8-2002

Modeling and Simulation of the Chemical Etching Process in Niobium Cavities

Qin Xue
University of Nevada, Las Vegas

MODELING AND SIMULATION OF THE CHEMICAL ETCHING PROCESS IN NIOBIUM CAVITIES

by

Qin Xue

Bachelor of Science
Taiyuan University of Technology
1995

A thesis submitted in partial fulfillment
of the requirements for

Master of Science Degree
Department of Mechanical Engineering
Howard R. Hughes College of Engineering

Graduate College
University of Nevada, Las Vegas
August 2002

ABSTRACT

Preparing and Submitting Your
Thesis or Dissertation

By

Qin Xue

Dr.Yitong Chen, Examination Committee Chair
Associate professor of Mechanical
Dr.Darrell Pepper, Examination Committee Chair
Professor of Mechanical
University of Nevada, Las Vegas

Niobium Cavities are important parts of the integrated NC/SC high-power linear accelerator (linac) that can accelerate over 100 mA of protons to several GeV. Surface finish of the niobium cavity plays an important role of achieving the best performance of niobium cavity. The chemical etching techniques have been widely used.

Chemical etching of the inner surface of the cavity is achieved by circulating acid through it. The acid interacts with the surface and eliminates imperfections. During the etching process, a pipe with baffles is inserted within the cavity to direct the flow along the surfaces.

A 2-D, axisymmetric, steady state, incompressible fluid flow model is developed to simulate the chemical process. The Femlab code based on the finite-element method is used.

Benchmark cases were used to check the feasibility and accuracy of Femlab.

Plausible results were achieved when the proved results were compared with the results got from FEMLAB software.

TABLE OF CONTENTS

LIST OF FIGURES

LIST OF TABLES

CHAPTER 1

INTRODUCTION

Nuclear industry provides a significant percentage of the world, as well as that of the United States, electricity. Nuclear power produce thousands of tons of spent fuel. Some of this spent fuel can be radioactive for thousands of years. The US DOE is currently exploring the possibility of creating a permanent storage site at Yucca Mountain, Nevada for nuclear spent nuclear fuel: Accelerator Transmuting of Waste (ATW). In this approach, a particle accelerator produces protons that react with a heavy metal target to produce neutrons. A major component of the system is a linac that can accelerate over 100 mA of protons to several GeV. Los Alamos National Laboratory (LANL) is currently developing a superconducting RF (SCRF) high-current linear accelerator. SCRF has three major components: niobium cavities, power couplers and cryomodules. This paper mainly deals with niobium cavities.

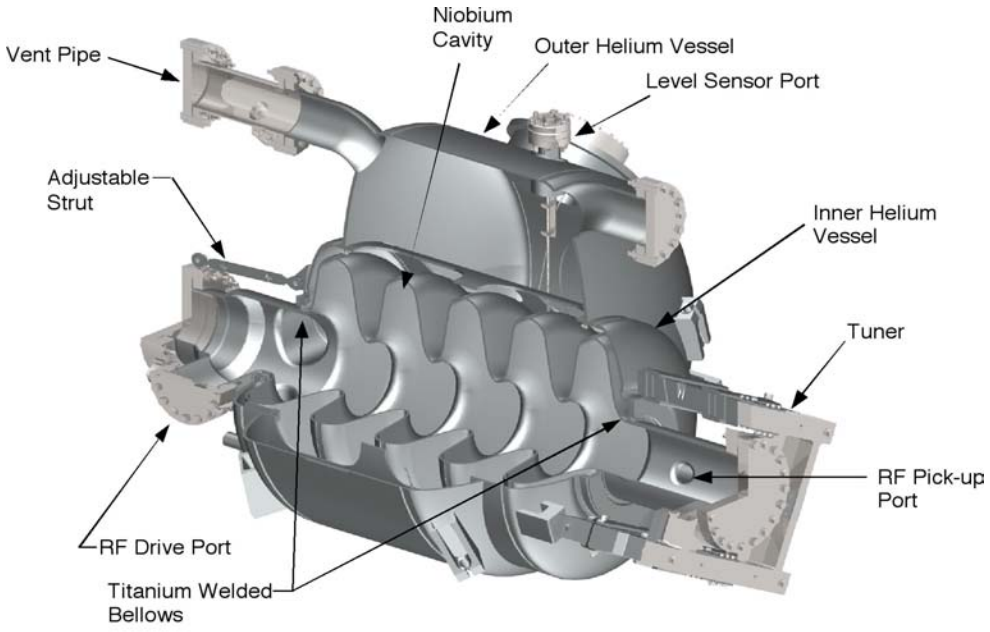

Figure 1. Schematic diagram of a niobium cavity (Executive summary: development and performance of medium-beta superconducting cavities (LANL))

The performance of niobium cavity is a function of multipacting, which is a resonant process in which number of electrons build up a multipacting, absorbing RF power so that it becomes impossible to increase the cavity fields by raising the incident power. The electrons collide with the structure walls leading to a large temperature rise and eventually to superconducting cavities, thermal breakdown. As a result, the Q_0 (quality factor) of the cavity is significantly reduced at the multipacting thresholds. A good cavity design should be able to eliminate, or at least to mimimize, multipacting. The factors that affect the multipacting includes: shape, surface finish, and coating.

Surface finish is so important that even microscopic contaminants on the surface of cavity can seriously affect its performance due to magnetic heating or electron field emission. As a consequence, the surface finish treatment is needed after fabrication of the cavity. The surface treatment techniques include chemical etching method, electropolishing methods, plasma-spray coating method, high-pressure water peening method, layer particle injection method, rolling and grinding method, honing, and lapping etc. Each method has advantage and disadvantage. For example, electropolishing method can provide a smooth, mirror like surface finish with no sharp steps at the grain boundaries, but the etching rate is slower than chemical etching method. On the other hand, surface contamination by sulfur must be removed by ultrasonic rinsing in hydrogen peroxide in chemical etching. A porous telflon membrane may also needed in cathode to keep the bubbles of hydrogen away from the niobium. Over the years, the researchers have concluded that chemical etching might not improve the performance after certain depth ($\cong$100 μm) and the surface of the cavity get more etching near the iris regions than the equaor regions of the cavity. Singer et al. used combination of electropolishing and chemical etching to improve the surface quality. Aune et al. presented a comprehensive study on developing nine-cell cavity. They applied chemical etching to the surface of the cavity during different stages of manufacturing.

To improve the performance of chemical etching, Los Alamos National Laboratory (LANL) employed a baffle to direct the etching fluid toward the walls of the cavity (Figure 2).

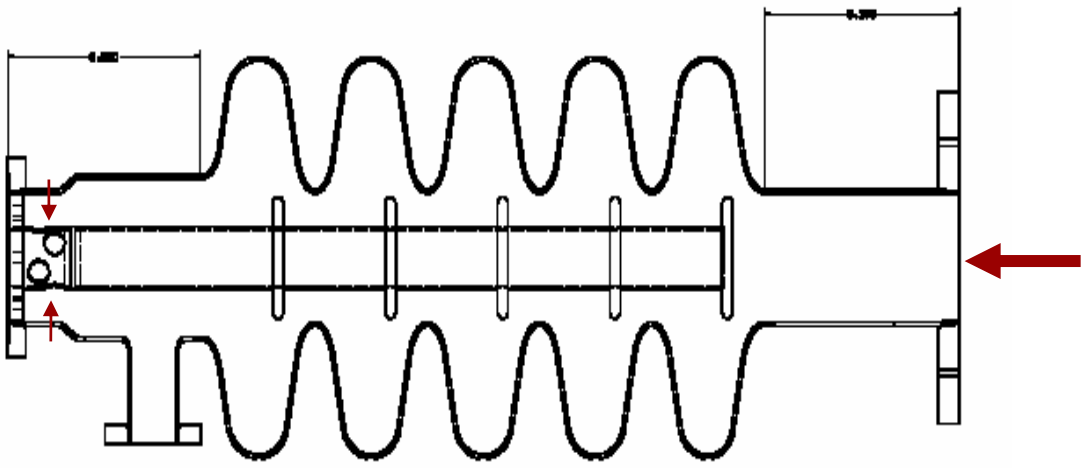

Figure 2. Current etching configuration of a niobium cavity

To study and understand the etching process, CFD technique now exerting a tremendous influence on the analysis of fluid flow phenomena, including heat transfer, mass transfer and chemical reaction is used to model the fluid flow problem. The well known discretization methods used in CFD are Finite Difference Method (FDM), Finite Volume Method (FVM), Finite Element Method (FEM), and Boundary Element Method (BEM). Comparing with the other methods, the FEM are especially flexible and efficient for discretizing the regions around complex configurations.

CHAPTER 2

MODELING CHEMICAL ETCHING PROCESS IN NIOBIUM CAVITIES

Modeling chemical etching process

In the field of Engineering we come across many complex practical problems, the quantitative analysis of which is extremely tedious and usually not possible. In such cases we have to resort to the modeling and numerical techniques.

To study the surface finish of niobium cavities, A model for a multiple-cell cavity based on “Executive Summary: Development and Performance of Medium-Beta Super conducting Cavities, LANL” is developed (Figure 3). In the chemical etching process, the actual cells in five-cell niobium cavities are vertically situated.

For simulating the process, CFD technique is employed. The problem is modeled as a 2-D, steady state, axisymmetric, incompressible, Newtonian fluid flow problem. During the chemical etching process the temperature of the cavity is maintained below $15^{o}C$, therefore heat factor is neglected. The governing equations are Continuity and Momentum equations.

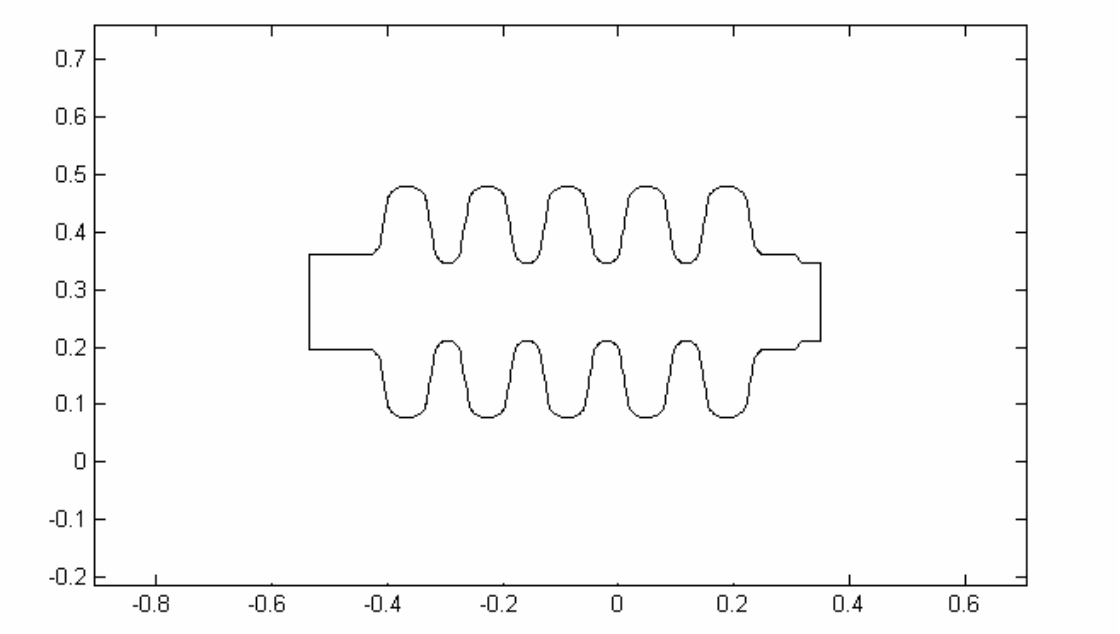

Figure 3. Five-cell niobium cavity geometry modeling

Basic Concepts of Fluid Mechanics

- Steady flow

  $\partial/\partial t \equiv 0$ and all properties are functions of position only.

- Incompressible flow

  The change of density is negligible, that is, the density of the flow is considered as constant. An explicit criterion for incompressible flow is:

$$\frac{V^2}{a^2} = Ma^2 << 1 \qquad (2.1)$$

  where Ma is the dimensionless Mach number of the flow. Commonly if $Ma \leq 0.3$ we consider it as incompressible flow.

- Viscosity

It is an internal property of a fluid inversely proportional to the shear strain rate or deformation rate. According to the viscosity, fluids can be classified as inviscid flow and viscid flow. For inviscid flow, the flow is frictionless and viscosity is zero. For viscid flow, the viscosity is nonzero. According to the relation of the shear stress and the deformation rate, fluids can be classified as Newtonian and non-Newtonian fluids. The linear fluid, the shear stress of which is directly proportional to deformation rate, is Newtonian fluid. The proportional constant is called the absolute or dynamic viscosity. Otherwise the fluid is non-Newtonian fluid.

- The Reynolds Number

  The Reynolds number is the most important dimensionless parameter in fluid dynamics and proportional to the ratio of inertial force to viscous force.

$$\mathrm{Re} = \frac{\rho VL}{\mu} = \frac{VL}{\nu} \tag{2.2}$$

  where Re is the Reynolds number; μ is viscosity; ρ is density; ν is kinematic viscosity; V and L are characteristic velocity and length of the flow.

- Laminar, Turbulent and Transition Flow

  According to Re, fluids are normally classified as laminar, turbulent and transition flow. Very low Re implies creeping motion. Moderate Re implies laminar motion in which the flow is smooth, steady and moves in layers. High Re implies turbulent motion in which the flow moves disorderly and has fluctuations. The transition motion happens in the changeover when the flow becomes irregular, unstable and fluctuating.

Fluid Mechanics Equations

The most important equations in fluid mechanics are the continuity equation (mass conservation equation) and momentum equations (motion equations).

The continuity can be derived by considering an elemental control volume and using the mass conservation relation in the element. The general compact form of continuity equation, which is always right no matter steady or unsteady, viscous or frictionless, compressible or incompressible flow, is:

$$\frac{\partial \rho}{\partial t} + \vec{\nabla} \cdot \rho \vec{V} = 0 \tag{2.3}$$

the gradient vector

$$\vec{\nabla} = \frac{\partial}{\partial x}\vec{i} + \frac{\partial}{\partial y}\vec{j} + \frac{\partial}{\partial z}\vec{k} \tag{2.4}$$

and $$\vec{V} = u\vec{i} + v\vec{j} + w\vec{k} \tag{2.5}$$

where u, v, w are x, y and z components of velocity respectively; ρ is density. Rewriting the vector equation in cartesian coordinate system:

$$\frac{\partial \rho}{\partial t} + \frac{\partial}{\partial x}(\rho u) + \frac{\partial}{\partial y}(\rho v) + \frac{\partial}{\partial z}(\rho w) = 0 \tag{2.6}$$

and in cylindrical coordinates:

$$\frac{\partial \rho}{\partial t} + \frac{1}{r}\frac{\partial}{\partial r}(\rho r v_r) + \frac{1}{r}\frac{\partial}{\partial \theta}(\rho v_\theta) + \frac{\partial}{\partial z}(\rho v_z) = 0 \tag{2.7}$$

Using the same elemental control volume, the momentum equation also can be derived by momentum relation in the infinitesimal control volume. The general compact momentum equation with gravitational type of body force is:

$$\rho \frac{d\vec{V}}{dt} = \rho \vec{g} - \vec{\nabla} p + \vec{\nabla} \cdot \overrightarrow{\tau_{ij}} \tag{2.8}$$

where p is pressure and

$$\frac{d\vec{V}}{dt} = \frac{\partial \vec{V}}{\partial t} + u\frac{\partial \vec{V}}{\partial x} + v\frac{\partial \vec{V}}{\partial y} + w\frac{\partial \vec{V}}{\partial z} \tag{2.9}$$

$$\tau_{ij} = \begin{bmatrix} \tau_{xx} & \tau_{yx} & \tau_{zx} \\ \tau_{xy} & \tau_{yy} & \tau_{zy} \\ \tau_{xz} & \tau_{yz} & \tau_{zz} \end{bmatrix} \tag{2.10}$$

Equation (2.8) is a brief vector equation valid for any fluid in general motion, and its component equations in Cartesian form are:

x-component $$\rho\left(\frac{\partial u}{\partial t} + u\frac{\partial u}{\partial x} + v\frac{\partial u}{\partial y} + w\frac{\partial u}{\partial z}\right) = \rho g_x - \frac{\partial p}{\partial x} + \frac{\partial \tau_{xx}}{\partial x} + \frac{\partial \tau_{yx}}{\partial y} + \frac{\partial \tau_{zx}}{\partial z}$$

(2.11a)

y-component $$\rho\left(\frac{\partial v}{\partial t} + u\frac{\partial v}{\partial x} + v\frac{\partial v}{\partial y} + w\frac{\partial v}{\partial z}\right) = \rho g_y - \frac{\partial p}{\partial y} + \frac{\partial \tau_{xy}}{\partial x} + \frac{\partial \tau_{yy}}{\partial y} + \frac{\partial \tau_{zy}}{\partial z}$$

(2.11b)

z-component $$\rho\left(\frac{\partial w}{\partial t} + u\frac{\partial w}{\partial x} + v\frac{\partial w}{\partial y} + w\frac{\partial w}{\partial z}\right) = \rho g_z - \frac{\partial p}{\partial z} + \frac{\partial \tau_{xz}}{\partial x} + \frac{\partial \tau_{yz}}{\partial y} + \frac{\partial \tau_{zz}}{\partial z}$$

(2.11c)

where g_x, g_y, g_z are x, y and z components of the acceleration of gravity; τ_{xx}, τ_{yy}, τ_{zz}, τ_{xy}, τ_{xz}, τ_{yx}, τ_{yz}, τ_{zx}, τ_{zy} are viscous stress components.

The general momentum equations in cylindrical coordinates are:

r-component $$\rho\left(\frac{\partial v_r}{\partial t} + v_r\frac{\partial v_r}{\partial r} + \frac{v_\theta}{r}\frac{\partial v_r}{\partial \theta} - \frac{v_\theta^{\,2}}{r} + v_z\frac{\partial v_r}{\partial z}\right) = -\frac{\partial p}{\partial r} + \rho g_r - \left(\frac{1}{r}\frac{\partial}{\partial r}(r\tau_{rr}) + \frac{1}{r}\frac{\partial \tau_{r\theta}}{\partial \theta} - \frac{\tau_{\theta\theta}}{r} + \frac{\partial \tau_{r\theta}}{\partial z}\right)$$

(2.12a)

θ-component

$$\rho\left(\frac{\partial v_\theta}{\partial t}+v_r\frac{\partial v_\theta}{\partial r}+\frac{v_\theta}{r}\frac{\partial v_\theta}{\partial \theta}+\frac{v_r v_\theta}{r}+v_z\frac{\partial v_\theta}{\partial z}\right)=-\frac{1}{r}\frac{\partial p}{\partial \theta}+\rho g_\theta$$
$$-\left(\frac{1}{r^2}\frac{\partial}{\partial r}(r^2\tau_{r\theta})+\frac{1}{r}\frac{\partial \tau_{\theta\theta}}{\partial \theta}+\frac{\partial \tau_{\theta z}}{\partial z}\right)$$

(2.12b)

z-component

$$\rho\left(\frac{\partial v_z}{\partial t}+v_r\frac{\partial v_z}{\partial r}+\frac{v_\theta}{r}\frac{\partial v_z}{\partial \theta}+v_z\frac{\partial v_z}{\partial z}\right)=-\frac{\partial p}{\partial z}+\rho g_z$$
$$-\left(\frac{1}{r}\frac{\partial}{\partial r}(r\tau_{rz})+\frac{1}{r}\frac{\partial \tau_{\theta z}}{\partial \theta}+\frac{\partial \tau_{zz}}{\partial z}\right)$$

(2.12c)

where v_r, v_θ, v_z are r, θ and z components of velocity respectively; g_r, g_θ, g_z are r, θ and z components of the acceleration of gravity; τ_{rr}, $\tau_{\theta\theta}$, τ_{zz}, $\tau_{r\theta}$, $\tau_{\theta r}$, $\tau_{\theta z}$, $\tau_{z\theta}$, τ_{zr}, τ_{rz} are viscous stress components.

Navier-Stokes Equations

For a Newtonian fluid, as described earlier the viscous stresses are proportional to the element strain rates and the coefficient of viscosity. In this case the stresses are:

$$\tau_{xx}=-\mu\left[2\frac{\partial u}{\partial x}-\frac{2}{3}(\vec{\nabla}\cdot\vec{V})\right] \quad (2.13a)$$

$$\tau_{yy}=-\mu\left[2\frac{\partial v}{\partial y}-\frac{2}{3}(\vec{\nabla}\cdot\vec{V})\right] \quad (2.13b)$$

$$\tau_{zz}=-\mu\left[2\frac{\partial w}{\partial z}-\frac{2}{3}(\vec{\nabla}\cdot\vec{V})\right] \quad (2.13c)$$

$$\tau_{xy} = \tau_{yx} = -\mu\left[r\frac{\partial u}{\partial y} + \frac{\partial v}{\partial x} \right] \tag{2.13d}$$

$$\tau_{yz} = \tau_{zy} = -\mu\left[\frac{\partial v}{\partial z} + \frac{\partial w}{\partial y} \right] \tag{2.13e}$$

$$\tau_{zx} = \tau_{xz} = -\mu\left[\frac{\partial w}{\partial x} + \frac{\partial u}{\partial z} \right] \tag{2.13f}$$

where

$$\vec{\nabla} \cdot \vec{V} = \frac{\partial u}{\partial x} + \frac{\partial v}{\partial y} + \frac{\partial w}{\partial z} \tag{2.14}$$

Substituting Equations (2.13) into Equations (2.11), the momentum equations becomes

x-component

$$\rho\left(\frac{\partial u}{\partial t} + u\frac{\partial u}{\partial x} + v\frac{\partial u}{\partial y} + w\frac{\partial u}{\partial z} \right) = \rho g_x - \frac{\partial p}{\partial x} + \frac{\partial}{\partial x}\left(2\mu\frac{\partial u}{\partial x} - \frac{2}{3}\mu\vec{\nabla} \cdot \vec{V} \right) + \frac{\partial}{\partial y}\left[\mu\left(\frac{\partial v}{\partial x} + \frac{\partial u}{\partial y} \right) \right] + \frac{\partial}{\partial z}\left[\mu\left(\frac{\partial u}{\partial z} + \frac{\partial w}{\partial x} \right) \right] \tag{2.15a}$$

y-component

$$\rho\left(\frac{\partial v}{\partial t} + u\frac{\partial v}{\partial x} + v\frac{\partial v}{\partial y} + w\frac{\partial v}{\partial z} \right) = \rho g_y - \frac{\partial p}{\partial y} + \frac{\partial}{\partial x}\left[\mu\left(\frac{\partial u}{\partial y} + \frac{\partial v}{\partial x} \right) \right] + \frac{\partial}{\partial y}\left(2\mu\frac{\partial v}{\partial y} - \frac{2}{3}\mu\vec{\nabla} \cdot \vec{V} \right) + \frac{\partial}{\partial z}\left[\mu\left(\frac{\partial v}{\partial z} + \frac{\partial w}{\partial y} \right) \right] \tag{2.15b}$$

z-component

$$\rho\left(\frac{\partial w}{\partial t} + u\frac{\partial w}{\partial x} + v\frac{\partial w}{\partial y} + w\frac{\partial w}{\partial z} \right) = \rho g_z - \frac{\partial p}{\partial z} + \frac{\partial}{\partial x}\left[\mu\left(\frac{\partial w}{\partial x} + \frac{\partial u}{\partial z} \right) \right] + \frac{\partial}{\partial y}\left[\mu\left(\frac{\partial v}{\partial z} + \frac{\partial w}{\partial y} \right) \right] + \frac{\partial}{\partial z}\left(2\mu\frac{\partial w}{\partial z} - \frac{2}{3}\mu\vec{\nabla} \cdot \vec{V} \right) \tag{2.15c}$$

Equations (2.15) are the Navier-Stokes equations. In the special case with constant viscosity and density, it can be simplified to:

x-component
$$\rho\left(\frac{\partial u}{\partial t}+u\frac{\partial u}{\partial x}+v\frac{\partial u}{\partial y}+w\frac{\partial u}{\partial z}\right)=\rho g_x-\frac{\partial p}{\partial x}+\mu\left(\frac{\partial^2 u}{\partial x^2}+\frac{\partial^2 u}{\partial y^2}+\frac{\partial^2 u}{\partial z^2}\right) \tag{2.16a}$$

y-component
$$\rho\left(\frac{\partial v}{\partial t}+u\frac{\partial v}{\partial x}+v\frac{\partial v}{\partial y}+w\frac{\partial v}{\partial z}\right)=\rho g_y-\frac{\partial p}{\partial y}+\mu\left(\frac{\partial^2 v}{\partial x^2}+\frac{\partial^2 v}{\partial y^2}+\frac{\partial^2 v}{\partial z^2}\right) \tag{2.16b}$$

z-component
$$\rho\left(\frac{\partial w}{\partial t}+u\frac{\partial w}{\partial x}+v\frac{\partial w}{\partial y}+w\frac{\partial w}{\partial z}\right)=\rho g_z-\frac{\partial p}{\partial z}+\mu\left(\frac{\partial^2 w}{\partial x^2}+\frac{\partial^2 w}{\partial y^2}+\frac{\partial^2 w}{\partial z^2}\right) \tag{2.16c}$$

Equations (2.16) are the Navier-Stokes equation for incompressible flow in cartesian coordinates, in cylindrical coordinates the equations become

r-component
$$\rho\left(v_r\frac{\partial v_r}{\partial r}+\frac{v_\theta}{r}\frac{\partial v_r}{\partial \theta}-\frac{v_\theta^{\,2}}{r}+v_z\frac{\partial v_r}{\partial z}\right)=-\frac{\partial p}{\partial r}+\rho g_r+\mu\left[\frac{\partial}{\partial r}\left(\frac{1}{r}\frac{\partial}{\partial r}(rv_r)\right)+\frac{1}{r^2}\frac{\partial^2 v_r}{\partial \theta^2}-\frac{2}{r^2}\frac{\partial v_\theta}{\partial \theta}+\frac{\partial^2 v_r}{\partial z^2}\right] \tag{2.17a}$$

θ-component
$$\rho\left(v_r\frac{\partial v_\theta}{\partial r}+\frac{v_\theta}{r}\frac{\partial v_\theta}{\partial \theta}+\frac{v_r v_\theta}{r}+v_z\frac{\partial v_\theta}{\partial z}\right)=-\frac{1}{r}\frac{\partial p}{\partial \theta}+\rho g_\theta+\mu\left[\frac{\partial}{\partial r}\left(\frac{1}{r}\frac{\partial}{\partial r}(rv_\theta)\right)+\frac{1}{r^2}\frac{\partial^2 v_\theta}{\partial \theta^2}+\frac{2}{r^2}\frac{\partial v_r}{\partial \theta}+\frac{\partial^2 v_\theta}{\partial z^2}\right] \tag{2.17b}$$

z-component
$$\rho\left(v_r\frac{\partial v_z}{\partial r}+\frac{v_\theta}{r}\frac{\partial v_z}{\partial \theta}+v_z\frac{\partial v_z}{\partial z}\right)=-\frac{\partial p}{\partial z}+\rho g_z+\mu\left[\frac{1}{r}\frac{\partial}{\partial r}\left(r\frac{\partial v_z}{\partial r}\right)+\frac{1}{r^2}\frac{\partial^2 v_z}{\partial \theta^2}+\frac{\partial^2 v_z}{\partial z^2}\right] \tag{2.17c}$$

Governing Equations for Chemical Etching Process Modeling

For the chemical etching process modeling problem, which is modeled as a 2-D, steady state, axisymmetric, incompressible, Newtonian fluid flow problem, the continuity and momentum equations are greatly simplified. For convenience, the cylindrical coordinate system is employed.

Due to the assumption that the viscosity and density of the etching fluid are constant, Equation (2.7) becomes

$$\frac{1}{r}\frac{\partial}{\partial r}(rv_r)+\frac{1}{r}\frac{\partial}{\partial \theta}(v_\theta)+\frac{\partial}{\partial z}(v_z)=0 \qquad (2.18)$$

Since the problem is in the steady state condition, the time term is removed. Furthermore, for axisymmetric fluid problems, v_θ and $\partial/\partial\theta$ are considered to be approximately zero and the 3-D problem is simplified to 2-D problem. Thus the equations (2.17) and (2.18) reduce to

The Continuity Equation:

$$\frac{1}{r}\frac{\partial}{\partial r}(rv_r)+\frac{\partial}{\partial z}(v_z)=0 \qquad (2.19)$$

The Momentum Equation:

r-component $$\rho\left(v_r\frac{\partial v_r}{\partial r}+v_z\frac{\partial v_r}{\partial z}\right)=-\frac{\partial p}{\partial r}+\rho g_r+\mu\left[\frac{\partial}{\partial r}\left(\frac{1}{r}\frac{\partial}{\partial r}(rv_r)\right)+\frac{\partial^2 v_r}{\partial z^2}\right]$$

(2.20a)

z-component $$\rho\left(v_r\frac{\partial v_z}{\partial r}+v_z\frac{\partial v_z}{\partial z}\right)=-\frac{\partial p}{\partial z}+\rho g_z+\mu\left[\frac{1}{r}\frac{\partial}{\partial r}\left(r\frac{\partial v_z}{\partial r}\right)+\frac{\partial^2 v_z}{\partial z^2}\right]$$

(2.20b)

where g_r=0. The equations (2.19) and (2.20) are governing equations for CFD simulation of chemical etching process.

CHAPTER 3

FINITE ELEMENT METHOD

Introduction

The finite element method (FEM) is a powerful numerical technique and computational tool. Although this method was first developed for use in the aircraft structural analysis. With the rapid advances in computer technology in recent years, the usage of the method has been extended into wide field of engineering ranging from the stress analysis of aeronautics, automotive and building to the field analysis of heat transfer, fluid flow and so on.

Comparing to other numerical method, such as the finite difference method (FDM) or the finite volume method (FDM) and boundary element method (BEM), the finite element method has the advantages as follows.

- The ease of handling irregular geometries.
- The ease of the uniform or non-uniform mesh discretization.
- The ease of incorporating the boundary conditions directly into the integral formulation.
- The ease of handling nonhomogeneous and anisotropic materials.
- The ease of establishing the governing equations, as well as the compact and well-defined linear algebra and matrix operations associated with it.

- The ease of implementing the high-order elements.

With all the ease as stated above, the finite element method has become very popular.

The basic idea of the FEM is to discretized the domain into small subdomains called finite elements or elements. Different shapes are available, such as straight line in one dimension, triangles and quadrilaterals in two dimensions, and tetrahedra, pentahedra, and hexahedra for three dimensions. These elements are interconnected at defined points called nodes. The nodes and the elements constitute the FEM mesh. Inside the elements, the value of the field variables such as velocity, pressure and temperature are specified by the interpolation functions, which are functions of the values at the nodes. A set of linear equations, which unknowns are the values of the field variable of the nodes, will be produced according to each element. At this point, the field can be calculated easily by any matrix algebra technique.

In the history of FEM, three approaches including direct approach, variational approach (such as Rayleigh-Ritz method) and weighted residual approach (such as Gelerkin method and least squares method) were developed. Among the three approaches, with the ease of being derived directly from the differential equations, the weighted residual approach is the most widely used one.

The Weighted Residual Method

A general representation of single governing equation with only a variable is:

$$f(\phi) = 0 \qquad \text{in } \Omega \tag{3.1}$$

$$g_1(\phi) = 0 \qquad \text{on } \Gamma_1 \tag{3.2a}$$

$$g_2(\phi) = 0 \qquad \text{on } \Gamma_2 \tag{3.2b}$$

where the variable ϕ is only function of x; f is a function of ϕ in the whole domain Ω; Γ_1 and Γ_2 are the boundary parts of Ω.

The approximate solution is given by

$$\phi(x) \cong \phi'(x) = \sum_{i=1}^{n} a_i N_i(x) \tag{3.3}$$

where a_i are constants and $N_i(x)$ are the shape functions; $\phi'(x)$ is approximate variable satisfying all the boundary conditions. R, residual, is defined as:

$$R = f(\phi') \tag{3.4}$$

where some conditions are required to make R small. In the weighted residual method, the criterion is takes as:

$$\int_{\Omega} w_i R dx = 0 \tag{3.5}$$

where w_i are the weighting functions or weights. R is zero when $\phi'(x)$ is equal to the exact solution $\phi(x)$.

Referring to the choice of the weighting function, several different methods like collocation, subdomain collocation, least square and Galerkin are applicable. Of these methods, Galerkin method is the most popular in recent years.

Galerkin Method

In the Galerkin method, the weighting functions are specified to be same as the shape function. Equation (3.5) changes to

$$\int_{\Omega} N_i R dx = 0 \tag{3.6}$$

Practically The finite element is always processed by step by step, the procedure in Galekin method can be stated by the steps below:

Step 1: Discretizing the domain.

Step 2: Selecting the interpolation function for $\phi^{(e)}$, such as shown below for two-dimensional problems.

$$\phi^{(e)}(x,y) = \sum_{i=1}^{n} N_i(x)\phi_i^{(e)} \tag{3.7}$$

Step 3: Setting up the integral equation like equation (3.6) and deriving the matrix. The weights are taken the same as the shape functions. We can use a one-dimensional problem to explain this step. The governing equation is

$$\frac{\partial^2 T}{\partial x^2} + \frac{\partial^2 T}{\partial y^2} = 0 \quad \text{in } \Omega \tag{3.8a}$$

with boundary condition:

$$T = T_0 \qquad \text{on } \Gamma_1 \tag{3.8b}$$

$$\frac{\partial T}{\partial n} = q \quad \text{on } \Gamma_2 \tag{3.8c}$$

Using the weighted residual method, we have equation

$$\iint_A w_i \left(\frac{\partial^2 T}{\partial x^2} + \frac{\partial^2 T}{\partial y^2} \right) dxdy = 0 \tag{3.9}$$

By applying the Green-Gauss theorem, a “weak” form will be produced.

$$\iint_A w_i\left(\frac{\partial^2 T}{\partial x^2}+\frac{\partial^2 T}{\partial y^2}\right)dxdy=-\iint_A\left(\frac{\partial w_i}{\partial x}\frac{\partial T}{\partial x}+\frac{\partial w_i}{\partial y}\frac{\partial T}{\partial y}\right)dxdy+\int_s w_i\frac{\partial T}{\partial n}ds=0 \tag{3.10}$$

Now substituting $w_i = N_i$ and $T^{(e)}(x,y)=\sum_{i=1}^{n} N_i(x)T_i^{(e)}$ into above equation,

$$\iint_A\left(\frac{\partial N_i}{\partial x}\frac{\partial N_j}{\partial x}+\frac{\partial N_i}{\partial y}\frac{\partial N_j}{\partial y}\right)dxdy\{T_j\}-\int_s N_i q ds=0 \tag{3.11}$$

so the stiffness matrix is

$$\left[K^{(e)}\right]=\iint_A\left(\frac{\partial N_i}{\partial x}\frac{\partial N_j}{\partial x}+\frac{\partial N_i}{\partial y}\frac{\partial N_j}{\partial y}\right)dxdy \tag{3.12}$$

and the load vector is

$$\left[P^{(e)}\right]=\int_s N_i q ds \tag{3.13}$$

Step 4: Assembling the element equations.

Step 5: Solving the matrix and getting the solutions for the field variables ϕ at the nodes.

Linear Triangular Element

In two-dimension problem, the field variable $\phi(x,y)$ could be approximated by linear, quadratic, cubic and high-order polynomial functions. The linear approximation is the most common one. It can be expressed as

$$\phi(x)=\alpha_1+\alpha_2 x+\alpha_3 y \tag{3.14}$$

For linear triangular element, each element has three nodes as shown in Figure 4. The node values are

$$\phi_1=\alpha_1+\alpha_2 x_1+\alpha_3 y_1 \tag{3.15a}$$

$$\phi_2 = \alpha_1 + \alpha_2 x_2 + \alpha_3 y_2 \tag{3.15b}$$

$$\phi_3 = \alpha_1 + \alpha_2 x_3 + \alpha_3 y_3 \tag{3.15c}$$

Where x_1, x_2, x_3 are the x coordinates of node 1,2 and 3 respectively; y_1, y_2, y_3 are the y coordinates of node 1,2 and 3 respectively.

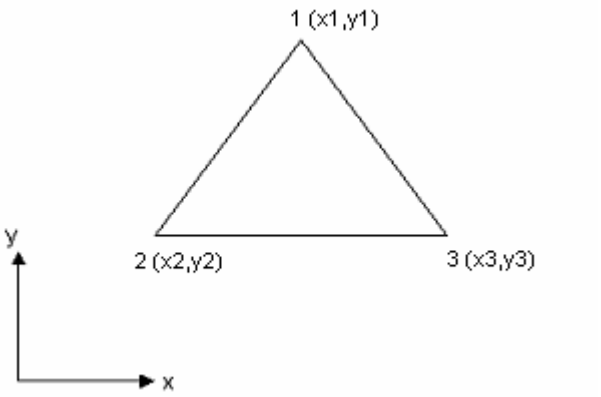

Figure 4. Two-dimensional linear triangular element

Now solving for α_1, α_2 and α_3

$$\alpha_1 = \frac{1}{2A^{(e)}}\left[(x_2 y_3 - x_3 y_2)\phi_1 + (x_3 y_1 - x_1 y_3)\phi_2 + (x_1 y_2 - x_2 y_1)\phi_3\right] \tag{3.16a}$$

$$\alpha_2 = \frac{1}{2A^{(e)}}\left[(y_2 - y_3)\phi_1 + (y_3 - y_1)\phi_2 + (y_1 - y_2)\phi_3\right] \tag{3.16b}$$

$$\alpha_3 = \frac{1}{2A^{(e)}}\left[(x_3 - x_2)\phi_1 + (x_1 - x_3)\phi_2 + (x_2 - x_1)\phi_3\right] \tag{3.16c}$$

where

$$A^{(e)} = \frac{1}{2}\left[(x_2 y_3 - x_3 y_2) + (x_3 y_1 - x_1 y_3) + (x_1 y_2 - x_2 y_1)\right] \tag{3.17}$$

The variable $\phi(x, y)$ also can be written according to the shape function

$$\phi = \phi_1 N_1 + \phi_2 N_2 + \phi_3 N_3 \tag{3.18}$$

The combination of Equation (3.7), (3.8), (3.9), (3.10) retains

$$N_1^{(e)} = \frac{1}{2A^{(e)}}\left[(x_2 y_3 - x_3 y_2) + (y_2 - y_3)x + (x_3 - x_2)y\right] \tag{3.19a}$$

$$N_2^{(e)} = \frac{1}{2A^{(e)}}\left[(x_3 y_1 - x_1 y_3) + (y_3 - y_1)x + (x_1 - x_3)y\right] \tag{3.19b}$$

$$N_3^{(e)} = \frac{1}{2A^{(e)}}\left[(x_1 y_2 - x_2 y_1) + (y_1 - y_2)x + (x_2 - x_1)y\right] \tag{3.19c}$$

For every N_1, N_2 and N_3 of linear triangular elements, there exists a relation

$$N_1 + N_2 + N_3 = 1 \tag{3.20}$$

Therefore the shape functions are not all independent. For convenience, the two independent shape functions are also represented by the natural coordinates ξ, η.

$$N_1 = \xi \tag{3.21a}$$

$$N_2 = \eta \tag{3.21b}$$

$$N_3 = 1 - \xi - \eta \tag{3.21c}$$

The isoparametric representation is:

$$x = x_1 N_1 + x_2 N_2 + x_3 N_3 \tag{3.22a}$$

$$y = y_1 N_1 + y_2 N_2 + y_3 N_3 \tag{3.22b}$$

The substitution of equations (3.13) into (3.14) gets

$$x = (x_1 - x_3)\xi + (x_2 - x_3)\eta + x_3 \tag{3.23a}$$

$$y = (y_1 - y_3)\xi + (y_2 - y_3)\eta + y_3 \tag{3.23b}$$

Now evaluating the partial derivatives of $\phi(x(\xi,\eta), y(\xi,\eta))$,

$$\frac{\partial u}{\partial \xi} = \frac{\partial u}{\partial x}\frac{\partial x}{\partial \xi} + \frac{\partial u}{\partial y}\frac{\partial y}{\partial \xi} \tag{3.24a}$$

$$\frac{\partial u}{\partial \eta} = \frac{\partial u}{\partial x}\frac{\partial x}{\partial \eta} + \frac{\partial u}{\partial y}\frac{\partial y}{\partial \eta} \tag{3.24b}$$

which can be written in matrix as

$$\begin{Bmatrix} \frac{\partial u}{\partial \xi} \\ \frac{\partial u}{\partial \eta} \end{Bmatrix} = \begin{bmatrix} \frac{\partial x}{\partial \xi} & \frac{\partial y}{\partial \xi} \\ \frac{\partial x}{\partial \eta} & \frac{\partial y}{\partial \eta} \end{bmatrix} \begin{Bmatrix} \frac{\partial u}{\partial x} \\ \frac{\partial u}{\partial y} \end{Bmatrix} \tag{3.25}$$

where the Jacobian J is defined as

$$J = \begin{bmatrix} \frac{\partial x}{\partial \xi} & \frac{\partial y}{\partial \xi} \\ \frac{\partial x}{\partial \eta} & \frac{\partial y}{\partial \eta} \end{bmatrix} \tag{3.26}$$

So the equation (3.20) is derived as follows

$$\begin{Bmatrix} \frac{\partial u}{\partial x} \\ \frac{\partial u}{\partial y} \end{Bmatrix} = J^{-1} \begin{Bmatrix} \frac{\partial u}{\partial \xi} \\ \frac{\partial u}{\partial \eta} \end{Bmatrix} \tag{3.27}$$

The Finite Element Method For Chemical Etching Process Modeling

The governing equations (2.19) and (2.20) of the chemical etching process modeling were given before. For avoiding the confusion, v_r and v_z are replaced by u and v respectively in the rest of this chapter. The equations (2.19) and (2.20) can be rewritten as

$$\rho\left(u\frac{\partial u}{\partial r} + v\frac{\partial u}{\partial z}\right) = -\frac{\partial p}{\partial r} + \rho g_r + \mu\left[\frac{\partial}{\partial r}\left(\frac{1}{r}\frac{\partial}{\partial r}(ru)\right) + \frac{\partial^2 u}{\partial z^2}\right] \tag{3.28a}$$

$$\rho\left(u\frac{\partial v}{\partial r} + v\frac{\partial v}{\partial z}\right) = -\frac{\partial p}{\partial z} + \rho g_z + \mu\left[\frac{1}{r}\frac{\partial}{\partial r}\left(r\frac{\partial v}{\partial r}\right) + \frac{\partial^2 v}{\partial z^2}\right] \tag{3.28b}$$

$$\frac{1}{r}\frac{\partial}{\partial r}(ru)+\frac{\partial z}{\partial z}=0 \tag{3.28c}$$

In the equations (3.28), we consider the pressure p, the velocity components v_r in the radian direction and v_z in the z direction as unknowns of the formulations. Assuming the approximations of p, u and v as

$$p^{(e)}(r,z)=\sum_{i=1}^{n} N_i{}^{p}(r,z)p_i{}^{(e)} \tag{3.29a}$$

$$u^{(e)}(r,z)=\sum_{i=1}^{n} N_i{}^{u}(r,z)u_i{}^{(e)} \tag{3.29b}$$

$$v^{(e)}(r,z)=\sum_{i=1}^{n} N_i{}^{v}(r,z)v_i{}^{(e)} \tag{3.29c}$$

where $N_i{}^{p}$, $N_i{}^{u}$ and $N_i{}^{v}$ are the shape functions. For simplicity, we set

$$N_i{}^{u}=N_i{}^{v}=N_i{}^{p}=N_i \tag{3.30}$$

If Galekin weighted residual method is applied to equations (3.28), we get

$$\iiint_{V^{(e)}} N_i\left[\rho^{(e)}\left(u^{(e)}\frac{\partial u^{(e)}}{\partial r}+v^{(e)}\frac{\partial u^{(e)}}{\partial z}\right)+\frac{\partial p^{(e)}}{\partial r}-\rho g_r-\mu\left(\frac{\partial}{\partial r}\left(\frac{1}{r}\frac{\partial}{\partial r}(ru^{(e)})\right)+\frac{\partial^2 u^{(e)}}{\partial z^2}\right)\right]dV=0 \tag{3.31a}$$

$$\iiint_{V^{(e)}} N_i\left[\rho\left(u^{(e)}\frac{\partial v^{(e)}}{\partial r}+v^{(e)}\frac{\partial v^{(e)}}{\partial z}\right)+\frac{\partial p^{(e)}}{\partial z}-\rho g_z-\mu\left(\frac{1}{r}\frac{\partial}{\partial r}\left(r\frac{\partial v^{(e)}}{\partial r}\right)+\frac{\partial^2 v^{(e)}}{\partial z^2}\right)\right]dV=0 \tag{3.31b}$$

$$\iiint_{V^{(e)}} N_i\left[\frac{1}{r}\frac{\partial}{\partial r}(ru^{(e)})+\frac{\partial v^{(e)}}{\partial z}\right]dV=0 \tag{3.31c}$$

where

$$dV=2\pi r dr dz \tag{3.32}$$

Substituting equation (3.32) into equations (3.31) and canceling the term 2π.

$$\iint_{\Omega^{(e)}} N_i \left[\rho\left(u^{(e)} \frac{\partial u^{(e)}}{\partial r} + v^{(e)} \frac{\partial u^{(e)}}{\partial z} \right) + \frac{\partial p^{(e)}}{\partial r} - \rho g_r - \mu\left(\frac{\partial}{\partial r}\left(\frac{1}{r}\frac{\partial}{\partial r}(ru^{(e)}) \right) + \frac{\partial^2 u^{(e)}}{\partial z^2} \right) \right] r dr dz = 0 \tag{3.33a}$$

$$\iint_{\Omega^{(e)}} N_i \left[\rho\left(u^{(e)} \frac{\partial v^{(e)}}{\partial r} + v^{(e)} \frac{\partial v^{(e)}}{\partial z} \right) + \frac{\partial p^{(e)}}{\partial z} - \rho g_z - \mu\left(\frac{1}{r}\frac{\partial}{\partial r}\left(r\frac{\partial v^{(e)}}{\partial r} \right) + \frac{\partial^2 v^{(e)}}{\partial z^2} \right) \right] r dr dz = 0 \tag{3.33b}$$

$$\iint_{\Omega^{(e)}} N_i \left[\frac{1}{r}\frac{\partial}{\partial r}(ru^{(e)}) + \frac{\partial v^{(e)}}{\partial z} \right] r dr dz = 0 \tag{3.33c}$$

Integrating the equations (3.33) by parts, at the same time, eliminating p, u and v by using equations (3.29), we get

$$\begin{aligned}
&\iint_{\Omega^{(e)}} N_i r\rho\left(N_j {u_j}^{(e)} \frac{\partial N_j}{\partial r} + N_j {v_j}^{(e)} \frac{\partial N_j}{\partial z} \right) {u_j}^{(e)} dr dz + \iint_{\Omega^{(e)}} N_i r \frac{\partial N_j}{\partial r} {p_j}^{(e)} dr dz \\
&- \iint_{\Omega^{(e)}} N_i r\rho g_r dr dz + \iint_{\Omega^{(e)}} \mu\left(\frac{\partial N_i}{\partial r}\frac{\partial}{\partial r}(rN_j) + r\frac{\partial N_i}{\partial z}\frac{\partial N_j}{\partial z} \right) {u_j}^{(e)} dr dz \\
&- \int_{\Gamma^{(e)}} \mu N_i \frac{\partial}{\partial r}(rN_j) n_r {u_j}^{(e)} d\Gamma - \int_{\Gamma^{(e)}} \mu r N_i \frac{\partial N_j}{\partial z} n_z {u_j}^{(e)} d\Gamma = 0
\end{aligned} \tag{3.34a}$$

$$\begin{aligned}
&\iint_{\Omega^{(e)}} N_i r\rho\left(N_j {u_j}^{(e)} \frac{\partial N_j}{\partial r} + N_j {v_j}^{(e)} \frac{\partial N_j}{\partial z} \right) {v_j}^{(e)} dr dz + \iint_{\Omega^{(e)}} N_i r \frac{\partial N_j}{\partial z} {p_j}^{(e)} dr dz \\
&- \iint_{\Omega^{(e)}} N_i r\rho g_z dr dz + \iint_{\Omega^{(e)}} \mu r\left(\frac{\partial N_i}{\partial r}\frac{\partial N_j}{\partial r} + \frac{\partial N_i}{\partial z}\frac{\partial N_j}{\partial z} \right) {v_j}^{(e)} dr dz \\
&- \int_{\Gamma^{(e)}} \mu N_i r \frac{\partial N_j}{\partial r} n_r {v_j}^{(e)} d\Gamma - \int_{\Gamma^{(e)}} \mu r N_i \frac{\partial N_j}{\partial z} n_z {v_j}^{(e)} d\Gamma = 0
\end{aligned} \tag{3.34b}$$

$$\iint_{\Omega^{(e)}} N_i \frac{\partial}{\partial r}(rN_j)u_i^{(e)}drdz + \iint_{\Omega^{(e)}} N_i r \frac{\partial N_j}{\partial z} v_j^{(e)} drdz = 0 \tag{3.34c}$$

Equations (3.34) can be written in the form

$$K_r^{(e)} u_i^{(e)} + K_{rp}^{(e)} p_i^{(e)} = f_r^{(e)} \tag{3.35a}$$

$$K_z^{(e)} v_i^{(e)} + K_{zp}^{(e)} p_i^{(e)} = f_z^{(e)} \tag{3.35b}$$

$$K_u^{(e)} u_i^{(e)} + K_v^{(e)} p_i^{(e)} = f_{uv}^{(e)} \tag{3.35c}$$

where

$$K_r^{(e)} = \iint_{\Omega^{(e)}} N_i r\rho \left(N_j u_j^{(e)} \frac{\partial N_j}{\partial r} + N_j v_j^{(e)} \frac{\partial N_j}{\partial z} \right) drdz + \iint_{\Omega^{(e)}} \mu \left(\frac{\partial N_i}{\partial r} \frac{\partial}{\partial r}(rN_j) + r \frac{\partial N_i}{\partial z} \frac{\partial N_j}{\partial z} \right) drdz$$

$$K_{rp}^{(e)} = \iint_{\Omega^{(e)}} N_i r \frac{\partial N_j}{\partial r} drdz$$

$$f_r^{(e)} = \iint_{\Omega^{(e)}} N_i r\rho g_r drdz + \int_{\Gamma^{(e)}} \mu N_i \frac{\partial}{\partial r}(rN_j) n_r u_j^{(e)} d\Gamma + \int_{\Gamma^{(e)}} \mu r N_i \frac{\partial N_j}{\partial z} n_z u_j^{(e)} d\Gamma$$

$$K_z^{(e)} = \iint_{\Omega^{(e)}} N_i r\rho \left(N_j u_j^{(e)} \frac{\partial N_j}{\partial r} + N_j v_j^{(e)} \frac{\partial N_j}{\partial z} \right) drdz + \iint_{\Omega^{(e)}} \mu r \left(\frac{\partial N_i}{\partial r} \frac{\partial N_j}{\partial r} + \frac{\partial N_i}{\partial z} \frac{\partial N_j}{\partial z} \right) drdz$$

$$K_{zp}^{(e)} = \iint_{\Omega^{(e)}} N_i r \frac{\partial N_j}{\partial z} drdz$$

$$f_z^{(e)} = \iint_{\Omega^{(e)}} N_i r\rho g_z drdz + \int_{\Gamma^{(e0}} \mu N_i r \frac{\partial N_j}{\partial r} n_r v_j^{(e)} d\Gamma + \int_{\Gamma^{(e)}} \mu r N_i \frac{\partial N_j}{\partial z} n_z v_j^{(e)} d\Gamma$$

$$K_u^{(e)} = \iint_{\Omega^{(e)}} N_i \frac{\partial}{\partial r}(rN_j) drdz$$

$$K_v^{(e)} = \iint_{\Omega^{(e)}} N_i r \frac{\partial N_j}{\partial z} drdz$$

$$f_{uv}^{(e)} = 0$$

(3.36)

The element equations (3.35a), (3.35b), (3.35c) can be combined into

$$K^{(e)} \phi_i^{(e)} = f^{(e)} \tag{3.37}$$

$$\begin{bmatrix} K_r^{(e)} & 0 & K_{rp}^{(e)} \\ 0 & K_z^{(e)} & K_{zp}^{(e)} \\ K_u^{(e)} & K_v^{(e)} & 0 \end{bmatrix} \begin{bmatrix} u_i^{(e)} \\ v_i^{(e)} \\ p_i^{(e)} \end{bmatrix} = \begin{bmatrix} f_r^{(e)} \\ f_z^{(e)} \\ 0 \end{bmatrix} \tag{3.38}$$

The element equations can be assembled to get the overall equations as

$$[K]\phi = f \tag{3.39}$$

where

$$[K] = \sum_{e=1}^{E} [K^{(e)}] \tag{3.40}$$

$$\phi = \sum_{e=1}^{E} \phi^{(e)} \tag{3.41}$$

$$f = \sum_{e=1}^{E} f^{(e)} \tag{3.42}$$

and E is the number of elements.

CHAPTER 4

FEMLAB SOFTWARE VERIFICATION

Introduction

FEMLAB is commercial software based on partial differential equations and the finite element method. FEMLAB is characterized as interactive and user-friendly graphical user interface, including CAD modeling, physics or equation coefficient definitions, boundary condition setting, automatic mesh generation, equation solving, visualization, and postprocessing. Another important advantage of FEMLAB is programming capabilities by using the specific programming language, an extension of the MATLAB language. Therefore, FEMLAB is widely used package for modeling and simulating scientific and engineering problems.

For checking the accuracy of FEMLAB, two well-known fluid flow cases are simulated using FEMLAB. One is square cavity flow case, and the other one is backward facing step case. The results are compared to proven results got by Odus R. Burggraf (136) and B.F.Armaly, et al. (957-960) respectively. It turns out FEMLAB is feasible in CFD problem.

Square Cavity Benchmarking

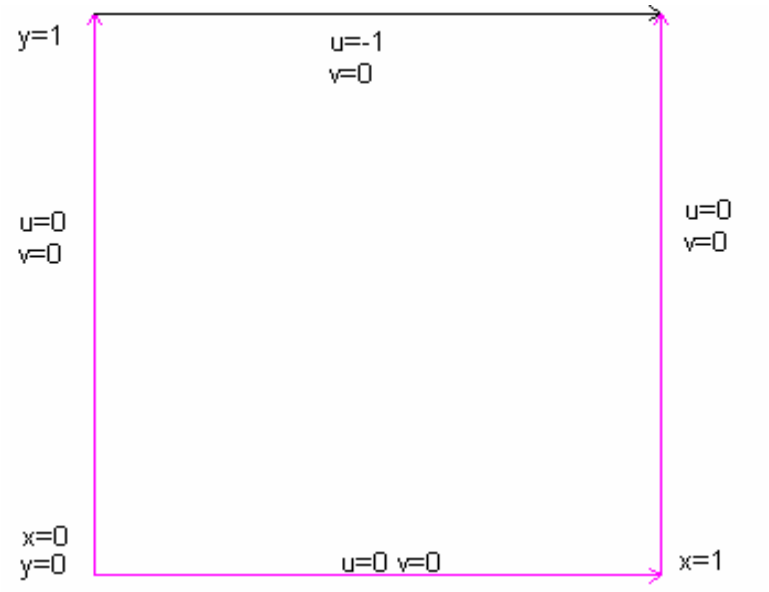

Figure 5. Geometry and boundary conditions for square cavity flow

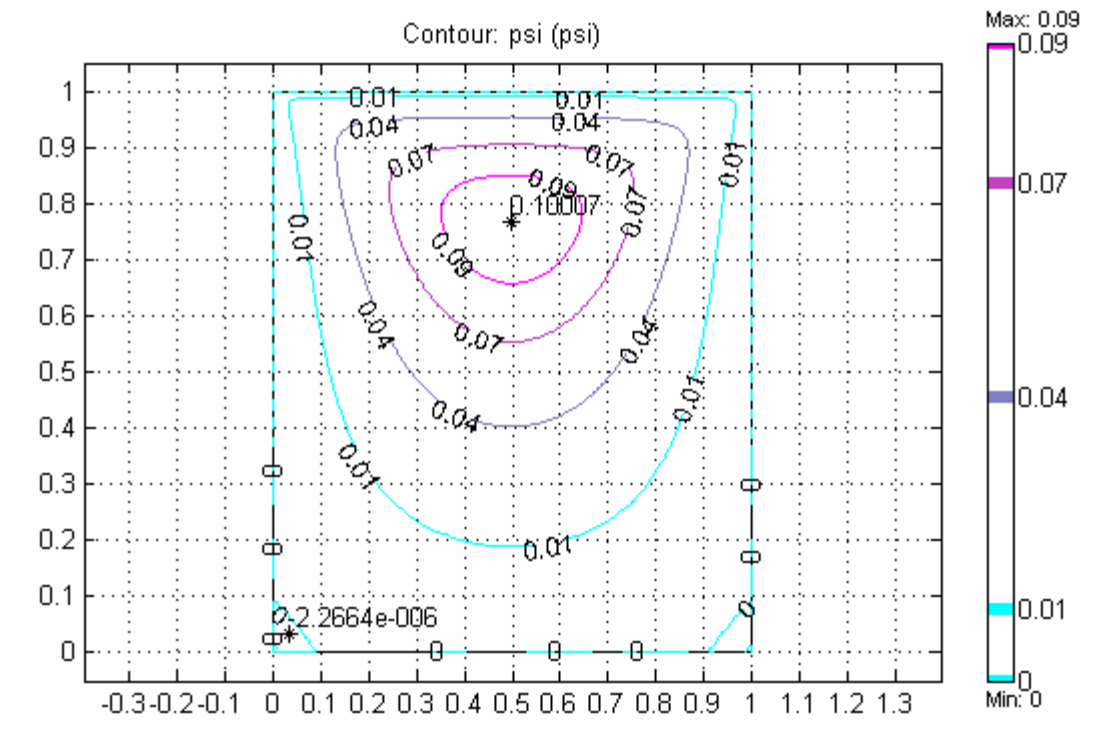

Figure 6. Streamline contours for square cavity flow at Re=1

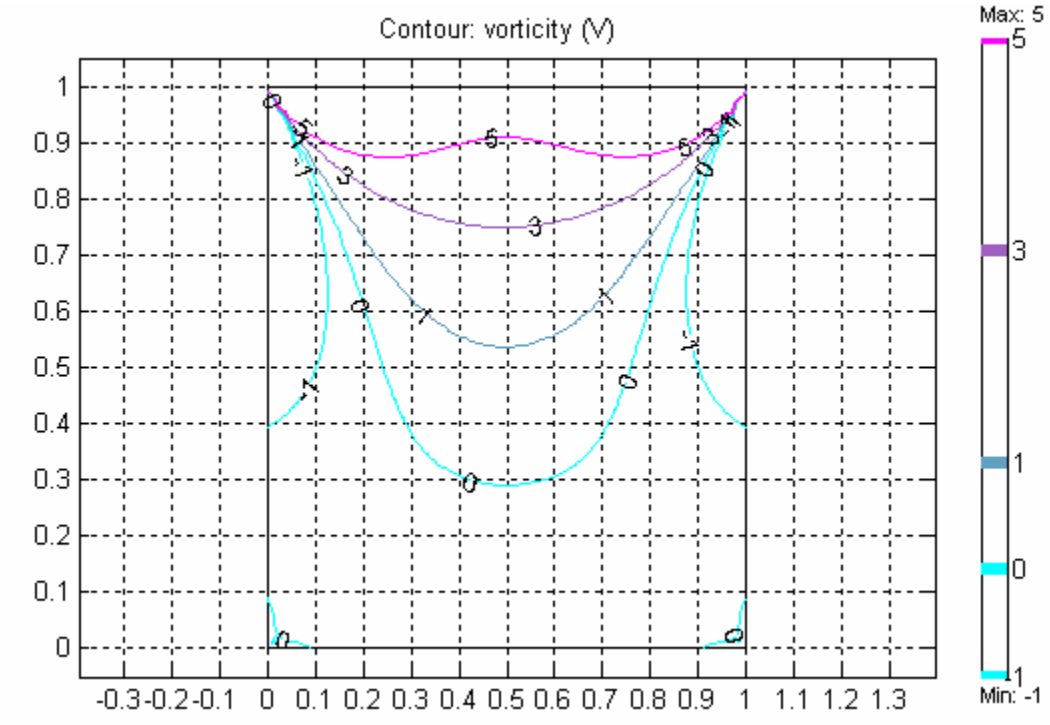

Figure 7. Vorticity contours for square cavity flow at Re=1

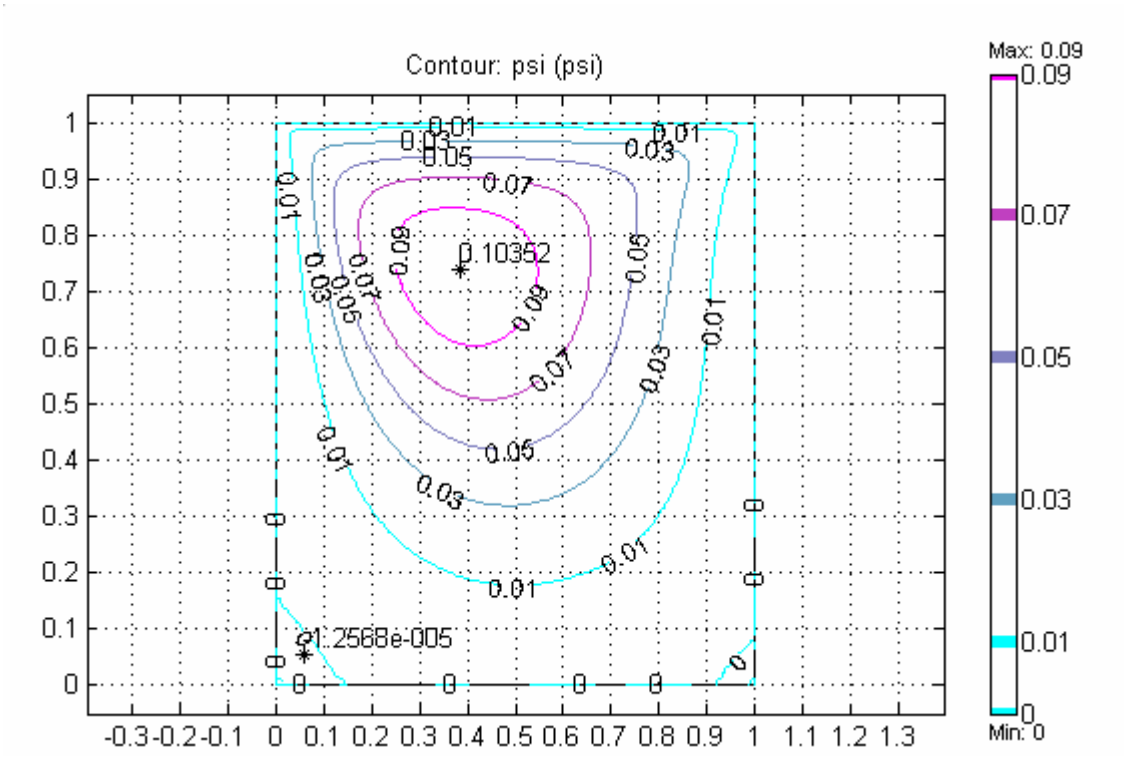

Figure 8. Streamline contours for square cavity flow at Re=100

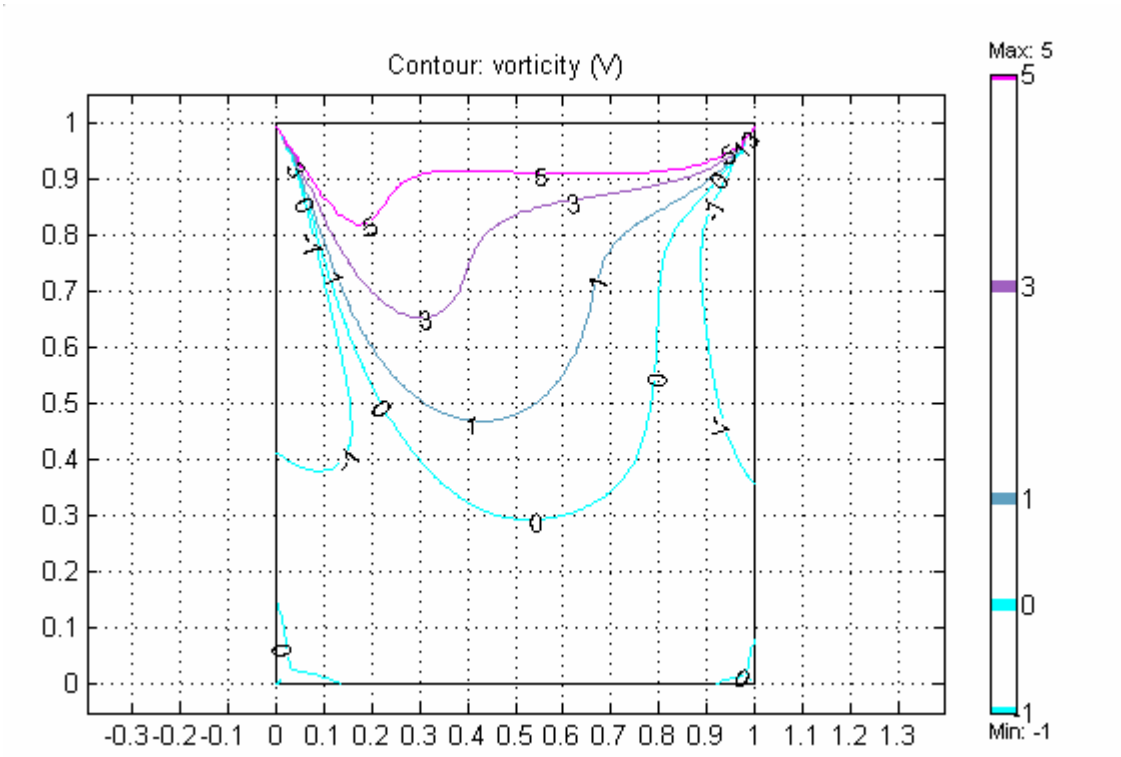

Figure 9. Vorticity contours for square cavity flow at Re=100

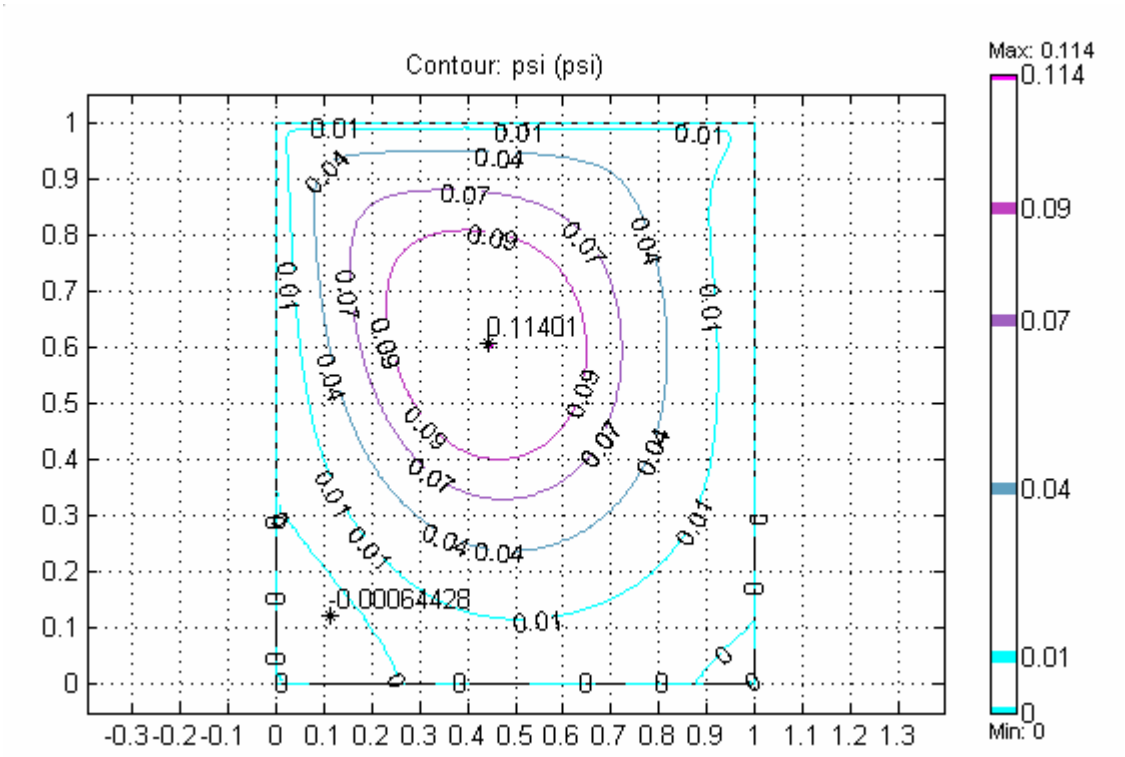

Figure 10. Streamline contours for square cavity flow at Re=400

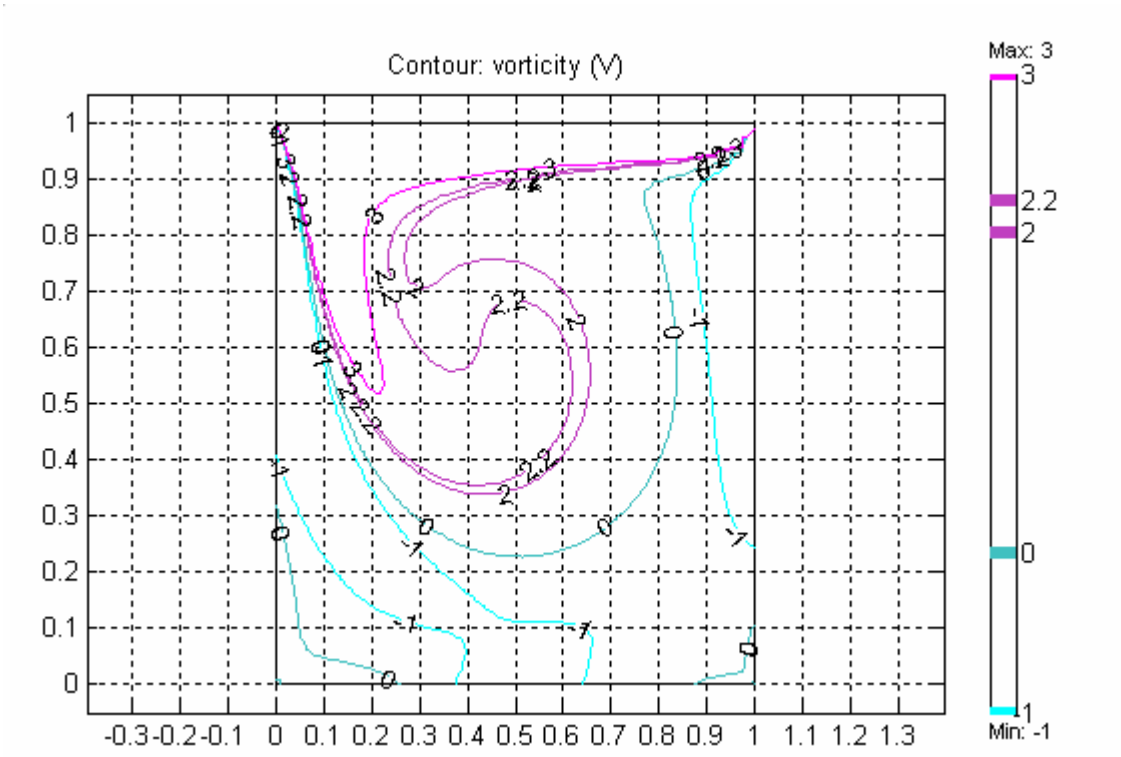

Figure 11. Vorticity contours for square cavity flow at Re=400

Table 1. Comparison of the proved results with Femlab results for square cavity

	Re=0		Re=1		Re=100		Re=400	
	ψ at vortex center	ω at vortex center	ψ at vortex center	ω at vortex center	ψ at vortex center	ω at vortex center	Ψ at vortex center	ω at vortex center
Burggraf	0.100	3.20			0.101	3.14	0.102	2.15
Current			0.100	3.23	0.104	3.18	0.114	2.29

Where ψ is streamline function and w is vorticity.

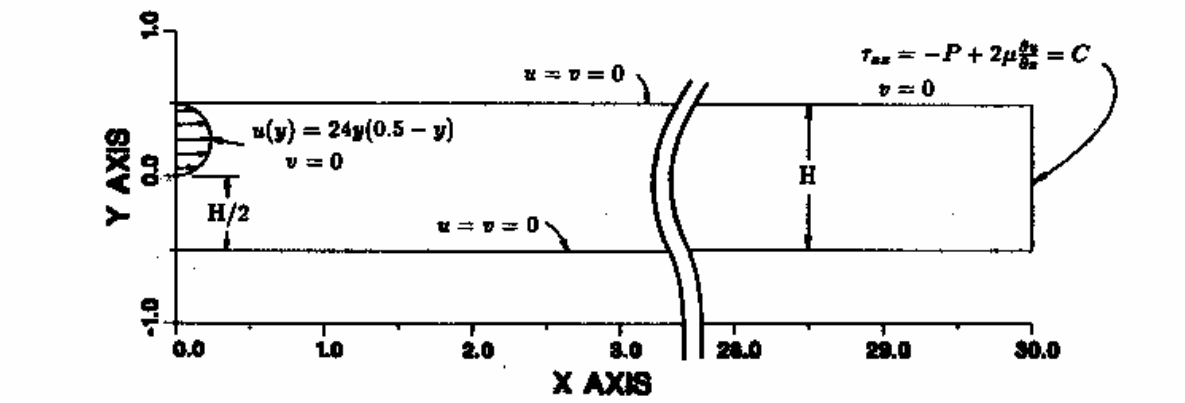

Figure 12. Geometry and boundary conditions for backward-facing step

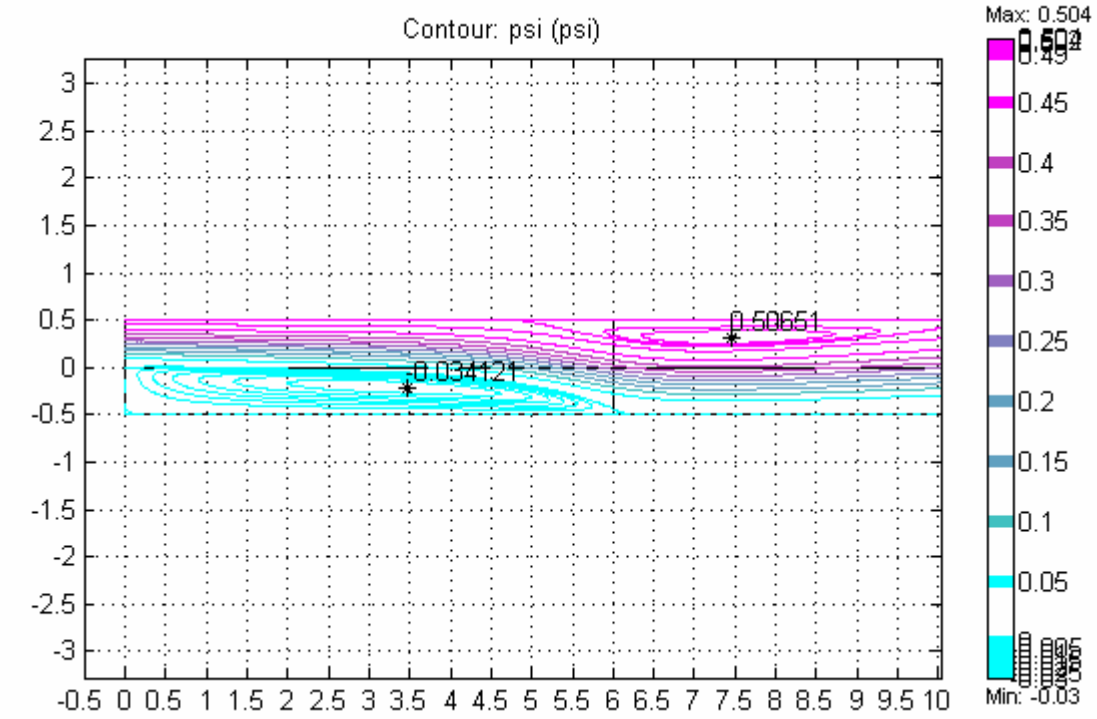

Figure 13. Streamline contours for backward-facing step at Re=800. Contour Level: -0.030, -0.025, -0.020, -0.015, -0.010, -0.005, 0, 0.050, 0.100, 0.150, 0.200, 0.250, 0.300, 0.350, 0.400, 0.450, 0.490, 0.500, 0.504.

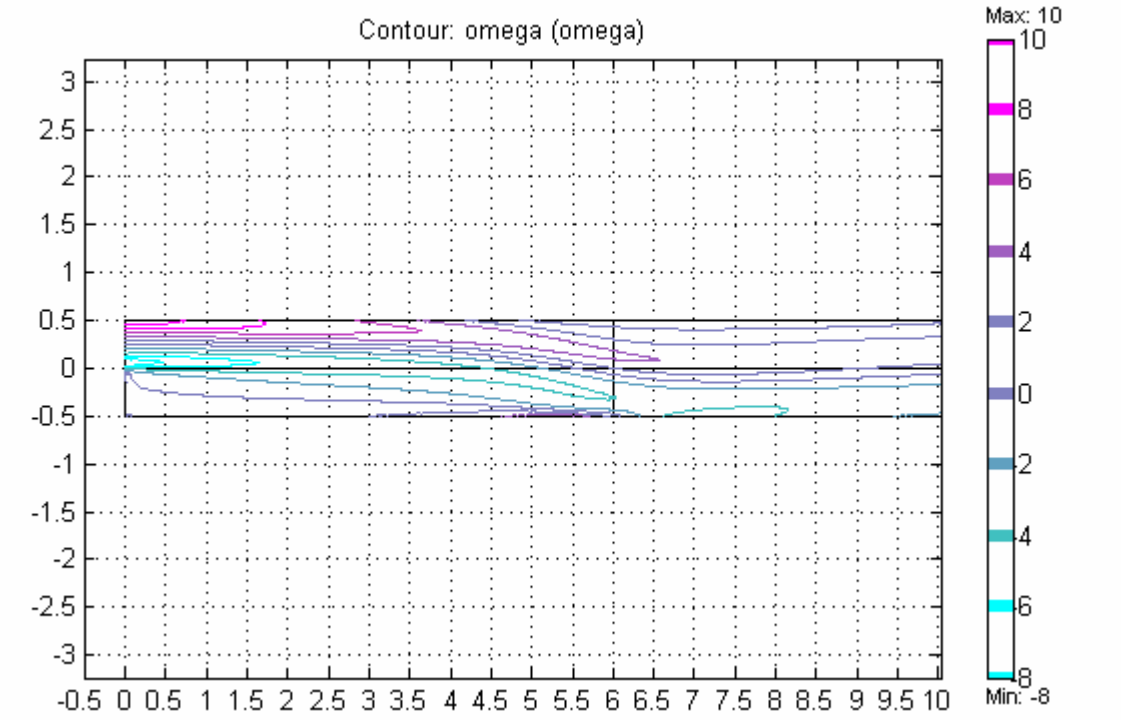

Figure 14. Vorticity contours for backward-facing step at Re=800
Contour level: -8, -6, -4, -2, 0, 2, 4, 6, 8, 10.

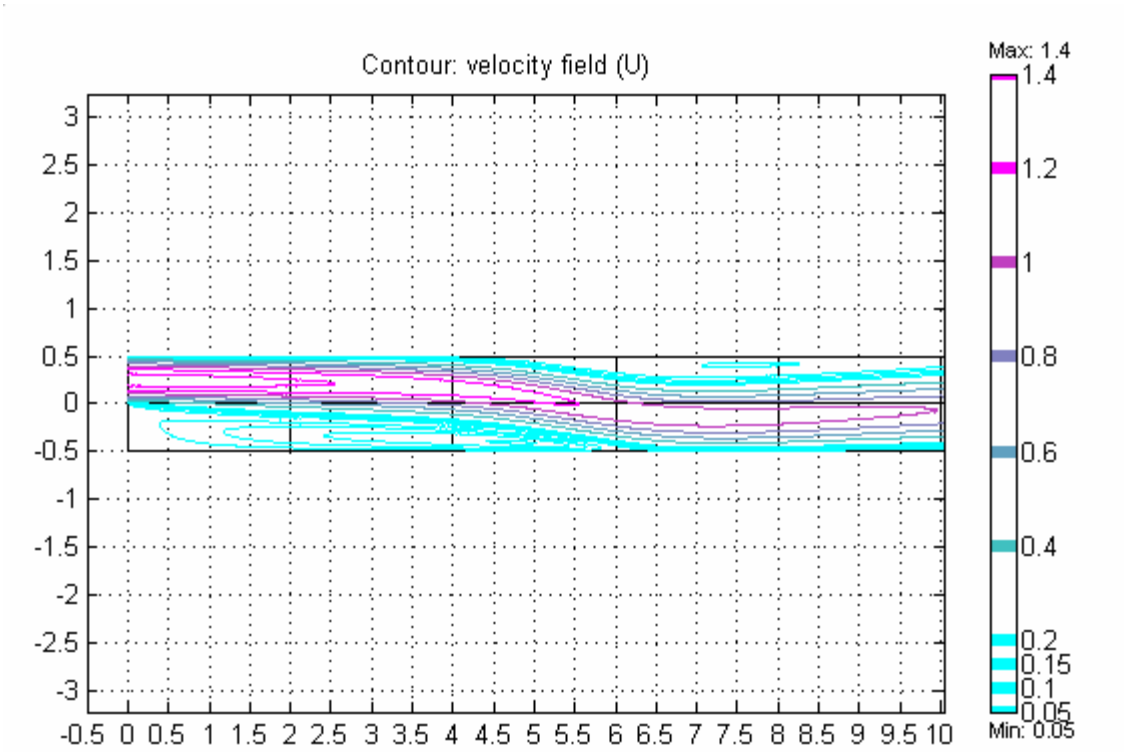

Figure 15. Velocity contours for backward-facing step at Re=800
Contour level: 0.05, 0.10, 0.15, 0.20, 0.40, 0.60, 0.80, 1.00, 1.20, 1.40.

Table 2. Comparison of the proven results with Femlab results of lower wall eddy for backward-facing step

	Vortex center (x,y)	Stream function at vortex center	Vorticity at vortex center	Length of recirculation region
Armaly et al.	(3.350, -0.200)	-0.0342	-2.283	6.10
Current	(3.480, -0.208)	-0.0341	-2.251	6.09

Table 3. Comparison of the proven results with Femlab results of upper wall eddy for backward-facing step

	Vortex center (x,y)	Stream function at vortex center	Vorticity at vortex center	Separation point (x,y)	Reattachment point (x,y)	Length of recirculation region
Armaly et al.	(7.400, 0.300)	0.5064	1.322	(4.85, 0.50)	(10.48, 0.50)	5.63
Current	(7.460, 0.313)	0.5065	1.181	(4.86, 0.50)	(10.50, 0.50)	5.64

CHAPTER 5

SIMULATION AND PARAMETER STUDIES

Introduction

In the LANL, the chemical etching method is applied to polish the inner surface of the niobium cavity. The etching fluid consists of Nitric Acid, Hydrofluoric Acid and Phosphoric Acid (Table 4). The circulating acids interact with the interior surface. During this process, a pipe with baffles is inserted into the cavity to direct the fluid along its inner surfaces. Using FEMLAB, this original case is first simulated to study the performance of the etching process.

Table 4. Chemical Composition of the Etching Fluid

Ratio (by Volume)	Acid	Reagent Grade
1	Nitric Acid (HNO_2)	(69-71%)
1	Hydrofluoric Acid (HF)	(48%)
2	Phosphoric Acid (H_2PO_4)	(85%)

From the fluid mechanics point of view, the parameter studies are also completed, by changing the sizes and location of the baffle.

A performance index (PI), using two variables, is defined to evaluate the performance of surface polishing. Based on the performance index, the results are compared and the optimum performance is obtained in this way.

The Simulation Of The Original Baffle Design Case

Etching fluid parameter

For the etching fluid, the values of density (ρ) and viscosity (μ) are shown below:

ρ = 1532 kg/m^3

μ = 0.0221 kg/ms

Reynolds number

$$\mathrm{Re} = \frac{\rho V D}{\mu} = \frac{1532 kg/m^3 \cdot 0.0475 m/s \cdot 0.127 m}{0.0221 kg/m \cdot s} = 418.18$$

so the flow is a laminar flow for the original baffle design. For all the other cases we will study next, since all the coefficients relative to Reynolds number are not changed, they are also laminar flows.

Niobium cavities geometry

Since the niobium cavities are axisymmetric, we could study half of the geometry instead of the whole geometry.

Half of the geometry of the niobium cavity with the baffle is shown in Figure 16. There is an internal line close to the inner surface. It is created to assess the performance index. In the next section it will be explained in more detail.

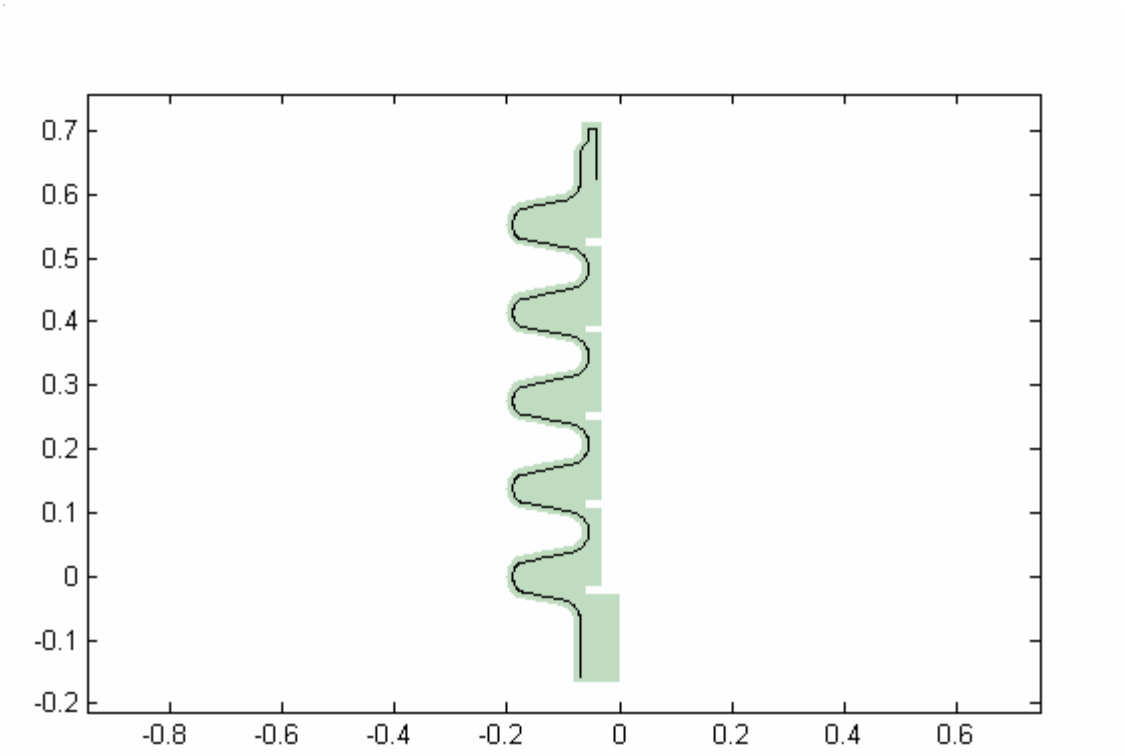

Figure 16. The half geometry with the baffle

The boundary conditions

The flow comes in from the bottom inlet and comes out of the small hole at the end of the baffle pipe. The top of the cavity is closed. At the inlet, z-direction velocity is a parabolic function $v_z = 0.09505(2s\text{-}s^2)$ and r-direction velocity is zero. At the outlet, the pressure is considered as zero. At the surface of the cavity and the baffle, the boundary condition is no slip.

The mesh

The mesh shown in Figure 17 consists of 9475 triangular elements. The geometry has the properties of a narrow flow area near the baffle and a relatively small flow outlet area. Considering the specific geometry, the dense mesh is given around the area mentioned above.

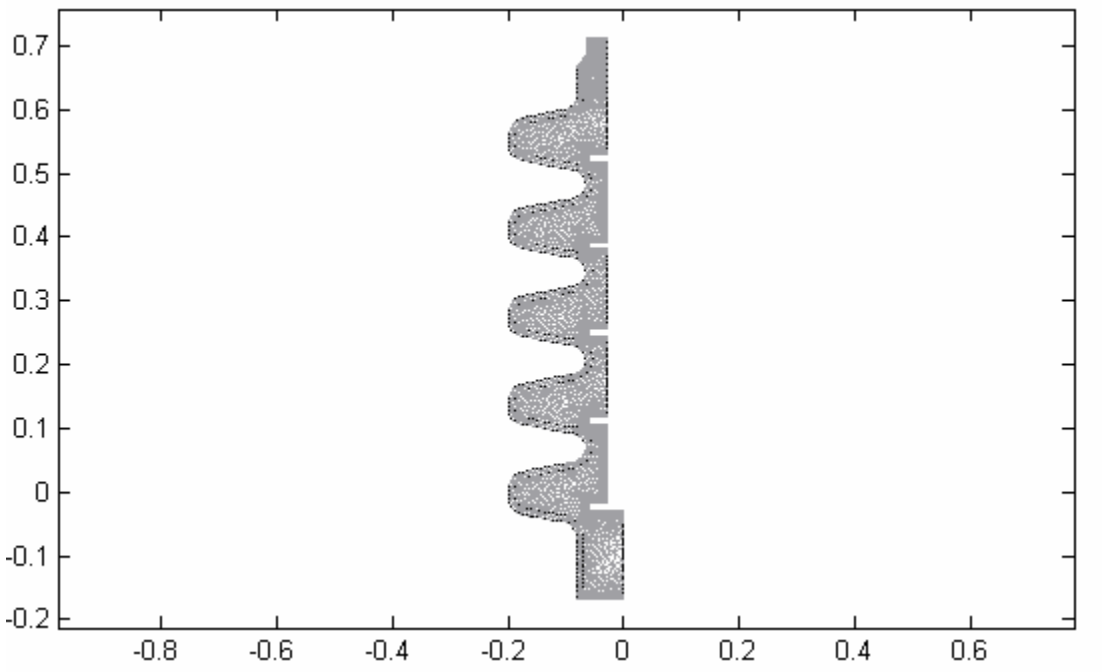

Figure 17. The mesh for the half geometry

Flow line

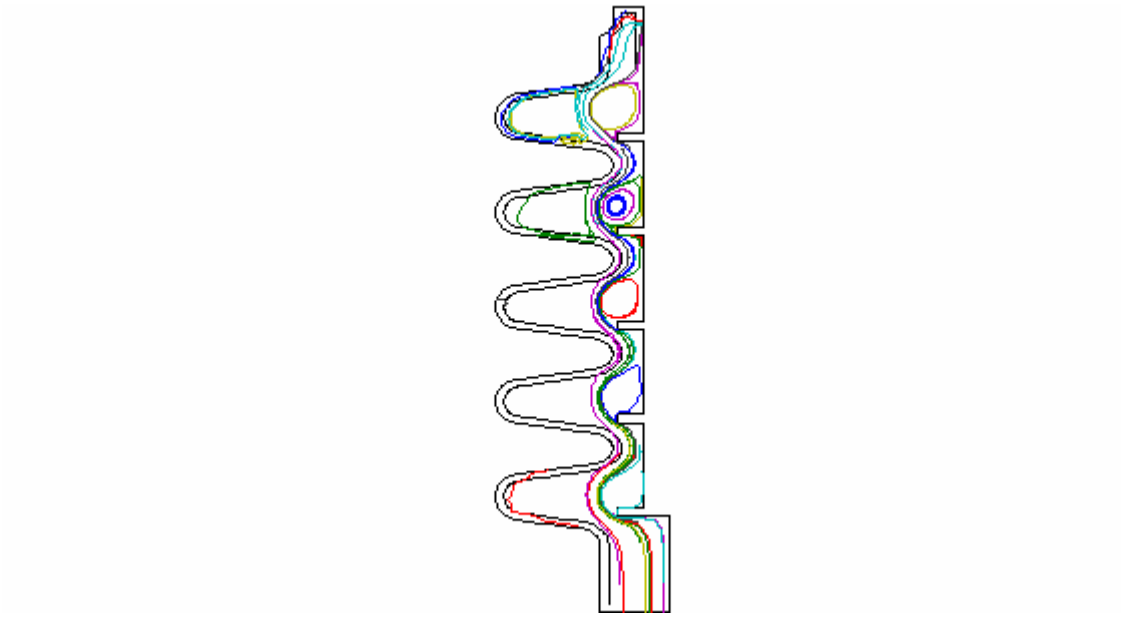

Figure 18. Flow line plot for the original design

Velocity Contour

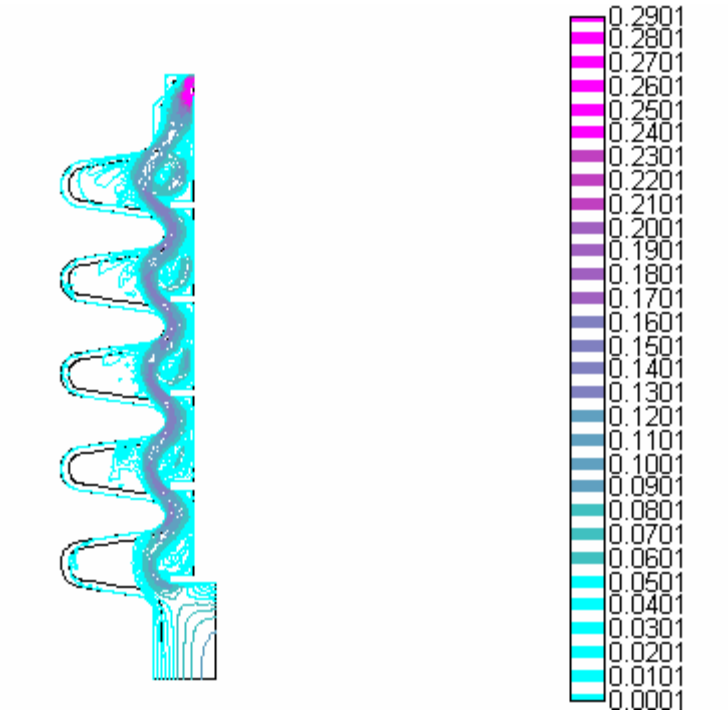

Figure 19. The velocity contour for the original design

The Performance Index Of The Original Baffle Design

Performance Index

As shown in Figure 16, the Internal line, a little gap away from the wall, is created for the convenience of the performance index. The line is a combination of the inlet segment, the outlet segment and the cavity segments. Each cavity is divided into six vertical segments (Figure 20), beginning from the bottom with segment 1, and continuing up through segment 2, 3, 4, 5 and 6.

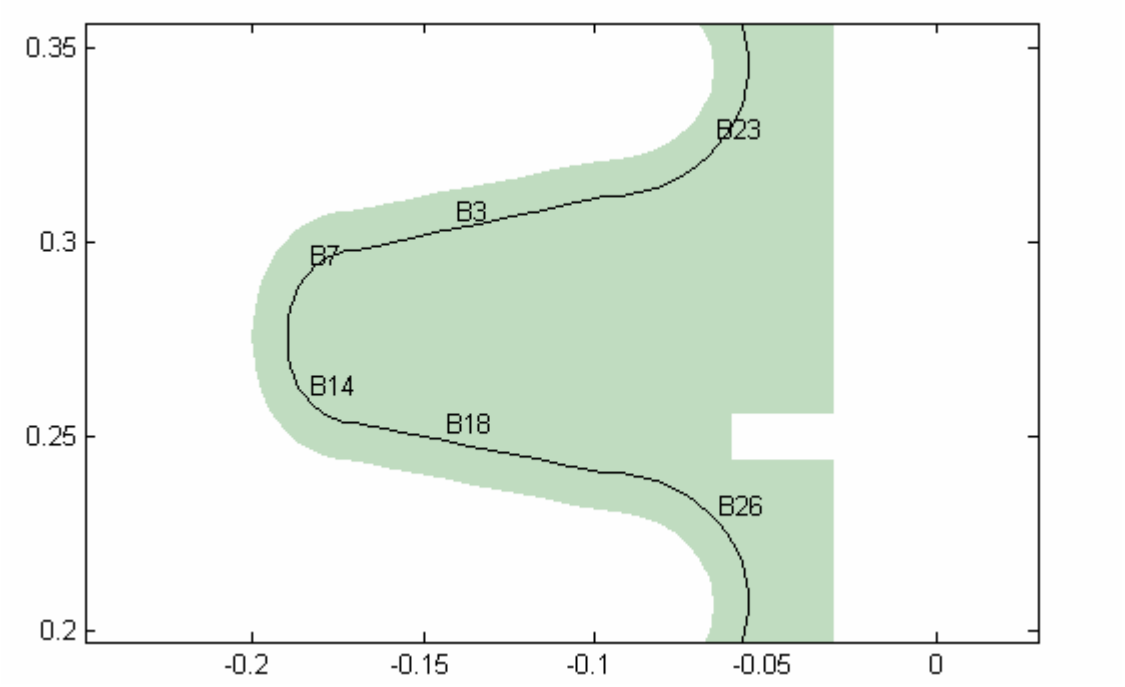

Figure 20. One cavity with the six inner segments

Performance index is defined using two variables:

$$V = \frac{\sum_{i=1}^{n} \frac{\int vds}{\int ds}}{n}$$

$$SDV = \frac{\sum_{i=1}^{n} \left[\frac{\int vds}{\int ds} - V \right]^2}{nV}$$

The first variable V describes the average velocity along the inner line; the second variable SDV defines its standard deviation. The optimum baffle design is acquired by maximizing the first variable and minimizing the second variable.

The results of the original design case (Table 5)

In table 5, the cavity cells are counted from the bottom to the top in the ascending order, so cavity cell 1 is the bottom cavity cell and the cavity cell 5 is the top cavity cell.

From the table, it is obvious that for every cavity the bottom iris (segment 1) and And the top iris (segment 6) have larger velocity. For the original design, V and SDV are 0.0482 and 0.2422 m/s respectively.

Table 5. The performance index of the original design case

Segment		Average Velocity (m/s)
Cavity Cell 1	Segment 1	0.0272
	Segment 2	0.0015
	Segment 3	0.0001
	Segment 4	0.0001
	Segment 5	0.0046
	Segment 6	0.1457
Cavity Cell 2	Segment 1	0.1326
	Segment 2	0.0061
	Segment 3	0.0015
	Segment 4	0.0011
	Segment 5	0.0147
	Segment 6	0.1751
Cavity Cell 3	Segment 1	0.1399
	Segment 2	0.0045
	Segment 3	0.0005
	Segment 4	0.0004
	Segment 5	0.0141
	Segment 6	0.1793
Cavity Cell 4	Segment 1	0.1459
	Segment 2	0.0044
	Segment 3	0.0003
	Segment 4	0.0005
	Segment 5	0.0161
	Segment 6	0.1871
Cavity Cell 5	Segment 1	0.1581
	Segment 2	0.0098
	Segment 3	0.0030
	Segment 4	0.0032
	Segment 5	0.0293
	Segment 6	0.0861
Inlet		0.0252
Outlet		0.0237
V		0.0482
SDV		0.2422

Parameter Studies

For getting the optimum baffle design, we choose five variables (Figure 21) representing the size and location of the baffle as the parameters and simulate the different baffle designs by changing the parameters.

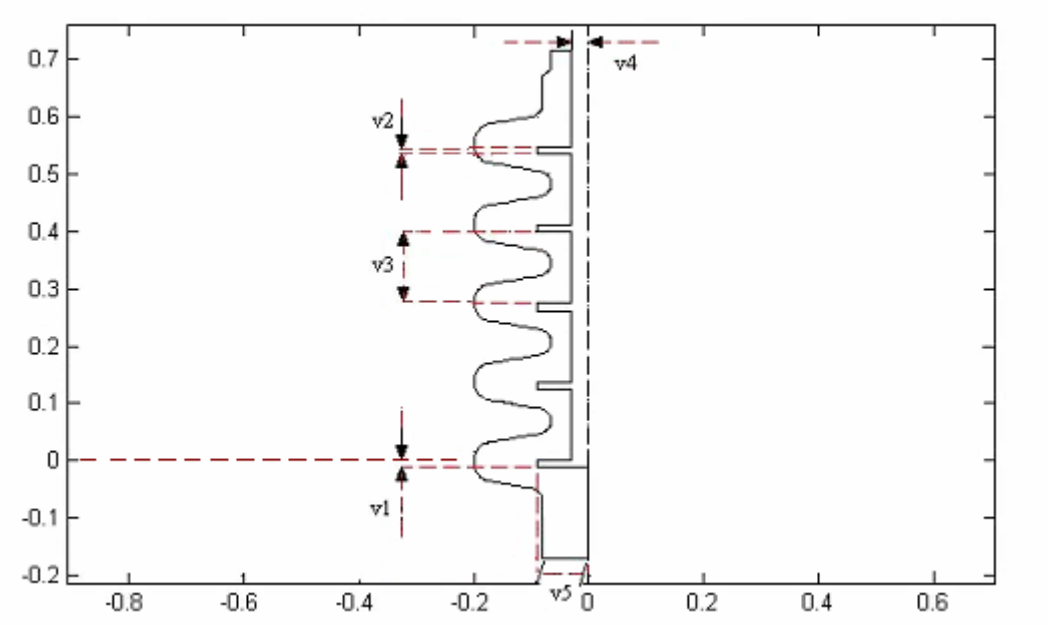

Figure 21. Niobium cavity with five parameters labeled

The parameters

In Figure 21, the parameters (the variables) are defined as

v1: location of the baffle (relative to the location y coordinate is 0)

v2: thickness of the baffle

v3: spacing between baffles

v4: radius of the pipe

v5: radius of the baffle

Parameter study 1

12 cases (Table 6) are studied. For each case, one parameter is changed from the original design. The simulation results are shown in flow line plots and velocity contours in Figures 22 through 45. The performance indexes are listed in Table 7.

Table 6. The cases of parameter study 1

	v1	v2	v3	v4	v5
Original Design	-0.03	0.012	0.125	0.03	0.06
Case 1	-0.006	0.012	0.125	0.03	0.06
Case 2	0	0.012	0.125	0.03	0.06
Case 3	0.03	0.012	0.125	0.03	0.06
Case 4	-0.03	0.009	0.125	0.03	0.06
Case 5	-0.03	0.015	0.125	0.03	0.06
Case 6	-0.03	0.012	0.135	0.03	0.06
Case 7	-0.03	0.012	0.125	0.02	0.06
Case 8	-0.03	0.012	0.125	0.04	0.06
Case 9	-0.03	0.012	0.125	0.03	0.04
Case 10	-0.03	0.012	0.125	0.03	0.05
Case 11	-0.03	0.012	0.125	0.03	0.07
Case 12	-0.03	0.012	0.125	0.03	0.08

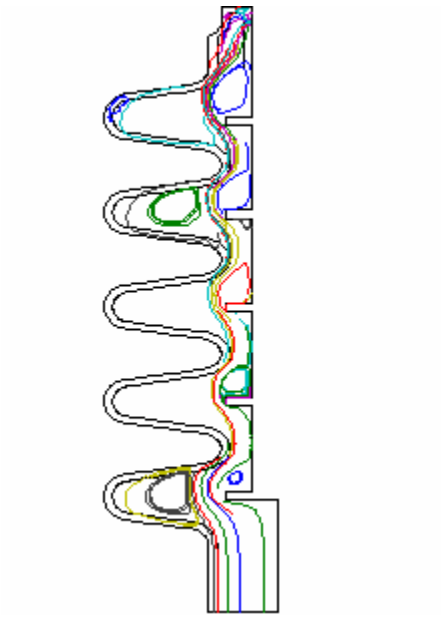

Figure 22. Flow line plot for case 1 (v1=-0.006) of parameter study 1

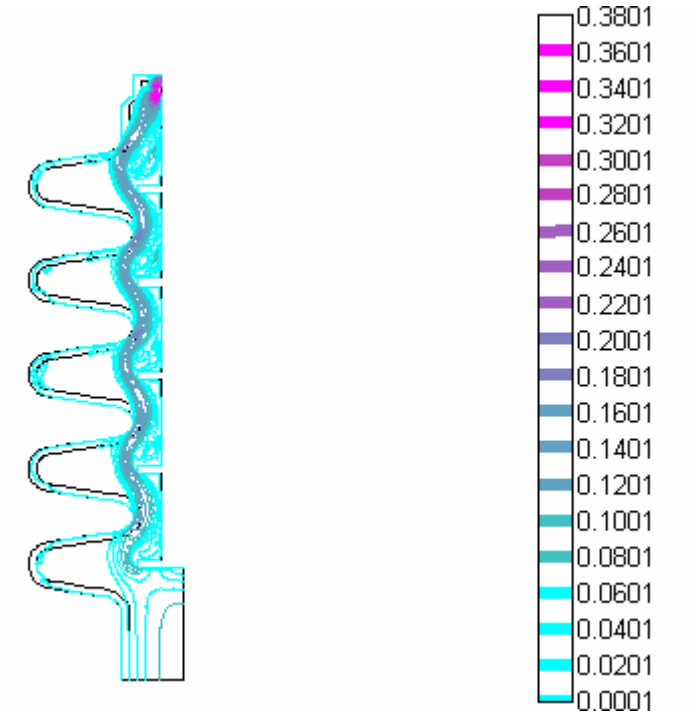

Figure 23. Velocity contour for case 1(v1=-0.006) of parameter study 1

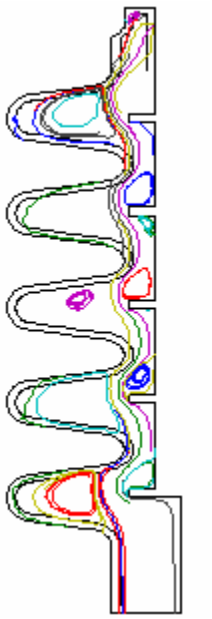

Figure 24. Flow line plot for case 2 (v1=0) of parameter study 1

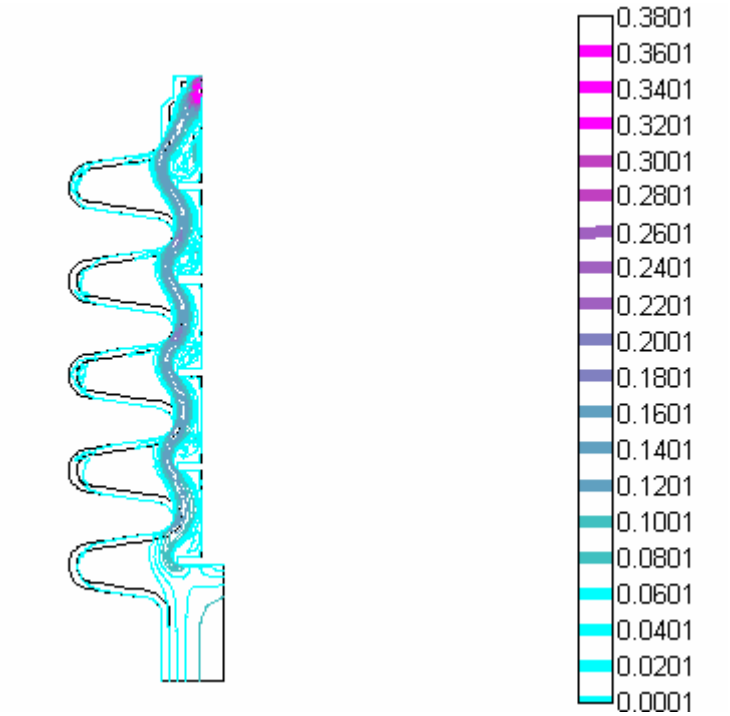

Figure 25. Velocity contour for case 2 (v1=0) of parameter study 1

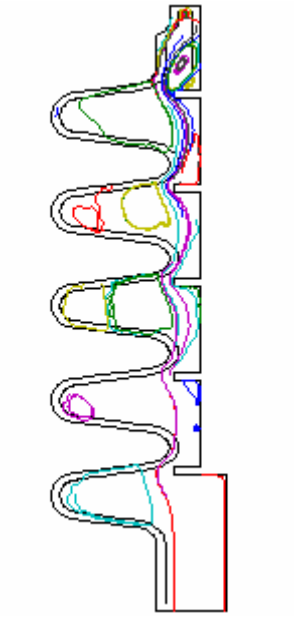

Figure 26. Flow line plot for case 3 (v1=0.03) of parameter study 1

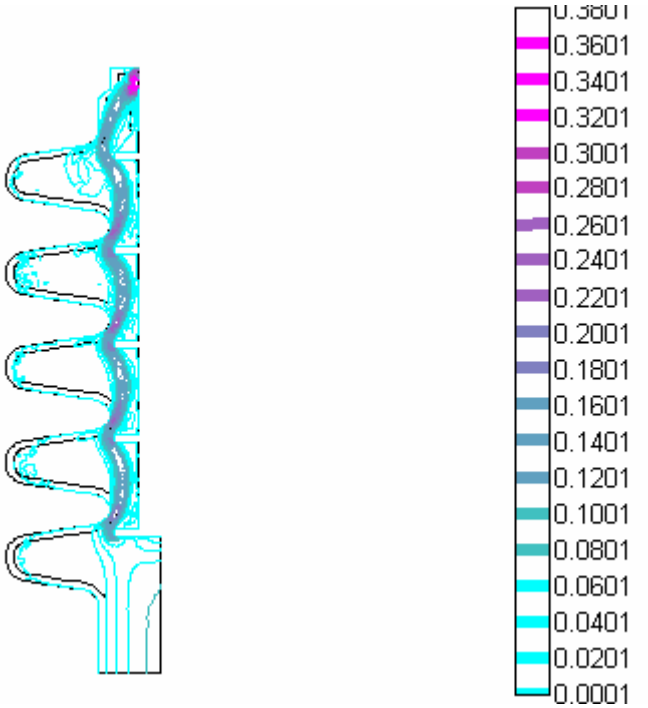

Figure 27. Velocity contour for case 3 (v1=0.03) of parameter study 1

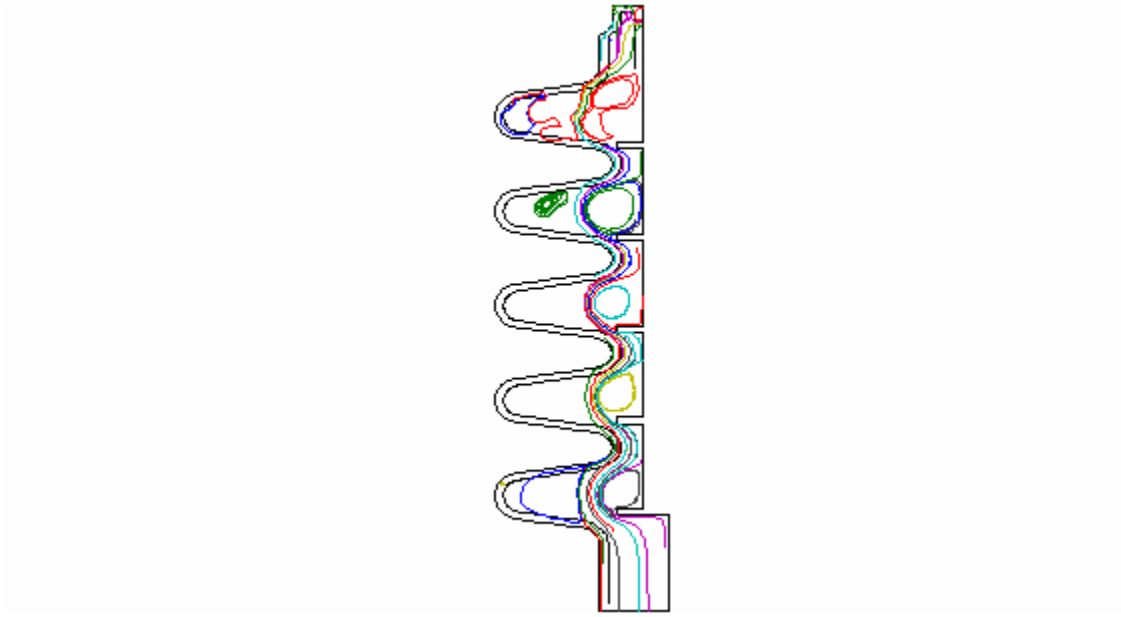

Figure 28. Flow line plot for case 4 (v2=0.009) of parameter study 1

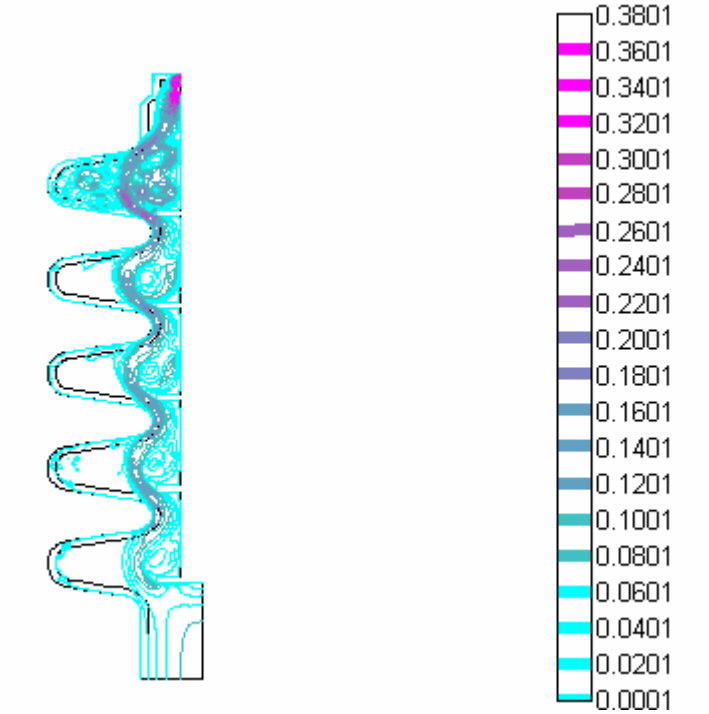

Figure 29. Velocity contour for case 4 (v2=0.009) of parameter study 1

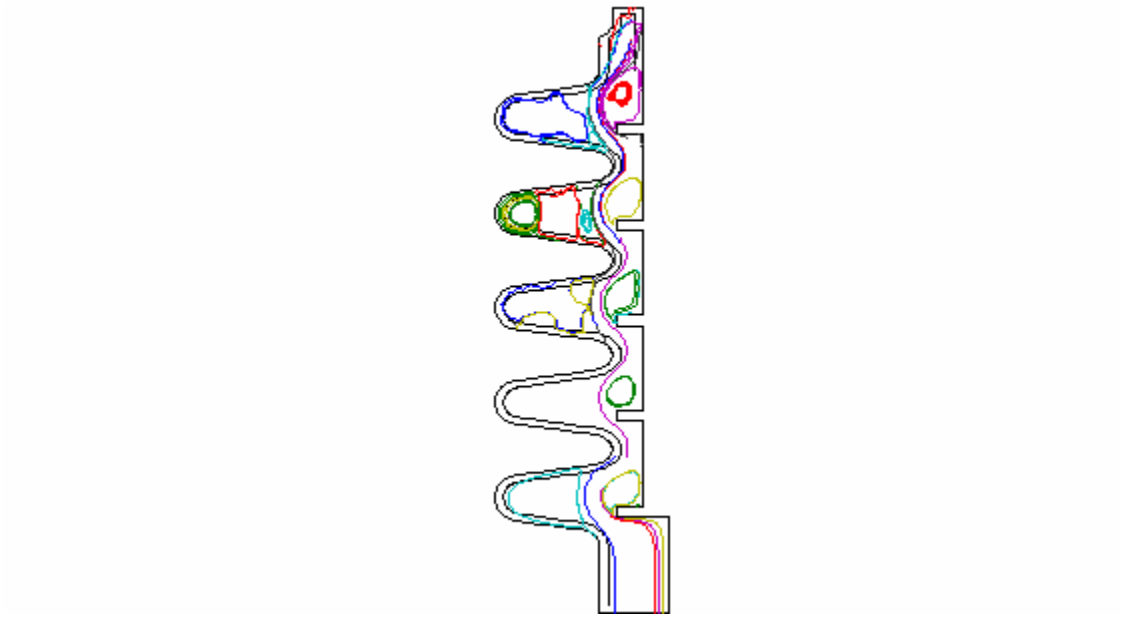

Figure 30. Flow line plot for case 5 (v2=0.015) of parameter study 1

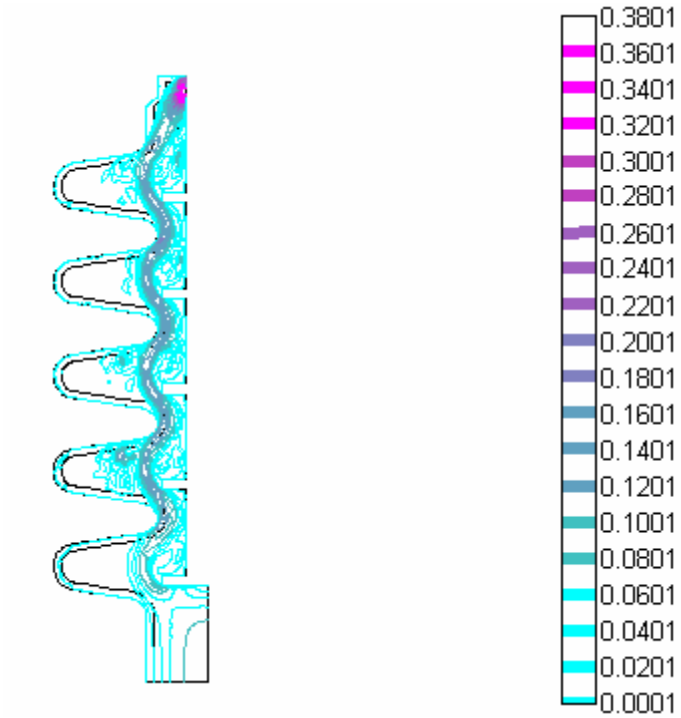

Figure 31. Velocity contour for case 5 (v2=0.015) of parameter study 1

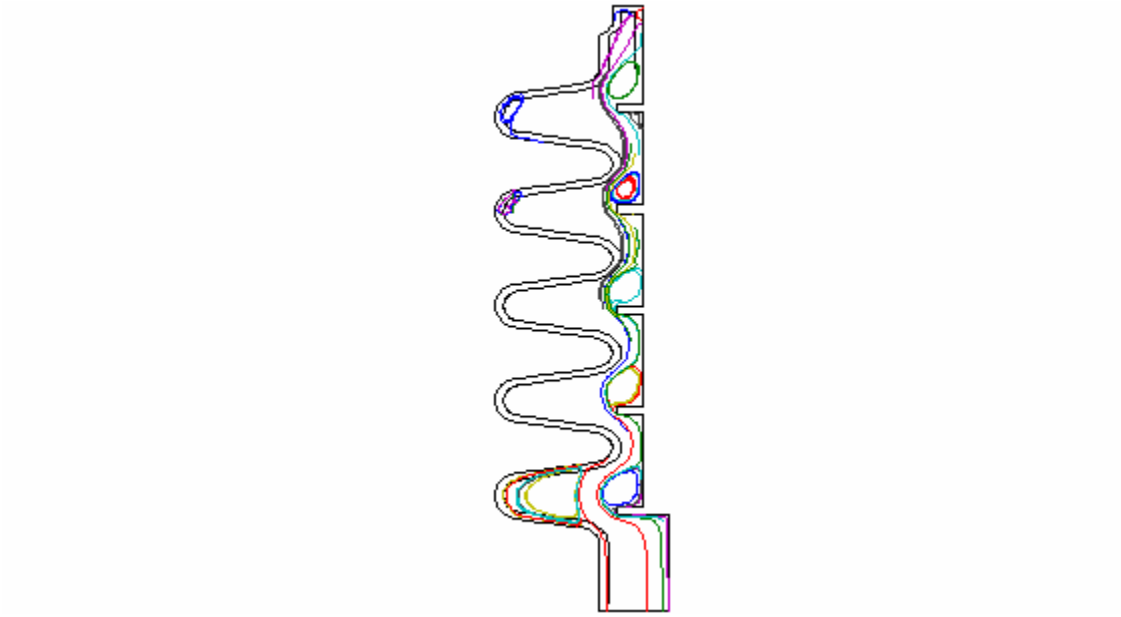

Figure 32. Flow line plot for case 6 (v3=0.135) of parameter study 1

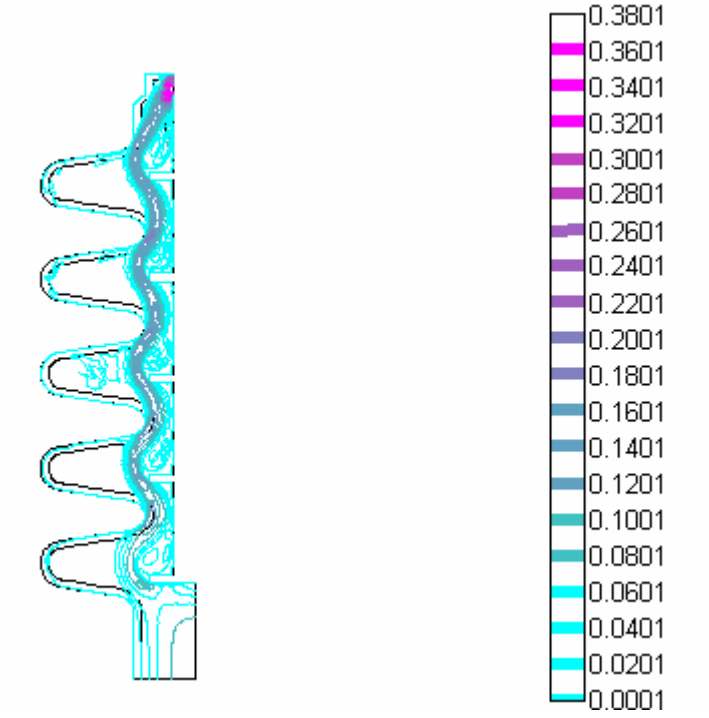

Figure 33. Velocity contour for case 6 (v3=0.135) of parameter study 1

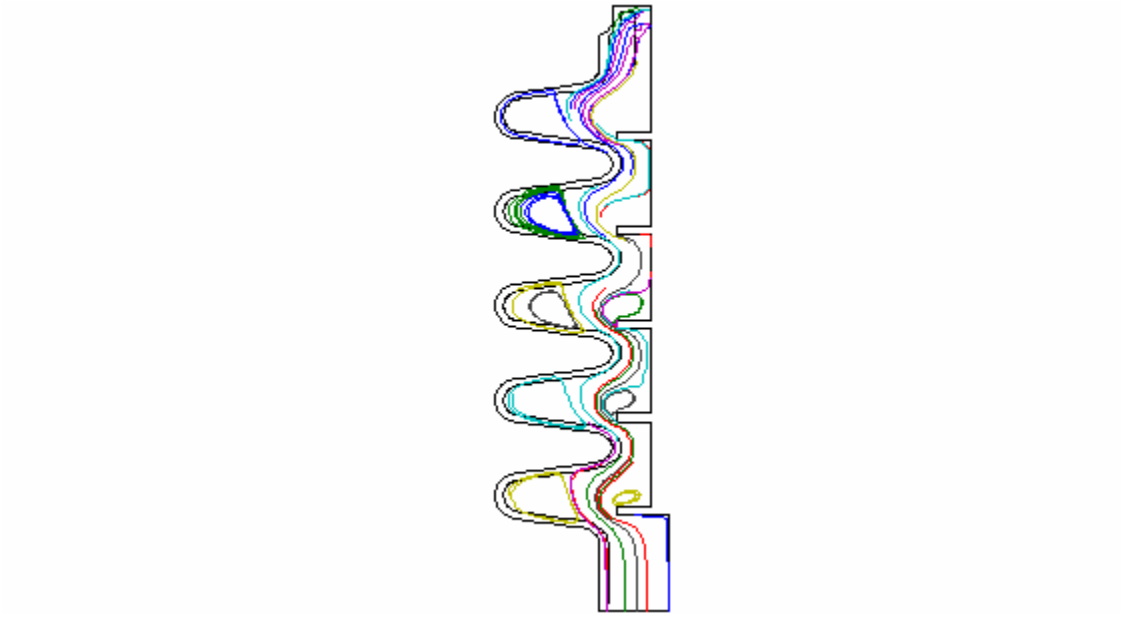

Figure 34. Flow line plot for case 7 (v4=0.02) of parameter study 1

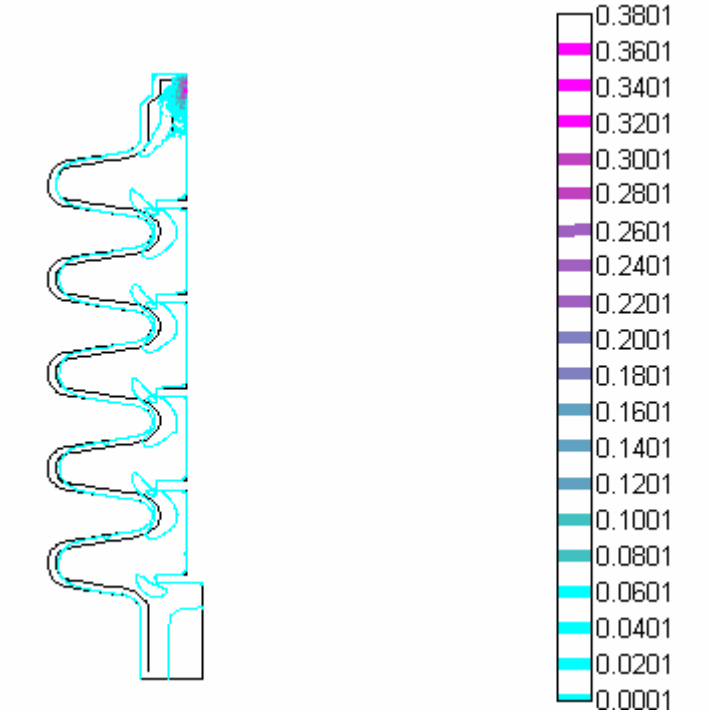

Figure 35. Velocity contour for case 7 (v4=0.02) of parameter study 1

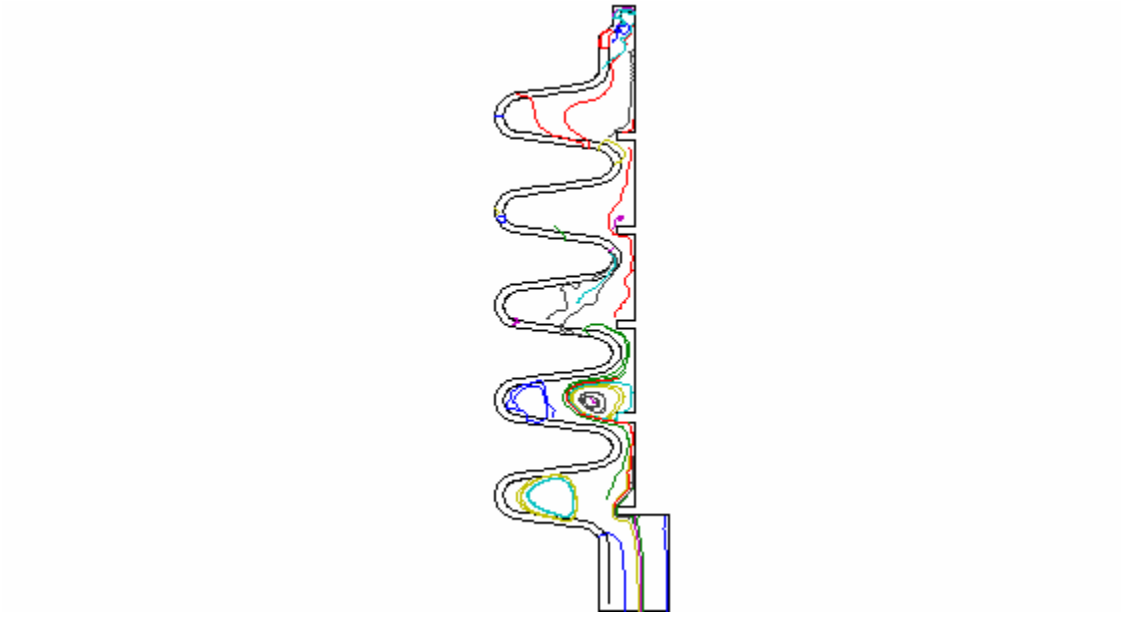

Figure 36. Flow line plot for case 8 (v4=0.04) of parameter study 1

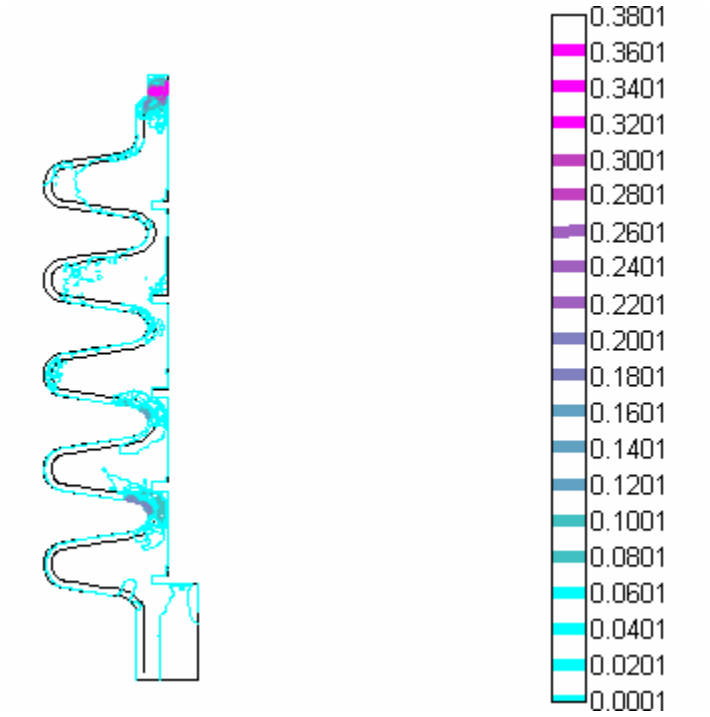

Figure 37. Velocity contour for case 8 (v4=0.04) of parameter study 1

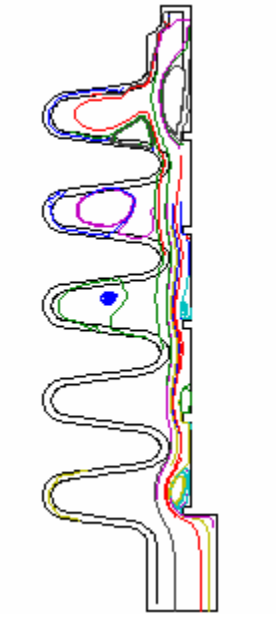

Figure 38. Flow line plot for case 9 (v5=0.04) of parameter study 1

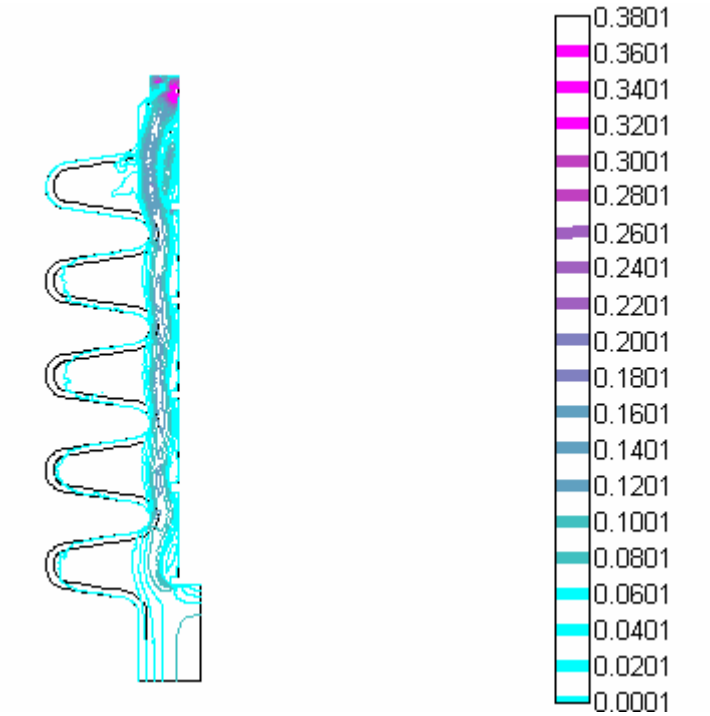

Figure 39. Velocity contour for case 9 (v5=0.04) of parameter study 1

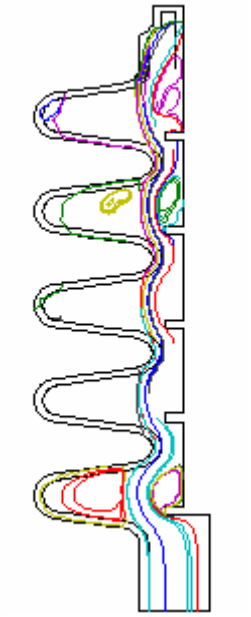

Figure 40. Flow line plot for case 10 (v5=0.05) of parameter study 1

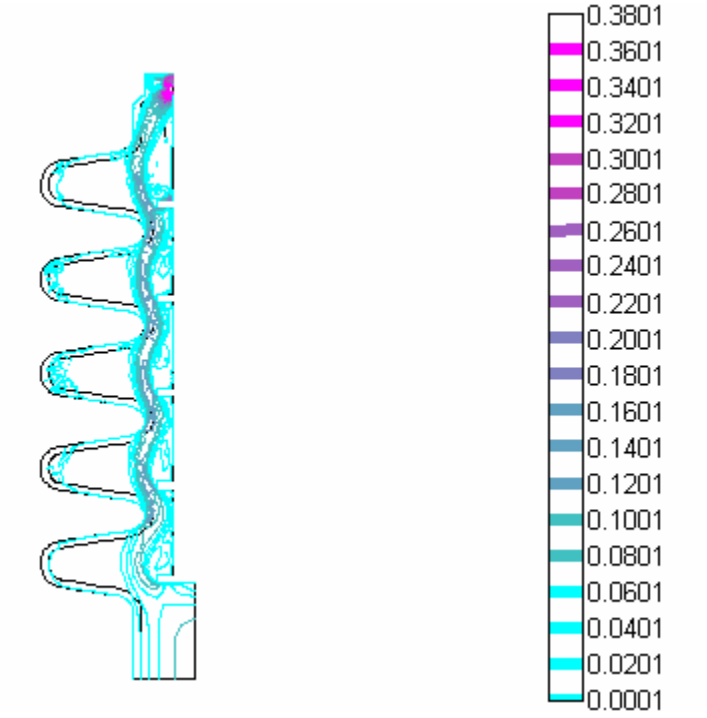

Figure 41. Velocity contour for case 10 (v5=0.05) of parameter study 1

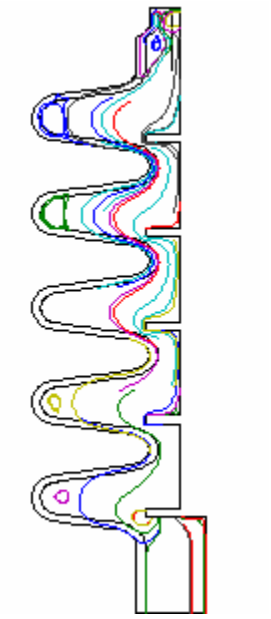

Figure 42. Flow line plot for case 11 (v5=0.07) of parameter study 1

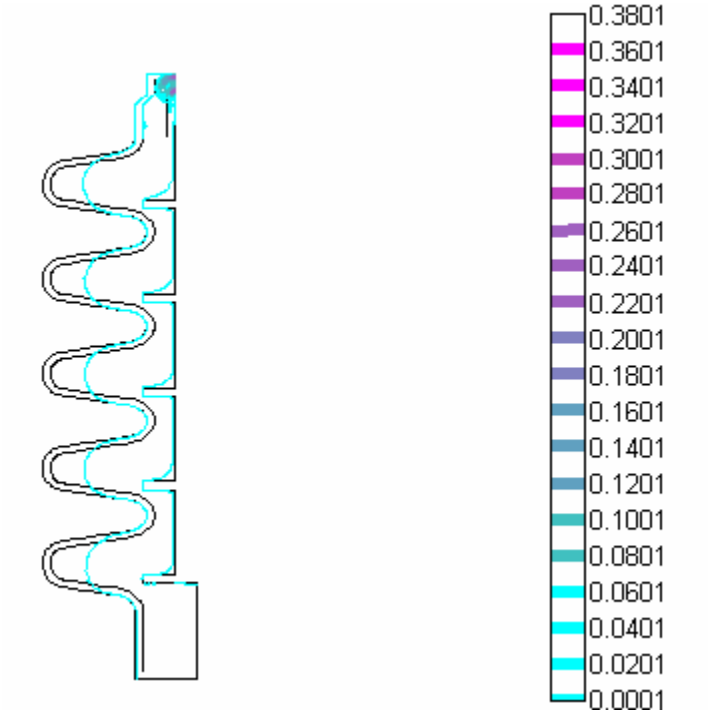

Figure 43. Velocity contour for case 11 (v5=0.07) of parameter study 1

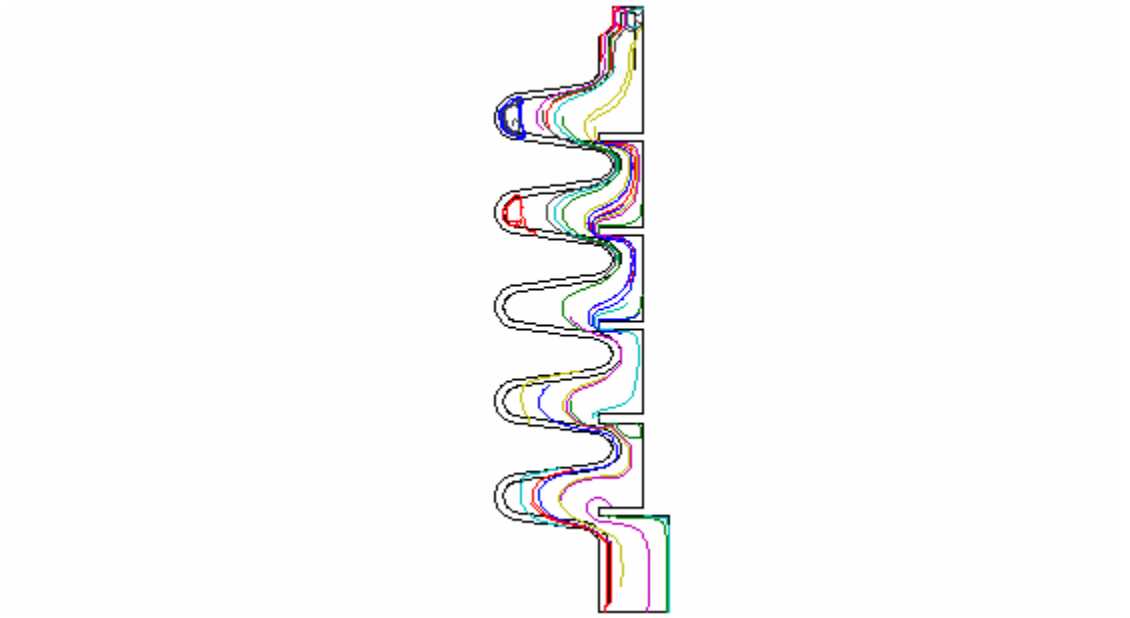

Figure 44. Flow line plot for case 12 (v5=0.08) of parameter study 1

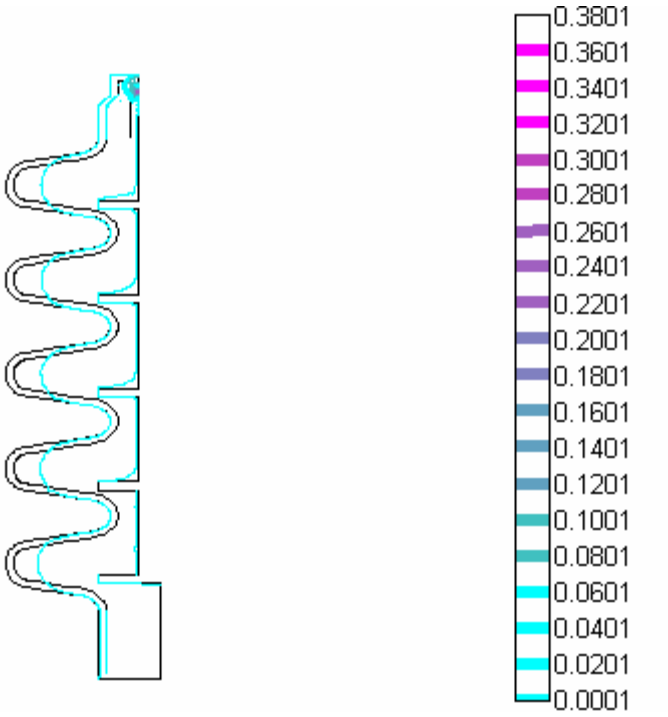

Figure 45. Velocity contour for case 12 (v5=0.08) of parameter study 1

Table 7. The performance indexes for the parameter study 1

Case	Parameter	V	SDV
Original Design		0.0482	0.2422
Case 1	v1=-0.006	0.0405	0.2685
Case 2	v1=0	0.0407	0.2697
Case 3	v1=0.03	0.0429	0.2702
Case 4	v2=0.009	0.0617	0.2381
Case 5	v2=0.015	0.0463	0.2432
Case 6	v3=0.135	0.0415	0.2558
Case 7	v4=0.02	0.0120	0.2557
Case 8	v4=0.04	0.0206	0.3500
Case 9	v5=0.04	0.0268	0 .2412
Case 10	v5=0.05	0.0330	0.2475
Case 11	v5=0.07	0.0023	0.2665
Case 12	v5=0.08	0.0023	0.2751

From the Table 7, we can see

- For the first three cases, the average velocities are a little lower than that of the original design, and the standard deviations increase when the baffle is moving up.
- In cases 4 and 5, the thickness of the baffle is adjusted. When the value of v2 is small (v2=0.009), a better design than the original one is produced.
- Case 6 is not good design since V becomes less and SDV larger compared to the original case.
- For cases 7 and 8, we get relatively smaller velocities.
- For the last four cases, the radius of the baffle, which is very important to direct the flow along the inner surface is the variable to study. The

performances are not improved. In the last two cases, the velocities are the lowest among all 12 cases.

Parameter study 2

In this parameter study (Table 8), the location of the baffle is fixed to the centerline of the cavities. This means v1 is -0.006. The radius of the baffle is increased from 0.04 m to 0.08 m. The simulation results are shown in Figures 46 through 51. The performance indexes are listed in Table 9.

Table 8. The cases of parameter study 2

Case	v1	v2	v3	v4	v5
Original Design	-0.030	0.012	0.125	0.03	0.06
Case 1(study 1)	-0.006	0.012	0.125	0.03	0.06
Case 1	-0.006	0.012	0.125	0.03	0.04
Case 2	-0.006	0.012	0.125	0.03	0.05
Case 3	-0.006	0.012	0.125	0.03	0.08

Figure 46. Flow line plot for case 1 (v1=-0.006, v5=0.04) of parameter study 2

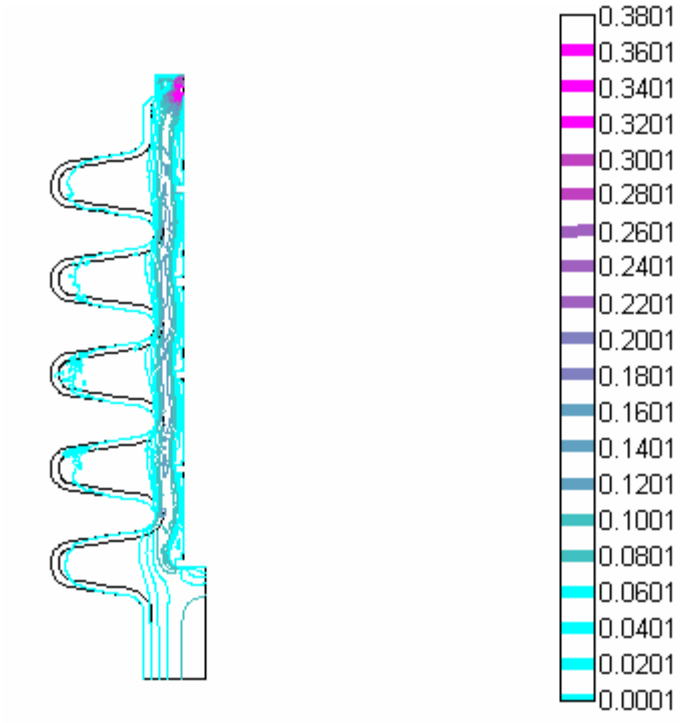

Figure 47. Velocity contour for case 1(v1=-0.006, v5=0.04) of parameter study 2

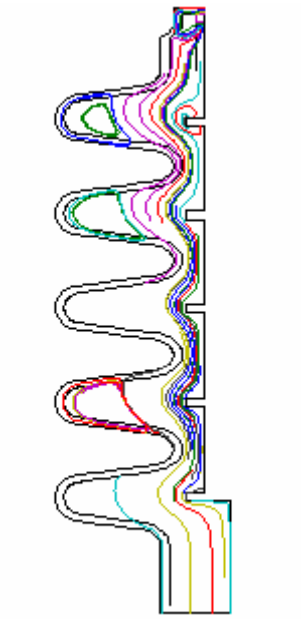

Figure 48. Flow line plot for case 2 (v1=-0.006, v5=0.05) of parameter study 2

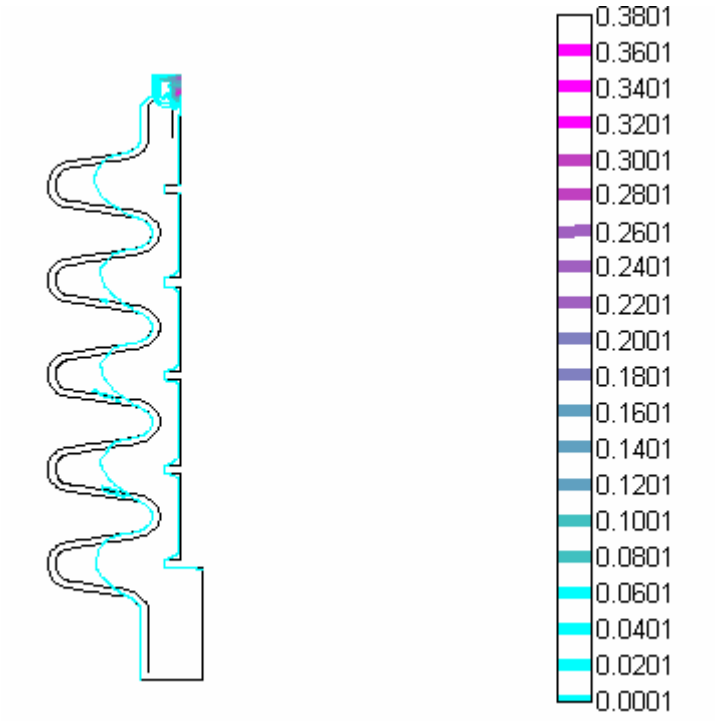

Figure 49. Velocity contour for case 2 (v1=-0.006, v5=0.04) of parameter study 2

Figure 50. Flow line plot for case 3 (v1=-0.006, v5=0.04) of parameter study 2

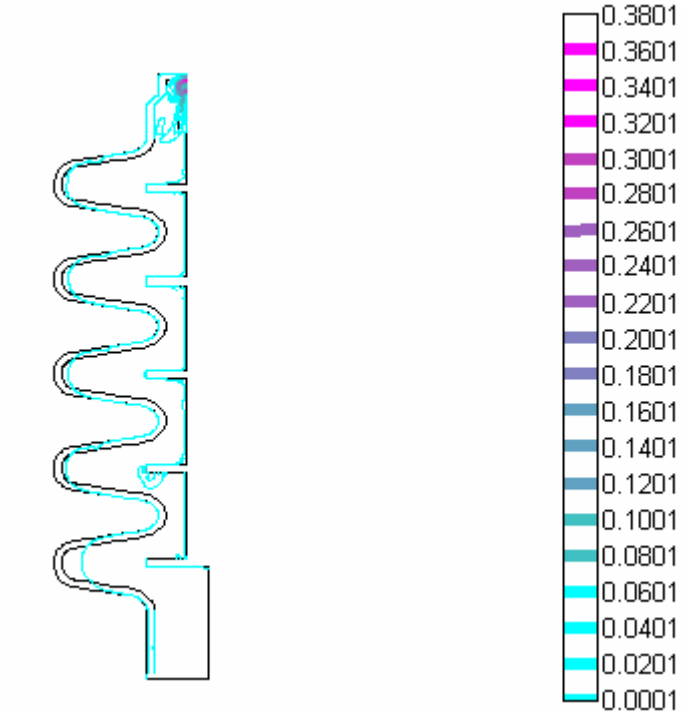

Figure 51. Velocity contour for case 3(v1=-0.006, v5=0.04) of parameter study 2

Table 9. The performance indexes for the parameter study 2

Case	Parameter	V	SDV
Original Design	v1=-0.030 v5= 0.060	0.0482	0.2422
Case 1(study 1)	v1=-0.006 v5= 0.060	0.0405	0.2685
Case 1	v1=-0.006 v5= 0.040	0.0225	0.2696
Case 2	v1=-0.006 v5= 0.050	0.0030	0.2614
Case 3	v1=-0.006 v5= 0.080	0.0045	0.2101

From the Table 9, we can observe that case 3 has the lowest SDV but the average velocity is very slow, and the original design has the largest velocity in the parameter study 2.

CHAPTER 6

CONCLUSIONS

From all the simulations and parametric studies, we conclude the baffle radius (v5) and baffle location (v1) variables play a very important role when compared to the other variables. The baffle radius is a more sensitive variable; it should be optimized so that it guides the fluid to the inner surface of the cavity.

We get one case, in which the thickness of baffle is reduced (case 4 of study 1), satisfied with lower standard deviation and higher velocity when comparing all cases with the original design case. That is the optimum design among all cases.

If possible, the experiments should be done to check all the theoretical simulations. 3-D analyses and simulations are recommended for further studies.

APPENDIX A

THE FEMLAB PROGRAM CODE FOR THE PARAMETER STUDIES

The FEMLAB code (.m file)

```
%  FEMLAB Model M-file
% Generated 17-Oct-2001 15:50:41 by FEMLAB 2.2.0.125.
% This file parameterize the geometry of the baffle
%v(1)   location of the baffle
%v(2)   thickness of the baffle
%v(3)   spacing between baffles
%v(4)   radius of the pipe
%v(5)   radius of the baffle
v(1)=-0.006*5;
v(2)=0.012;
v(3)=0.125;
v(4)=0.03;
v(5)=0.06;

flclear fem
% FEMLAB Version
```

```
clear vrsn;
vrsn.name='FEMLAB 2.2';
vrsn.major=0;
vrsn.build=125;
fem.version=vrsn;

% Recorded command sequence

% New geometry 1
fem.sdim={'r','z'};

% Geometry
clear s c p
p=[-0.200 -0.200 -0.200  ...
-0.200 -0.200 -0.200  ...
-0.200 -0.200 -0.200  ...
-0.200 -0.200 -0.200  ...
-0.200 -0.200 -0.200  ...
-0.172 -0.172 -0.172  ...
-0.172 -0.172 -0.172  ...
-0.172 -0.172 -0.170  ...
-0.170 -0.112 -0.112 -0.098  ...
-0.098 -0.098 -0.098  ...
```

-0.098 -0.098 -0.098 ...

-0.098 -0.080 -0.080 ...

-0.080 -0.080 -0.080 ...

-0.080 -0.065 -0.065 ...

-0.065 -0.065 -0.065 ...

-0.065 -0.065 -0.065 ...

-0.065 -0.065 -0.065 ...

-0.065 -0.065 -0.065 ...

-v(5) -v(5) -v(5) ...

-v(5) -v(5) -v(5) ...

-v(5) -v(5) -v(5) ...

-v(5) -v(4) -v(4) ...

-v(4) -v(4) -v(4) ...

-v(4) -v(4) -v(4) ...

-v(4) -v(4) -v(4) ...

-v(4) -v(4) 0 0 0;

-0.036 0.0 0.0320 ...

0.106 0.138 0.170 ...

0.244 0.276 0.308 ...

0.382 0.414 0.446 0.52 ...

0.552 0.588 0.0320 0.106 ...

0.170 0.244 0.308 0.382 ...

0.446 0.52 -0.036 ...

```
0.588 -0.046 0.598  ...
0.045 0.093 0.183 0.231  ...
0.321 0.369 0.459  ...
0.507 -0.169 -0.070  ...
-0.046 0.599 0.621 0.670  ...
0.045 0.0699 0.093 0.183  ...
0.207 0.231 0.321  ...
0.345 0.369 0.459  ...
0.483 0.507 0.684  ...
0.714 v(1) v(1)+v(2)  v(1)+v(2)+v(3) v(1)+2*v(2)+v(3)  ...
v(1)+2*v(2)+2*v(3) v(1)+3*v(2)+2*v(3) v(1)+3*v(2)+3*v(3)  ...
v(1)+4*v(2)+3*v(3) v(1)+4*v(2)+4*v(3) v(1)+5*v(2)+4*v(3) v(1)  ...
v(1)+v(2) v(1)+v(2)+v(3) v(1)+2*v(2)+v(3) v(1)+2*v(2)+2*v(3)  ...
v(1)+3*v(2)+2*v(3) v(1)+3*v(2)+3*v(3) v(1)+4*v(2)+3*v(3)  ...
v(1)+4*v(2)+4*v(3) v(1)+5*v(2)+4*v(3) 0.684  ...
0.694 0.714 -0.169  ...
-0.069 v(1)];

rb={[2 5 8 11 14 16 17 18 19 20 21 22 23 24 25 26 27 28 29 30 31 32 33 34  ...
35 36 37 40 41 43 46 49 52 54 55 56 57 58 59 60 61 62 63 64 65 66 67 68 69  ...
70 71 72 73 74 75 76 77 78 79 80 81],[16 17 18 19 20 21 22 23 24 25 36 36  ...
40 41 54 55 56 56 57 58 58 59 60 60 61 62 62 63 64 64 65 66 67 69 71 73 75  ...
76 77 79 80;28 29 30 31 32 33 34 35 26 27 37 79 41 54 55 78 57 66 67 59 68  ...
```

69 61 70 71 63 72 73 65 74 75 81 68 70 72 74 76 77 78 80 81],[2 2 5 5 8 8 ...

11 11 14 14 26 27 28 29 30 31 32 33 34 35;3 1 4 6 7 9 10 12 13 15 38 39 42 ...

44 45 47 48 50 51 53;16 24 17 18 19 20 21 22 23 25 37 40 43 43 46 46 49 49 ...

52 52],zeros(4,0)};

wt={zeros(1,0),ones(2,41),[1 1 1 1 1 1 1 1 1 1 1 1 1 1 1 1 1 1 1 1 1; ...

0.70710678118654746 0.70710678118654746 0.70710678118654746 ...

0.70710678118654746 0.70710678118654746 0.70710678118654746 ...

0.70710678118654746 0.70710678118654746 0.70710678118654746 ...

0.70710678118654746 0.70710678118654746 0.70710678118654746 ...

0.70710678118654746 0.70710678118654746 0.70710678118654746 ...

0.70710678118654746 0.70710678118654746 0.70710678118654746 ...

0.70710678118654746 0.70710678118654746;1 1 1 1 1 1 1 1 1 1 1 1 1 1 1 1 1

...

1 1],zeros(4,0)};

lr={[NaN NaN NaN NaN NaN NaN NaN NaN NaN NaN NaN NaN NaN NaN NaN

NaN NaN ...

NaN NaN NaN NaN NaN NaN NaN NaN NaN NaN NaN NaN NaN NaN NaN

NaN NaN NaN NaN ...

NaN NaN NaN NaN NaN NaN NaN NaN NaN NaN NaN NaN NaN NaN NaN

NaN NaN NaN NaN ...

NaN NaN NaN NaN NaN NaN],[0 1 0 1 0 1 0 1 1 0 0 1 0 0 0 0 1 0 1 1 0 1 1 0 1

...

1 0 1 1 0 1 0 1 1 1 1 1 1 1 1 1;1 0 1 0 1 0 1 0 0 1 1 0 1 1 1 1 0 1 0 0 1 0 ...

```
0 1 0 0 1 0 0 1 0 1 0 0 0 0 0 0 0 0],[0 1 1 0 1 0 1 0 1 0 1 0 0 1 0 1 0 1  ...
0 1;1 0 0 1 0 1 0 1 0 1 0 1 1 0 1 0 1 0 1 0],zeros(2,0)};
CO1=solid2(p,rb,wt,lr);
objs={CO1};
names={'CO1'};
s.objs=objs;
s.name=names;

%Generate Boundaries to measure the performance indes of the flow
x=[-0.171 -0.097];
y=[0.16 0.174];
B1=curve2(x,y);
x=[-0.171 -0.097];
y=[0.022 0.036];
B2=curve2(x,y);
x=[-0.171 -0.097];
y=[0.298 0.312];
B3=curve2(x,y);
x=[-0.171 -0.097];
y=[0.436 0.450];
B4=curve2(x,y);
p=[-0.19 -0.19 -0.171;0 0.022  ...
0.022];
```

```
rb={[1 3],zeros(2,0),(1:3)',zeros(4,0)};
wt={zeros(1,0),zeros(2,0),[1;0.70710678118654746;1],zeros(4,0)};
lr={[NaN NaN],zeros(2,0),[0;0],zeros(2,0)};
B5=curve2(p,rb,wt,lr);
p=[-0.19 -0.19 -0.171;0.138 0.16 0.16];
rb={[1 3],zeros(2,0),(1:3)',zeros(4,0)};
wt={zeros(1,0),zeros(2,0),[1;0.70710678118654746;1],zeros(4,0)};
lr={[NaN NaN],zeros(2,0),[0;0],zeros(2,0)};
B6=curve2(p,rb,wt,lr);
p=[-0.19 -0.19 -0.171; ...
0.276 0.298 0.298];
rb={[1 3],zeros(2,0),(1:3)',zeros(4,0)};
wt={zeros(1,0),zeros(2,0),[1;0.70710678118654746;1],zeros(4,0)};
lr={[NaN NaN],zeros(2,0),[0;0],zeros(2,0)};
B7=curve2(p,rb,wt,lr);
p=[-0.19 -0.19 -0.171;0.414 0.436  ...
0.436];
rb={[1 3],zeros(2,0),(1:3)',zeros(4,0)};
wt={zeros(1,0),zeros(2,0),[1;0.70710678118654746;1],zeros(4,0)};
lr={[NaN NaN],zeros(2,0),[0;0],zeros(2,0)};
B8=curve2(p,rb,wt,lr);
p=[-0.19 -0.19 -0.170;-0.025 0  ...
-0.025];
```

```
rb={[2 3],zeros(2,0),[2;1;3],zeros(4,0)};
wt={zeros(1,0),zeros(2,0),[1;0.70710678118654746;1],zeros(4,0)};
lr={[NaN NaN],zeros(2,0),[0;0],zeros(2,0)};
B9=curve2(p,rb,wt,lr);
x=[-0.170 -0.112];
y=[-0.0250 -0.036];
B10=curve2(x,y);
p=[-0.112 -0.070 -0.070; ...
-0.036 -0.070 -0.036];
rb={[1 2],zeros(2,0),[1;3;2],zeros(4,0)};
wt={zeros(1,0),zeros(2,0),[1;0.70710678118654746;1],zeros(4,0)};
lr={[NaN NaN],zeros(2,0),[0;0],zeros(2,0)};
B11=curve2(p,rb,wt,lr);
x=[-0.070 -0.070];
y=[-0.070 -0.159];
B12=curve2(x,y);
p=[-0.19 -0.19 -0.172;0.138 0.116  ...
0.116];
rb={[1 3],zeros(2,0),(1:3)',zeros(4,0)};
wt={[],zeros(2,0),[1;0.70710678118654746;1],zeros(4,0)};
lr={[NaN NaN],zeros(2,0),[0;0],zeros(2,0)};
B13=curve2(p,rb,wt,lr);
p=[-0.19 -0.19 -0.172;0.276 0.254 0.254];
```

```
rb={[1 3],zeros(2,0),(1:3)',zeros(4,0)};
wt={[],zeros(2,0),[1;0.70710678118654746;1],zeros(4,0)};
lr={[NaN NaN],zeros(2,0),[0;0],zeros(2,0)};
B14=curve2(p,rb,wt,lr);
p=[-0.19 -0.19 -0.172;0.414 0.392  ...
0.392];
rb={[1 3],zeros(2,0),(1:3)',zeros(4,0)};
wt={[],zeros(2,0),[1;0.70710678118654746;1],zeros(4,0)};
lr={[NaN NaN],zeros(2,0),[0;0],zeros(2,0)};
B15=curve2(p,rb,wt,lr);
p=[-0.19 -0.19 -0.172;0.552 0.53  ...
0.53];
rb={[1 3],zeros(2,0),(1:3)',zeros(4,0)};
wt={[],zeros(2,0),[1;0.70710678118654746;1],zeros(4,0)};
lr={[NaN NaN],zeros(2,0),[0;0],zeros(2,0)};
B16=curve2(p,rb,wt,lr);
x=[-0.172 -0.098];
y=[0.116 0.103];
B17=curve2(x,y);
x=[-0.172 -0.098];
y=[0.254 0.241];
B18=curve2(x,y);
x=[-0.172 -0.098];
```

```
y=[0.392 0.379];
B19=curve2(x,y);
x=[-0.172 -0.098];
y=[0.53 0.517];
B20=curve2(x,y);
p=[-0.097 -0.055 -0.055;0.036  ...
0.036 0.070];
rb={[1 3],zeros(2,0),(1:3)',zeros(4,0)};
wt={zeros(1,0),zeros(2,0),[1;0.70710678118654746;1],zeros(4,0)};
lr={[NaN NaN],zeros(2,0),[0;0],zeros(2,0)};
B21=curve2(p,rb,wt,lr);
p=[-0.097 -0.055 -0.055;0.174  ...
0.174 0.208];
rb={[1 3],zeros(2,0),(1:3)',zeros(4,0)};
wt={zeros(1,0),zeros(2,0),[1;0.70710678118654746;1],zeros(4,0)};
lr={[NaN NaN],zeros(2,0),[0;0],zeros(2,0)};
B22=curve2(p,rb,wt,lr);
p=[-0.097 -0.055 -0.055;0.312 0.312 0.346];
rb={[1 3],zeros(2,0),(1:3)',zeros(4,0)};
wt={zeros(1,0),zeros(2,0),[1;0.70710678118654746;1],zeros(4,0)};
lr={[NaN NaN],zeros(2,0),[0;0],zeros(2,0)};
B23=curve2(p,rb,wt,lr);
p=[-0.097 -0.055 -0.055;0.450  ...
```

```
0.450 0.484];
rb={[1 3],zeros(2,0),(1:3)',zeros(4,0)};
wt={zeros(1,0),zeros(2,0),[1;0.70710678118654746;1],zeros(4,0)};
lr={[NaN NaN],zeros(2,0),[0;0],zeros(2,0)};
B24=curve2(p,rb,wt,lr);
p=[-0.0980 -0.055 -0.055; ...
0.103 0.070 0.103];
rb={[1 2],zeros(2,0),[1;3;2],zeros(4,0)};
wt={zeros(1,0),zeros(2,0),[1;0.70710678118654746;1],zeros(4,0)};
lr={[NaN NaN],zeros(2,0),[0;0],zeros(2,0)};
B25=curve2(p,rb,wt,lr);
p=[-0.0980 -0.055 -0.055; ...
0.241 0.208 0.241];
rb={[1 2],zeros(2,0),[1;3;2],zeros(4,0)};
wt={zeros(1,0),zeros(2,0),[1;0.70710678118654746;1],zeros(4,0)};
lr={[NaN NaN],zeros(2,0),[0;0],zeros(2,0)};
B26=curve2(p,rb,wt,lr);
p=[-0.0980 -0.055 -0.055;0.379  ...
0.346 0.379];
rb={[1 2],zeros(2,0),[1;3;2],zeros(4,0)};
wt={zeros(1,0),zeros(2,0),[1;0.70710678118654746;1],zeros(4,0)};
lr={[NaN NaN],zeros(2,0),[0;0],zeros(2,0)};
B27=curve2(p,rb,wt,lr);
```

```
p=[-0.0980 -0.055 -0.055; ...
0.517 0.484 0.517];
rb={[1 2],zeros(2,0),[1;3;2],zeros(4,0)};
wt={zeros(1,0),zeros(2,0),[1;0.70710678118654746;1],zeros(4,0)};
lr={[NaN NaN],zeros(2,0),[0;0],zeros(2,0)};
B28=curve2(p,rb,wt,lr);
p=[-0.19 -0.19 -0.170;0.552 0.578  ...
0.578];
rb={[1 3],zeros(2,0),(1:3)',zeros(4,0)};
wt={zeros(1,0),zeros(2,0),[1;0.70710678118654746;1],zeros(4,0)};
lr={[NaN NaN],zeros(2,0),[0;0],zeros(2,0)};
B29=curve2(p,rb,wt,lr);
x=[-0.170 -0.112];
y=[0.578 0.589];
B30=curve2(x,y);
p=[-0.112 -0.070 -0.070; ...
0.589 0.589 0.62];
rb={[1 3],zeros(2,0),(1:3)',zeros(4,0)};
wt={zeros(1,0),zeros(2,0),[1;0.70710678118654746;1],zeros(4,0)};
lr={[NaN NaN],zeros(2,0),[0;0],zeros(2,0)};
B31=curve2(p,rb,wt,lr);
x=[-0.070 -0.070];
y=[0.62 0.670];
```

```
B32=curve2(x,y);
p=[-0.070000000000000007 -0.054999999999999993 -0.054999999999999993;
...
0.67000000000000004 0.68400000000000005 0.70399999999999996];
rb={1:3,[1 2;2 3],zeros(3,0),zeros(4,0)};
wt={zeros(1,0),ones(2,2),zeros(3,0),zeros(4,0)};
lr={[NaN NaN NaN],zeros(2,2),zeros(2,0),zeros(2,0)};
B33=curve2(p,rb,wt,lr);
p=[-0.054999999999999993 -0.040000000000000001 -0.040000000000000001;
...
0.70399999999999996 0.624 0.70399999999999996];
rb={1:3,[1 2;3 3],zeros(3,0),zeros(4,0)};
wt={zeros(1,0),ones(2,2),zeros(3,0),zeros(4,0)};
lr={[NaN NaN NaN],zeros(2,2),zeros(2,0),zeros(2,0)};
B34=curve2(p,rb,wt,lr);
objs={B1,B2,B3,B4,B5,B6,B7,B8,B9,B10,B11,B12,B13,B14,B15,B16,B17,B18,B1
9, ...
B20,B21,B22,B23,B24,B25,B26,B27,B28,B29,B30,B31,B32,B33,B34};
names={'B1','B2','B3','B4','B5','B6','B7','B8','B9','B10','B11','B12','B13', ...
'B14','B15','B16','B17','B18','B19','B20','B21','B22','B23','B24','B25', ...
'B26','B27','B28','B29','B30','B31','B32','B33','B34'};
c.objs=objs;
c.name=names;
```

```
objs={};
names={};
p.objs=objs;
p.name=names;

drawstruct=struct('s',s,'c',c,'p',p);
fem.draw=drawstruct;
fem.geom=geomcsg(fem);

clear appl

% Application mode 1
appl{1}.mode='flpdecns2d("dim",{"u","v","p"},"sdim",{"r","z"},"submode","std","tdif
f","on")';
appl{1}.dim={'u','v','p'};
appl{1}.form='general';
appl{1}.border='off';
appl{1}.name='cns';
appl{1}.var={};
appl{1}.assign={'Fx';'Fx';'Fy';'Fy';'Kx';'Kx';'Ky';'Ky';'U';'U';'V';'V'; ...
'eta';'eta';'rho';'rho'};
appl{1}.equ.rho={'rh'};
```

```
appl{1}.equ.eta={'et'};

appl{1}.equ.Fx={'0'};

appl{1}.equ.Fy={'g*rh'};

appl{1}.equ.gporder={{2;2;2}};

appl{1}.equ.cporder={{1;1;1}};

appl{1}.equ.shape={1:3};

appl{1}.equ.init={{{'0'};{'0'};{'0'}}};

appl{1}.equ.usage={1};

appl{1}.equ.ind=1;

appl{1}.bnd.u={'0','0','0','0','0'};

appl{1}.bnd.v={'0','0','vmax*(2.*s.-s.^2)','0','0'};

appl{1}.bnd.p={'0','0','0','0','0'};

appl{1}.bnd.type={'noslip','neutral','uv','strout','slip'};

appl{1}.bnd.gporder={{0;0;0},{0;0;0},{0;0;0},{0;0;0},{0;0;0}};

appl{1}.bnd.cporder={{0;0;0},{0;0;0},{0;0;0},{0;0;0},{0;0;0}};

appl{1}.bnd.shape={0,0,0,0,0};

appl{1}.bnd.ind=[1 1 2 1 1 2 1 1 2 1 1 2 2 2 2 2 1 2 2 1 1 3 1 1 2 2 2 1 1  ...

1 1 1 1 1 1 1 1 1 1 1 1 1 1 1 1 2 2 2 1 1 1 1 1 1 4 4 5 5 1 1 1 1 1 1 1 1 1  ...

2 2 2 2 2 2 2 2 2 2 1 2 2 1 1 1 2 1 1 2 1 1 2 1 1 2 2 2 2 2];

appl{1}.sdim={'r','z'};

appl{1}.elemdefault='Lag1';

appl{1}.sshape=1;

appl{1}.shape={'shlag(1,''u'')','shlag(1,''v'')','shlag(1,''p'')'};
```

```
fem.appl=appl;

% Initialize mesh
fem.mesh=meshinit(fem,...
        'Out',    {'mesh'},...
        'jiggle', 'mean',...
        'Hcurve', 0.29999999999999999,...
        'Hgrad',  1.3,...
        'Hmax',   {[],zeros(1,0),zeros(1,0),zeros(1,0)},...
        'Hnum',   {[],[22 30 26 17 27 17 28 30 29 10 30 17 31 17 32 10 33 17 34
17  ...
35 10 36 17 37 17 38 10 39 17 40 17 41 10 42 17 43 17 44 10 45 17 46 17 47  ...
40 48 17 49 40 50 5 51 15 52 40 53 10 82 10 85 10]},...
        'Hpnt',   {12,zeros(1,0)});

% Dimension
fem.dim={'u','v','p'};

% Boundary conditions
fem.border=1;

% Problem form
```

```
fem.form='general';

% Geometry element order
fem.sshape=1;

% Differentiation
fem.diff={'ga','g','f','r'};

% Differentiation simplification
fem.simplify='on';

% Differentiation rules
fem.rules={};

% Define application mode variables
fem.var={};

% Point settings
clear pnt
pnt.var={};
pnt.ind=ones(1,98);
pnt.weak={{{'0'};{'0'};{'0'}}};
pnt.dweak={{{'0'};{'0'};{'0'}}};
```

```
pnt.constr={{{'0'};{'0'};{'0'}}};
pnt.init={{{''};{''};{''}}};
pnt.shape={1:3};
pnt.expr={};
fem.pnt=pnt;

% Boundary conditions
clear bnd
bnd.var={'U','sqrt(u^2+v^2)','Kx',{'nr*(2*(et)*ur)+nz*((et)*(uz+vr))', ...
'nr*(2*(et)*ur)+nz*((et)*(uz+vr))','nr*(2*(et)*ur)+nz*((et)*(uz+vr))', ...
'nr*(2*(et)*ur)+nz*((et)*(uz+vr))','nr*(2*(et)*ur)+nz*((et)*(uz+vr))'},'Ky', ...
{'nr*((et)*(vr+uz))+nz*(2*(et)*vz)','nr*((et)*(vr+uz))+nz*(2*(et)*vz)', ...
'nr*((et)*(vr+uz))+nz*(2*(et)*vz)','nr*((et)*(vr+uz))+nz*(2*(et)*vz)', ...
'nr*((et)*(vr+uz))+nz*(2*(et)*vz)'}};
bnd.vart={};
bnd.varu={};
bnd.ind=[1 1 2 1 1 2 1 1 2 1 1 2 2 2 2 2 1 2 2 1 1 3 1 1 2 2 2 1 1 1 1 1 1  ...
1 1 1 1 1 1 1 1 1 1 1 2 2 2 1 1 1 1 1 1 4 4 5 5 1 1 1 1 1 1 1 1 1 1 2 2 2 2  ...
2 2 2 2 2 2 1 2 2 1 1 1 2 1 1 2 1 1 2 1 1 2 2 2 2 2];
bnd.q={{{'0'},{'0'},{'0'};{'0'},{'0'},{'0'};{'0'},{'0'},{'0'}},{{'0'},{'0'}, ...
{'0'};{'0'},{'0'},{'0'};{'0'},{'0'},{'0'}},{{'0'},{'0'},{'0'};{'0'},{'0'}, ...
{'0'};{'0'},{'0'},{'0'}},{{'0'},{'0'},{'0'};{'0'},{'0'},{'0'};{'0'},{'0'}, ...
{'0'}},{{'0'},{'0'},{'0'};{'0'},{'0'},{'0'};{'0'},{'0'},{'0'}}};
```

```
bnd.g={{{'0'};{'0'};{'0'}},{{'0'};{'0'};{'0'}},{{'0'};{'0'};{'0'}},{{'0'}; ...
{'0'};{'0'}},{{'0'};{'0'};{'0'}}};
bnd.h={{{'1'},{'0'},{'0'};{'0'},{'1'},{'0'};{'0'},{'0'},{'0'}},{{'0'},{'0'}, ...
{'0'};{'0'},{'0'},{'0'};{'0'},{'0'},{'0'}},{{'1'},{'0'},{'0'};{'0'},{'1'}, ...
{'0'};{'0'},{'0'},{'0'}},{{'tr'},{'tz'},{'0'};{'0'},{'0'},{'0'};{'0'},{'0'}, ...
{'1'}},{{'nr'},{'nz'},{'0'};{'0'},{'0'},{'0'};{'0'},{'0'},{'0'}}};
bnd.r={{{'-u'};{'-v'};{'0'}},{{'0'};{'0'};{'0'}},{{'-u'}; ...
{'vmax*(2*s-s^2)-v'};{'0'}},{{'-(u*tr+v*tz)'};{'0'};{'-p'}}, ...
{{'-(u*nr+v*nz)'};{'0'};{'0'}}};
bnd.weak={{{'0'};{'0'};{'0'}},{{'0'};{'0'};{'0'}},{{'0'};{'0'};{'0'}}, ...
{{'0'};{'0'};{'0'}},{{'0'};{'0'};{'0'}}};
bnd.dweak={{{'0'};{'0'};{'0'}},{{'0'};{'0'};{'0'}},{{'0'};{'0'};{'0'}}, ...
{{'0'};{'0'};{'0'}},{{'0'};{'0'};{'0'}}};
bnd.constr={{{'0'};{'0'};{'0'}},{{'0'};{'0'};{'0'}},{{'0'};{'0'};{'0'}}, ...
{{'0'};{'0'};{'0'}},{{'0'};{'0'};{'0'}}};
bnd.init={{{''};{''};{''}},{{''};{''};{''}},{{''};{''};{''}},{{''};{''}; ...
{''}},{{''};{''};{''}}};
bnd.gporder={{2;2;2},{1;1;1},{2;2;2},{2;2;2},{2;2;2}};
bnd.cporder={{1;1;1},{1;1;1},{1;1;1},{1;1;1},{1;1;1}};
bnd.shape={1:3,1:3,1:3,1:3,1:3};
bnd.expr={};
fem.bnd=bnd;
```

```
% PDE coefficients
clear equ
equ.var={'U','sqrt(u^2+v^2)','V','vr-uz','rho',{'rh'},'eta',{'et'},'Fx', ...
{'0'},'Fy',{'g*rh'}};
equ.vart={};
equ.varu={};
equ.ind=1;
equ.da={{{'rh*r'},{'0'},{'0'};{'0'},{'rh*r'},{'0'};{'0'},{'0'},{'0'}}};
equ.c={{{'2*et*r','0';'0','et*r'},{'0','0';'et*r','0'},{'0','0';'0','0'}; ...
{'0','et*r';'0','0'},{'et*r','0';'0','2*et*r'},{'0','0';'0','0'};{'0','0'; ...
'0','0'},{'0','0';'0','0'},{'0','0';'0','0'}}};
equ.al={{{'0';'0'},{'0';'0'},{'0';'0'};{'0';'0'},{'0';'0'},{'0';'0'};{'0'; ...
'0'},{'0';'0'},{'0';'0'}}};
equ.ga={{{'-2*et*r*ur';'-et*r*(uz+vr)'};{'-et*r*(vr+uz)';'-2*et*r*vz'};{'0'; ...
'0'}}};
equ.be={{{'r*rh*u';'r*rh*v'},{'0';'0'},{'r';'0'};{'0';'0'},{'r*rh*u'; ...
'r*rh*v'},{'0';'r'};{'r';'0'},{'0';'r'},{'0';'0'}}};
equ.a={{{'r*rh*ur+2*et/r'},{'r*rh*uz'},{'0'};{'r*rh*vr'},{'r*rh*vz'},{'0'}; ...
{'1'},{'0'},{'0'}}};
equ.f={{{'-(r*(pr+rh*(u*ur+v*uz))+2*et*u/r)'}; ...
{'r*(g*rh-pz-rh*(u*vr+v*vz))'};{'-(r*(ur+vz)+u)'}}};
equ.weak={{{'0'};{'0'};{'0'}}};
equ.dweak={{{'0'};{'0'};{'0'}}};
```

```
equ.constr={{{'0'};{'0'};{'0'}}};
equ.init={{{'0'};{'0'};{'0'}}};
equ.gporder={{2;2;2}};
equ.cporder={{1;1;1}};
equ.shape={1:3};
equ.expr={};
fem.equ=equ;

% Shape functions
fem.shape={'shlag(1,''u'')','shlag(1,''v'')','shlag(1,''p'')'};

% Define variables
fem.variables={...
        'vmax',   0.095049999999999996,...
        'rh',     1532,...
        'g',      -9.8100000000000005,...
        'et',     0.022100000000000002};

% Extend the mesh
fem.xmesh=meshextend(fem,'context','local');

% Evaluate initial condition
u0=asseminit(fem,...
```

```
        'context','local',...
        'init',   fem.xmesh.eleminit);

% Solve nonlinear problem
fem.sol=femnlin(fem,...
        'out',    'sol',...
        'stop',   'on',...
        'init',   u0,...
        'report', 'on',...
        'initstep',0.0001,...
        'minstep',1e-008,...
        'context','local',...
        'sd',     'off',...
        'nullfun','flspnull',...
        'blocksize',5000,...
        'solcomp',{'p','u','v'},...
        'linsolver','matlab',...
        'bsteps', 1,...
        'ntol',   0.001,...
        'hnlin',  'off',...
        'jacobian','equ',...
        'maxiter',50,...
        'method', 'eliminate');
```

```
% Save current fem structure for restart purposes
fem0=fem;
% Plot solution
figure;
postplot(fem,...
        'geomnum',1,...
        'context','local',...
        'tridata',{'U','cont','on'},...
        'trifacestyle','interp',...
        'triedgestyle','none',...
        'trimap', 'jet',...
        'trimaxmin','off',...
        'tribar', 'on',...
        'geom',   'on',...
        'geomcol','bginv',...
        'refine', 1,...
        'contorder',1,...
        'phase',  0,...
        'title',  'Surface: velocity field (U)  ',...
        'renderer','zbuffer',...
        'solnum', 1,...
        'axisvisible','on')
```

```
AXIS([-0.6 0.4 -0.2 0.8])


% Plot solution
postplot(fem,...
        'geomnum',1,...
        'context','local',...
        'contdata',{'U','cont','internal'},...
        'contlevels',[0.0001:0.02:0.4000],...
        'contstyle','color',...
        'contlabel','off',...
        'contmaxmin','off',...
        'contbar','on',...
        'contmap','cool',...
        'geom',   'on',...
        'geomcol','bginv',...
        'refine', 3,...
        'contorder',2,...
        'phase',  0,...
        'title',  'Contour: velocity field (U)  ',...
        'renderer','zbuffer',...
        'solnum', 1,...
        'axisvisible','on')
AXIS([-0.6 0.4 -0.2 0.8])
```

```
% Plot solution
figure;
postplot(fem,...
        'geomnum',1,...
        'context','local',...
        'flowdata',{{'u','cont','internal'},{'v','cont','internal'}},...
        'flowcolor','cycle',...
        'flowlines',40,...
        'flowback','on',...
        'flownormal','off',...
        'flowsteps',400,...
        'flowstop',Inf,...
        'flowtol',0.001,...
        'flowstattol',0.01,...
        'flowstart','centers',...
        'geom',   'on',...
        'geomcol','bginv',...
        'refine', 3,...
        'contorder',2,...
        'phase',  0,...
        'title',  'Flow: [r velocity (u),z velocity (v)]  ',...
        'renderer','zbuffer',...
```

```
        'solnum', 1,...
        'axisvisible','on')
AXIS([-0.6 0.4 -0.2 0.8])

%calculate length
L(1)=-0.070-(-0.159);
L(2)=0.25*pi*(-0.036-(-.070)+(-.070-(-0.112)));
L(3)=sqrt((0.112-.170)^2+(.036-.025)^2);
L(4)=0.25*pi*(+0.000-(-.025)+(-.170-(-0.190)));
L(5)=L(4);
L(6)=sqrt((0.171-.097)^2+(.036-.022)^2);
L(7)=0.25*pi*(0.055-0.036+0.097-0.07);
L(8)=L(7);
L(9)=L(6);
L(10)=L(4);
L(11)=L(5);
L(12)=L(6);
L(13)=L(7);
L(14)=L(8);
L(15)=L(12);
L(16)=L(10);
L(17)=L(11);
L(18)=L(15);
```

```
L(19)=L(13);

L(20)=L(14);

L(21)=L(18);

L(22)=L(16);

L(23)=L(17);

L(24)=L(21);

L(25)=L(19);

L(26)=L(20);

L(27)=L(24);

L(28)=L(22);

L(29)=L(23);

L(30)=L(3);

L(31)=L(2);

L(32)=0.67-0.62;



%PI for the Entrance

% Integrate on subdomains

I1=postint(fem,'U',...

        'cont',   'on',...

        'contorder',1,...

        'edim',   1,...
```

```
        'solnum', 1,...
        'phase',  0,...
        'geomnum',1,...
        'dl',     25,...
        'intorder',2,...
        'context','local');
P(1)=I1/L(1);

%PI for the 1st length
% Integrate on subdomains
I2=postint(fem,'U',...
        'cont',   'on',...
        'contorder',1,...
        'edim',   1,...
        'solnum', 1,...
        'phase',  0,...
        'geomnum',1,...
        'dl',     79,...
        'intorder',2,...
        'context','local');
P(2)=I2/L(2);
%PI for the  length 2
% Integrate on subdomains
```

```
I3=postint(fem,'U',...
        'cont',   'on',...
        'contorder',1,...
        'edim',   1,...
        'solnum', 1,...
        'phase',  0,...
        'geomnum',1,...
        'dl',     18,...
        'intorder',2,...
        'context','local');
P(3)=I3/L(3);
%PI for the  length 3
% Integrate on subdomains
I4=postint(fem,'U',...
        'cont',   'on',...
        'contorder',1,...
        'edim',   1,...
        'solnum', 1,...
        'phase',  0,...
        'geomnum',1,...
        'dl',     69,...
        'intorder',2,...
        'context','local');
```

```
P(4)=I4/L(4);
%PI for the  length 4
% Integrate on subdomains
I5=postint(fem,'U',...
        'cont',   'on',...
        'contorder',1,...
        'edim',   1,...
        'solnum', 1,...
        'phase',  0,...
        'geomnum',1,...
        'dl',     68,...
        'intorder',2,...
        'context','local');
P(5)=I5/L(5);
% Integrate on subdomains
I6=postint(fem,'U',...
        'cont',   'on',...
        'contorder',1,...
        'edim',   1,...
        'solnum', 1,...
        'phase',  0,...
        'geomnum',1,...
        'dl',     13,...
```

```
        'intorder',2,...
        'context','local');
P(6)=I6/L(6);
% Integrate on subdomains
I7=postint(fem,'U',...
        'cont',   'on',...
        'contorder',1,...
        'edim',   1,...
        'solnum', 1,...
        'phase',  0,...
        'geomnum',1,...
        'dl',     94,...
        'intorder',2,...
        'context','local');


%P(2)=(I1+I2+I3+I4+I5+I6)/L(2);
P(7)=I7/L(7);
%PI for the 2nd Cell
% Integrate on subdomains
I8=postint(fem,'U',...
        'cont',   'on',...
        'contorder',1,...
        'edim',   1,...
```

```
        'solnum', 1,...
        'phase',  0,...
        'geomnum',1,...
        'dl',     84,...
        'intorder',2,...
        'context','local');
P(8)=I8/L(8);
% Integrate on subdomains
I9=postint(fem,'U',...
        'cont',   'on',...
        'contorder',1,...
        'edim',   1,...
        'solnum', 1,...
        'phase',  0,...
        'geomnum',1,...
        'dl',     3,...
        'intorder',2,...
        'context','local');
P(9)=I9/L(9);
% Integrate on subdomains
I10=postint(fem,'U',...
        'cont',   'on',...
        'contorder',1,...
```

```
        'edim',   1,...
        'solnum', 1,...
        'phase',  0,...
        'geomnum',1,...
        'dl',     70,...
        'intorder',2,...
        'context','local');
P(10)=I10/L(10);
% Integrate on subdomains
I11=postint(fem,'U',...
        'cont',   'on',...
        'contorder',1,...
        'edim',   1,...
        'solnum', 1,...
        'phase',  0,...
        'geomnum',1,...
        'dl',     71,...
        'intorder',2,...
        'context','local');
P(11)=I11/L(11);
% Integrate on subdomains
I12=postint(fem,'U',...
        'cont',   'on',...
```

```
        'contorder',1,...
        'edim',   1,...
        'solnum', 1,...
        'phase',  0,...
        'geomnum',1,...
        'dl',     14,...
        'intorder',2,...
        'context','local');
P(12)=I12/L(12);
% Integrate on subdomains
I13=postint(fem,'U',...
        'cont',   'on',...
        'contorder',1,...
        'edim',   1,...
        'solnum', 1,...
        'phase',  0,...
        'geomnum',1,...
        'dl',     95,...
        'intorder',2,...
        'context','local');
P(13)=I13/L(13);
%P(3)=(I1+I2+I3+I4+I5+I6)/L(3);
```

```
%PI for the 3rd Cell
% Integrate on subdomains
I14=postint(fem,'U',...
        'cont',   'on',...
        'contorder',1,...
        'edim',   1,...
        'solnum', 1,...
        'phase',  0,...
        'geomnum',1,...
        'dl',     87,...
        'intorder',2,...
        'context','local');
P(14)=I14/L(14);
% Integrate on subdomains
I15=postint(fem,'U',...
        'cont',   'on',...
        'contorder',1,...
        'edim',   1,...
        'solnum', 1,...
        'phase',  0,...
        'geomnum',1,...
        'dl',     6,...
        'intorder',2,...
```

```
        'context','local');
P(15)=I15/L(15);
% Integrate on subdomains
I16=postint(fem,'U',...
        'cont',   'on',...
        'contorder',1,...
        'edim',   1,...
        'solnum', 1,...
        'phase',  0,...
        'geomnum',1,...
        'dl',     72,...
        'intorder',2,...
        'context','local');
P(16)=I16/L(16);
% Integrate on subdomains
I17=postint(fem,'U',...
        'cont',   'on',...
        'contorder',1,...
        'edim',   1,...
        'solnum', 1,...
        'phase',  0,...
        'geomnum',1,...
        'dl',     73,...
```

```
        'intorder',2,...
        'context','local');
P(17)=I17/L(17);
% Integrate on subdomains
I18=postint(fem,'U',...
        'cont',   'on',...
        'contorder',1,...
        'edim',   1,...
        'solnum', 1,...
        'phase',  0,...
        'geomnum',1,...
        'dl',     15,...
        'intorder',2,...
        'context','local');
P(18)=I18/L(18);
% Integrate on subdomains
I19=postint(fem,'U',...
        'cont',   'on',...
        'contorder',1,...
        'edim',   1,...
        'solnum', 1,...
        'phase',  0,...
        'geomnum',1,...
```

```
        'dl',     96,...
        'intorder',2,...
        'context','local');
P(19)=I19/L(19);
%P(4)=(I1+I2+I3+I4+I5+I6)/L(4);

%PI for the 4th Cell
% Integrate on subdomains
I20=postint(fem,'U',...
        'cont',   'on',...
        'contorder',1,...
        'edim',   1,...
        'solnum', 1,...
        'phase',  0,...
        'geomnum',1,...
        'dl',     90,...
        'intorder',2,...
        'context','local');
P(20)=I20/L(20);
% Integrate on subdomains
I21=postint(fem,'U',...
        'cont',   'on',...
        'contorder',1,...
```

```
        'edim',   1,...
        'solnum', 1,...
        'phase',  0,...
        'geomnum',1,...
        'dl',     9,...
        'intorder',2,...
        'context','local');
P(21)=I21/L(21);
% Integrate on subdomains
I22=postint(fem,'U',...
        'cont',   'on',...
        'contorder',1,...
        'edim',   1,...
        'solnum', 1,...
        'phase',  0,...
        'geomnum',1,...
        'dl',     74,...
        'intorder',2,...
        'context','local');
P(22)=I22/L(22);
% Integrate on subdomains
I23=postint(fem,'U',...
        'cont',   'on',...
```

```
        'contorder',1,...
        'edim',   1,...
        'solnum', 1,...
        'phase',  0,...
        'geomnum',1,...
        'dl',     75,...
        'intorder',2,...
        'context','local');
P(23)=I23/L(23);
% Integrate on subdomains
I24=postint(fem,'U',...
        'cont',   'on',...
        'contorder',1,...
        'edim',   1,...
        'solnum', 1,...
        'phase',  0,...
        'geomnum',1,...
        'dl',     16,...
        'intorder',2,...
        'context','local');
P(24)=I24/L(24);
% Integrate on subdomains
I25=postint(fem,'U',...
```

```
        'cont',   'on',...
        'contorder',1,...
        'edim',   1,...
        'solnum', 1,...
        'phase',  0,...
        'geomnum',1,...
        'dl',     97,...
        'intorder',2,...
        'context','local');
P(25)=I25/L(25);
%P(5)=(I1+I2+I3+I4+I5+I6)/L(5);

%PI for the 5th Cell
% Integrate on subdomains
I26=postint(fem,'U',...
        'cont',   'on',...
        'contorder',1,...
        'edim',   1,...
        'solnum', 1,...
        'phase',  0,...
        'geomnum',1,...
        'dl',     93,...
        'intorder',2,...
```

```
        'context','local');
P(26)=I26/L(26);
% Integrate on subdomains
I27=postint(fem,'U',...
        'cont',   'on',...
        'contorder',1,...
        'edim',   1,...
        'solnum', 1,...
        'phase',  0,...
        'geomnum',1,...
        'dl',     12,...
        'intorder',2,...
        'context','local');
P(27)=I27/L(27);
% Integrate on subdomains
I28=postint(fem,'U',...
        'cont',   'on',...
        'contorder',1,...
        'edim',   1,...
        'solnum', 1,...
        'phase',  0,...
        'geomnum',1,...
        'dl',     76,...
```

```
        'intorder',2,...
        'context','local');
P(28)=I28/L(28);
% Integrate on subdomains
I29=postint(fem,'U',...
        'cont',   'on',...
        'contorder',1,...
        'edim',   1,...
        'solnum', 1,...
        'phase',  0,...
        'geomnum',1,...
        'dl',     77,...
        'intorder',2,...
        'context','local');
P(29)=I29/L(29);
% Integrate on subdomains
I30=postint(fem,'U',...
        'cont',   'on',...
        'contorder',1,...
        'edim',   1,...
        'solnum', 1,...
        'phase',  0,...
        'geomnum',1,...
```

```
        'dl',     19,...
        'intorder',2,...
        'context','local');
P(30)=I30/L(30);
% Integrate on subdomains
I31=postint(fem,'U',...
        'cont',   'on',...
        'contorder',1,...
        'edim',   1,...
        'solnum', 1,...
        'phase',  0,...
        'geomnum',1,...
        'dl',     80,...
        'intorder',2,...
        'context','local');
P(31)=I31/L(31);
%P(6)=(I1+I2+I3+I4+I5+I6)/L(6);


%PI for the Exit



% Integrate on subdomains
I32=postint(fem,'U',...
```

```
        'cont',   'on',...
        'contorder',1,...
        'edim',   1,...
        'solnum', 1,...
        'phase',  0,...
        'geomnum',1,...
        'dl',     26,...
        'intorder',2,...
        'context','local');
P(32)=I32/L(32);
%P(7)=I1/L(7);
P'
%aveP=sum(P)/7
aveP=sum(P)/32
stdevP=0.0;
%for i=1:7
for i=1:32
   stdevP=stdevP+(P(i)-aveP)^2;
end;
stdevP=(sqrt(stdevP)/32)/aveP
```

APPENDIX B

INDEX PERFORMANCES FOR THE CASES OF PARAMETER STUDY 1

Table 10. The performance index for case 1 of parameter study 1

Segment		Average Velocity (m/s)
Cavity cell 1	Segment 1	0.0113
	Segment 2	0.0011
	Segment 3	0.0001
	Segment 4	0.0001
	Segment 5	0.0036
	Segment 6	0.1482
Cavity cell 2	Segment 1	0.0811
	Segment 2	0.0024
	Segment 3	0.0002
	Segment 4	0.0004
	Segment 5	0.0068
	Segment 6	0.1744
Cavity cell 3	Segment 1	0.0914
	Segment 2	0.0043
	Segment 3	0.0002
	Segment 4	0.0002
	Segment 5	0.0124
	Segment 6	0.1957
Cavity cell 4	Segment 1	0.0859
	Segment 2	0.0049
	Segment 3	0.0002
	Segment 4	0.0002
	Segment 5	0.0144
	Segment 6	0.2088
Cavity cell 5	Segment 1	0.0838
	Segment 2	0.0045
	Segment 3	0.0004
	Segment 4	0.0002
	Segment 5	0.0128
	Segment 6	0.0870
Inlet		0.0233
Outlet		0.0372
V		0.0405
SDV		0.2685

Table 11. The performance index for case 2 of parameter study 1

Segment		Average Velocity (m/s)
Cavity cell 1	Segment 1	0.0099
	Segment 2	0.0010
	Segment 3	0.0001
	Segment 4	0.0001
	Segment 5	0.0036
	Segment 6	0.1510
Cavity cell 2	Segment 1	0.0771
	Segment 2	0.0029
	Segment 3	0.0001
	Segment 4	0.0001
	Segment 5	0.0096
	Segment 6	0.1839
Cavity cell 3	Segment 1	0.0822
	Segment 2	0.0046
	Segment 3	0.0002
	Segment 4	0.0002
	Segment 5	0.0132
	Segment 6	0.2017
Cavity cell 4	Segment 1	0.0876
	Segment 2	0.0034
	Segment 3	0.0001
	Segment 4	0.0000
	Segment 5	0.0095
	Segment 6	0.2004
Cavity cell 5	Segment 1	0.0864
	Segment 2	0.0047
	Segment 3	0.0002
	Segment 4	0.0002
	Segment 5	0.0124
	Segment 6	0.0912
Inlet		0.0230
Outlet		0.0428
V		0.0407
SDV		0.2697

Table 12. The performance index for case 3 of parameter study 1

Segment		Average Velocity (m/s)
Cavity cell 1	Segment 1	0.0069
	Segment 2	0.0007
	Segment 3	0.0001
	Segment 4	0.0001
	Segment 5	0.0022
	Segment 6	0.1783
Cavity cell 2	Segment 1	0.0818
	Segment 2	0.0019
	Segment 3	0.0001
	Segment 4	0.0001
	Segment 5	0.0071
	Segment 6	0.1875
Cavity cell 3	Segment 1	0.0842
	Segment 2	0.0023
	Segment 3	0.0001
	Segment 4	0.0001
	Segment 5	0.0074
	Segment 6	0.2014
Cavity cell 4	Segment 1	0.0883
	Segment 2	0.0027
	Segment 3	0.0001
	Segment 4	0.0001
	Segment 5	0.0087
	Segment 6	0.2059
Cavity cell 5	Segment 1	0.0948
	Segment 2	0.0056
	Segment 3	0.0002
	Segment 4	0.0002
	Segment 5	0.0084
	Segment 6	0.0884
Inlet		0.0200
Outlet		0.0880
V		0.0429
SDV		0.2702

Table 13. The performance index for case 4 of parameter study 1

Segment		Average Velocity (m/s)
Cavity cell 1	Segment 1	0.0256
	Segment 2	0.0013
	Segment 3	0.0001
	Segment 4	0.0001
	Segment 5	0.0042
	Segment 6	0.1406
Cavity cell 2	Segment 1	0.1451
	Segment 2	0.0018
	Segment 3	0.0001
	Segment 4	0.0002
	Segment 5	0.0098
	Segment 6	0.1755
Cavity cell 3	Segment 1	0.1864
	Segment 2	0.0064
	Segment 3	0.0010
	Segment 4	0.0008
	Segment 5	0.0216
	Segment 6	0.1860
Cavity cell 4	Segment 1	0.2250
	Segment 2	0.0128
	Segment 3	0.0015
	Segment 4	0.0012
	Segment 5	0.0295
	Segment 6	0.2078
Cavity cell 5	Segment 1	0.2879
	Segment 2	0.0396
	Segment 3	0.0541
	Segment 4	0.0188
	Segment 5	0.0246
	Segment 6	0.1287
Inlet		0.0241
Outlet		0.0121
V		0.0617
SDV		0.2381

Table 14. The performance index for case 5 of parameter study 1

Segment		Average Velocity (m/s)
Cavity cell 1	Segment 1	0.0275
	Segment 2	0.0028
	Segment 3	0.0002
	Segment 4	0.0002
	Segment 5	0.0032
	Segment 6	0.1444
Cavity cell 2	Segment 1	0.1242
	Segment 2	0.0143
	Segment 3	0.0010
	Segment 4	0.0007
	Segment 5	0.0392
	Segment 6	0.1839
Cavity cell 3	Segment 1	0.1194
	Segment 2	0.0052
	Segment 3	0.0005
	Segment 4	0.0009
	Segment 5	0.0252
	Segment 6	0.1957
Cavity cell 4	Segment 1	0.1122
	Segment 2	0.0041
	Segment 3	0.0008
	Segment 4	0.0007
	Segment 5	0.0069
	Segment 6	0.1961
Cavity cell 5	Segment 1	0.1128
	Segment 2	0.0028
	Segment 3	0.0005
	Segment 4	0.0011
	Segment 5	0.0122
	Segment 6	0.0825
Inlet		0.0360
Outlet		0.0251
V		0.0463
SDV		0.2432

Table 15. The performance index for case 6 of parameter study 1

Segment		Average Velocity (m/s)
Cavity cell 1	Segment 1	0.0272
	Segment 2	0.0015
	Segment 3	0.0002
	Segment 4	0.0002
	Segment 5	0.0046
	Segment 6	0.1456
Cavity cell 2	Segment 1	0.0976
	Segment 2	0.0034
	Segment 3	0.0004
	Segment 4	0.0003
	Segment 5	0.0049
	Segment 6	0.1717
Cavity cell 3	Segment 1	0.0844
	Segment 2	0.0081
	Segment 3	0.0016
	Segment 4	0.0042
	Segment 5	0.0149
	Segment 6	0.1964
Cavity cell 4	Segment 1	0.0862
	Segment 2	0.0053
	Segment 3	0.0001
	Segment 4	0.0001
	Segment 5	0.0137
	Segment 6	0.1986
Cavity cell 5	Segment 1	0.0763
	Segment 2	0.0058
	Segment 3	0.0002
	Segment 4	0.0002
	Segment 5	0.0119
	Segment 6	0.0859
Inlet		0.0252
Outlet		0.0523
V		0.0415
SDV		0.2558

Table 16. The performance index for case 7 of parameter study 1

Segment		Average Velocity (m/s)
Cavity cell 1	Segment 1	0.0085
	Segment 2	0.0008
	Segment 3	0.0001
	Segment 4	0.0001
	Segment 5	0.0012
	Segment 6	0.0377
Cavity cell 2	Segment 1	0.0393
	Segment 2	0.0010
	Segment 3	0.0001
	Segment 4	0.0001
	Segment 5	0.0014
	Segment 6	0.0401
Cavity cell 3	Segment 1	0.0415
	Segment 2	0.0010
	Segment 3	0.0001
	Segment 4	0.0001
	Segment 5	0.0014
	Segment 6	0.0406
Cavity cell 4	Segment 1	0.0437
	Segment 2	0.0010
	Segment 3	0.0001
	Segment 4	0.0001
	Segment 5	0.0014
	Segment 6	0.0408
Cavity cell 5	Segment 1	0.0474
	Segment 2	0.0010
	Segment 3	0.0001
	Segment 4	0.0001
	Segment 5	0.0009
	Segment 6	0.0152
Inlet		0.0076
Outlet		0.0092
V		0.0120
SDV		0.2557

Table 17. The performance index for case 8 of parameter study 1

Segment		Average Velocity (m/s)
Cavity cell 1	Segment 1	0.0179
	Segment 2	0.0033
	Segment 3	0.0004
	Segment 4	0.0006
	Segment 5	0.0032
	Segment 6	0.0228
Cavity cell 2	Segment 1	0.2021
	Segment 2	0.0052
	Segment 3	0.0005
	Segment 4	0.0009
	Segment 5	0.0065
	Segment 6	0.0567
Cavity cell 3	Segment 1	0.1164
	Segment 2	0.0063
	Segment 3	0.0005
	Segment 4	0.0003
	Segment 5	0.0008
	Segment 6	0.0419
Cavity cell 4	Segment 1	0.0622
	Segment 2	0.0010
	Segment 3	0.0002
	Segment 4	0.0001
	Segment 5	0.0001
	Segment 6	0.0218
Cavity cell 5	Segment 1	0.0257
	Segment 2	0.0007
	Segment 3	0.0000
	Segment 4	0.0000
	Segment 5	0.0001
	Segment 6	0.0168
Inlet		0.0087
Outlet		0.0365
V		0.0206
SDV		0.3500

Table 18. The performance index for case 9 of parameter study 1

Segment		Average Velocity (m/s)
Cavity cell 1	Segment 1	0.0135
	Segment 2	0.0009
	Segment 3	0.0001
	Segment 4	0.0000
	Segment 5	0.0021
	Segment 6	0.0992
Cavity cell 2	Segment 1	0.0754
	Segment 2	0.0009
	Segment 3	0.0001
	Segment 4	0.0001
	Segment 5	0.0012
	Segment 6	0.0780
Cavity cell 3	Segment 1	0.0736
	Segment 2	0.0006
	Segment 3	0.0000
	Segment 4	0.0000
	Segment 5	0.0011
	Segment 6	0.0814
Cavity cell 4	Segment 1	0.0751
	Segment 2	0.0005
	Segment 3	0.0000
	Segment 4	0.0001
	Segment 5	0.0011
	Segment 6	0.0834
Cavity cell 5	Segment 1	0.1049
	Segment 2	0.0053
	Segment 3	0.0011
	Segment 4	0.0021
	Segment 5	0.0085
	Segment 6	0.0646
Inlet		0.0240
Outlet		0.0577
V		0.0268
SDV		0.2412

Table 19. The performance index for case 10 of parameter study 1

Segment		Average Velocity (m/s)
Cavity cell 1	Segment 1	0.0178
	Segment 2	0.0011
	Segment 3	0.0001
	Segment 4	0.0001
	Segment 5	0.0035
	Segment 6	0.1163
Cavity cell 2	Segment 1	0.0926
	Segment 2	0.0013
	Segment 3	0.0001
	Segment 4	0.0001
	Segment 5	0.0052
	Segment 6	0.1237
Cavity cell 3	Segment 1	0.0950
	Segment 2	0.0014
	Segment 3	0.0001
	Segment 4	0.0001
	Segment 5	0.0058
	Segment 6	0.1257
Cavity cell 4	Segment 1	0.0977
	Segment 2	0.0022
	Segment 3	0.0001
	Segment 4	0.0002
	Segment 5	0.0090
	Segment 6	0.1296
Cavity cell 5	Segment 1	0.0874
	Segment 2	0.0017
	Segment 3	0.0001
	Segment 4	0.0001
	Segment 5	0.0048
	Segment 6	0.0551
Inlet		0.0235
Outlet		0.0559
V		0.0330
SDV		0.2475

Table 20. The performance index for case 11 of parameter study 1

Segment		Average Velocity (m/s)
Cavity cell 1	Segment 1	0.0044
	Segment 2	0.0002
	Segment 3	0.0000
	Segment 4	0.0000
	Segment 5	0.0001
	Segment 6	0.0049
Cavity cell 2	Segment 1	0.0097
	Segment 2	0.0004
	Segment 3	0.0000
	Segment 4	0.0000
	Segment 5	0.0002
	Segment 6	0.0053
Cavity cell 3	Segment 1	0.0100
	Segment 2	0.0003
	Segment 3	0.0000
	Segment 4	0.0000
	Segment 5	0.0002
	Segment 6	0.0052
Cavity cell 4	Segment 1	0.0104
	Segment 2	0.0003
	Segment 3	0.0000
	Segment 4	0.0000
	Segment 5	0.0002
	Segment 6	0.0051
Cavity cell 5	Segment 1	0.0106
	Segment 2	0.0004
	Segment 3	0.0000
	Segment 4	0.0000
	Segment 5	0.0001
	Segment 6	0.0011
Inlet		0.0011
Outlet		0.0033
V		0.0023
SDV		0.2665

Table 21. The performance index for case 12 of parameter study 1

Segment		Average Velocity (m/s)
Cavity cell 1	Segment 1	0.0041
	Segment 2	0.0004
	Segment 3	0.0000
	Segment 4	0.0000
	Segment 5	0.0004
	Segment 6	0.0023
Cavity cell 2	Segment 1	0.0076
	Segment 2	0.0008
	Segment 3	0.0000
	Segment 4	0.0000
	Segment 5	0.0003
	Segment 6	0.0053
Cavity cell 3	Segment 1	0.0111
	Segment 2	0.0006
	Segment 3	0.0000
	Segment 4	0.0000
	Segment 5	0.0003
	Segment 6	0.0054
Cavity cell 4	Segment 1	0.0114
	Segment 2	0.0006
	Segment 3	0.0000
	Segment 4	0.0000
	Segment 5	0.0003
	Segment 6	0.0053
Cavity cell 5	Segment 1	0.0117
	Segment 2	0.0006
	Segment 3	0.0000
	Segment 4	0.0000
	Segment 5	0.0002
	Segment 6	0.0013
Inlet		0.0014
Outlet		0.0012
V		0.0023
SDV		0.2751

APPENDIX C

INDEX PERFORMANCES FOR THE CASES OF PARAMETER STUDY 2

Table 22. The performance index for case 1 of parameter study 2

Segment		Average Velocity (m/s)
Cavity cell 1	Segment 1	0.0090
	Segment 2	0.0008
	Segment 3	0.0001
	Segment 4	0.0000
	Segment 5	0.0023
	Segment 6	0.0980
Cavity cell 2	Segment 1	0.0682
	Segment 2	0.0008
	Segment 3	0.0001
	Segment 4	0.0001
	Segment 5	0.0024
	Segment 6	0.0869
Cavity cell 3	Segment 1	0.0693
	Segment 2	0.0015
	Segment 3	0.0001
	Segment 4	0.0001
	Segment 5	0.0035
	Segment 6	0.0897
Cavity cell 4	Segment 1	0.0709
	Segment 2	0.0014
	Segment 3	0.0000
	Segment 4	0.0000
	Segment 5	0.0032
	Segment 6	0.0926
Cavity cell 5	Segment 1	0.0672
	Segment 2	0.0005
	Segment 3	0.0000
	Segment 4	0.0000
	Segment 5	0.0007
	Segment 6	0.0101
Inlet		0.0229
Outlet		0.0171
V		0.0225
SDV		0.2696

Table 23. The performance index for case 2 of parameter study 2

Segment		Average Velocity (m/s)
Cavity cell 1	Segment 1	0.0015
	Segment 2	0.0000
	Segment 3	0.0000
	Segment 4	0.0000
	Segment 5	0.0003
	Segment 6	0.0123
Cavity cell 2	Segment 1	0.0081
	Segment 2	0.0001
	Segment 3	0.0000
	Segment 4	0.0000
	Segment 5	0.0002
	Segment 6	0.0123
Cavity cell 3	Segment 1	0.0086
	Segment 2	0.0001
	Segment 3	0.0000
	Segment 4	0.0000
	Segment 5	0.0002
	Segment 6	0.0122
Cavity cell 4	Segment 1	0.0085
	Segment 2	0.0001
	Segment 3	0.0000
	Segment 4	0.0000
	Segment 5	0.0002
	Segment 6	0.0121
Cavity cell 5	Segment 1	0.0091
	Segment 2	0.0001
	Segment 3	0.0000
	Segment 4	0.0000
	Segment 5	0.0001
	Segment 6	0.0038
Inlet		0.0025
Outlet		0.0045
V		0.0030
SDV		0.2614

Table 24. The performance index for case 3 of parameter study 2

Segment		Average Velocity (m/s)
Cavity cell 1	Segment 1	0.0016
	Segment 2	0.0004
	Segment 3	0.0000
	Segment 4	0.0000
	Segment 5	0.0011
	Segment 6	0.0106
Cavity cell 2	Segment 1	0.0112
	Segment 2	0.0017
	Segment 3	0.0001
	Segment 4	0.0001
	Segment 5	0.0017
	Segment 6	0.0130
Cavity cell 3	Segment 1	0.0119
	Segment 2	0.0023
	Segment 3	0.0001
	Segment 4	0.0001
	Segment 5	0.0011
	Segment 6	0.0144
Cavity cell 4	Segment 1	0.0114
	Segment 2	0.0023
	Segment 3	0.0000
	Segment 4	0.0001
	Segment 5	0.0011
	Segment 6	0.0145
Cavity cell 5	Segment 1	0.0111
	Segment 2	0.0020
	Segment 3	0.0001
	Segment 4	0.0001
	Segment 5	0.0007
	Segment 6	0.0086
Inlet		0.0067
Outlet		0.0138
V		0.0045
SDV		0.2101

BIBLIOGRAPHY

"A Roadmap for Developing Accelerator Transmuting of Waste (ATW) Technology." DOE/RW-0519, October 1999.

Singer, W., et al. "Hydro Forming of TESLA Cavities at DESY." Proceedings of EPAC 2000. p. 324-326.

Aune, B., et al. "The Superconducting TESLA Cavities." http://documents.cern.ch/archive/electronic/physics/0003/0003011.pdf.

Burggraf, Odus R. "Analytical and numerical studies of the structure of steady separated flows." J. Fluid Mech. (1966), vol. 24 part 1. pp.113-151.

Armaly, B. F., et al. "Experimental and theoretical investigation of backward-facing step flow." J. Fluid Mech. (1993), vol. 127. pp. 473-496.

Chandrupatla, Tirupathi R., Belegundu, Ashok D. Introduction to finite elements in engineering. New Jersey: Prentice Hall, 1997.

White, Frank M. Fluid Mechanics. McGraw-Hill, 1999.

Stasa, Frank L. Applied finite element analysis for engineers. New York: Holt, Rinehart and Winston, 1985.

Fletcher Clive A. J. Computational techniques for fluid dynamics. Berlin Heidelberg: Spring-Verlag, 1988.

Fletcher Clive A. J. Computational techniques for fluid dynamics. Berlin Heidelberg: Spring-Verlag, 1991.

Pepper, Darrell W., Heinrich, Juan C. The finite element method basic concepts and applications. Hemisphere Publishing Corporation, 1992.

Rao, Singiresu S. The finite element method in engineering. Butterworth-Heinemann, 1999.

Emrich, R. J., ed. Fluid dynamics. New York: Academic Press, 1981.
Roache, Patrick J. Computational fluid dynamics. Albuqueque, N. M. : Hermosa Publishers, 1976.

Wendt, John F., et al, ed. Computational fluid dynamics. Berlin; New York: Springer-Verlag, 1992.

Wendt, John F., et al, ed. Computational fluid dynamics. Berlin; New York: Springer-Verlag, 1996.

Abbott, M. B., Basco, D. R. Computational fluid dynamics: an introduction for engineers. Harlow, Essex, England: Longman Scientific & Technical; New York: Wiley, 1989.

Hoffmann, Klaus A., Chiang, Steve T. Computational fluid dynamics for engineers. Wichita, Kan.: Engineering Education System, 1993.